NTNU
Det skapende universitet

Simulering av marine løfteoperasjoner med fokus på kontroll av konstruksjonsrepons

Andreas Andersen

Marin teknikk
Innlevert: juni 2015
Hovedveileder: Jørgen Amdahl, IMT

Norges teknisk-naturvitenskapelige universitet
Institutt for marin teknikk

NTNU
Norges teknisk-naturvitenskapelige universitet
Institutt for marin teknikk

MASTER THESIS 2014

for

Stud. Techn. Andreas Andersen

Simulation of marine lift operations with focus on structural response control

Simulering av marine løfteoperasjoner med fokus på kontroll av konstruksjonsrepons

Offshore oil and gas activities moves steadily into deeper waters and harsher environment Subsea installations become more and more common for extraction of hydrocarbons. This development put heavy demands on contractors to be able to perform safe and efficient installations, inspections and interventions. At present many operations require benign environmental conditions and are thus limited to the summer period. Time constraints may be by increased efficiency, i.e by reduction of time for each individual operation. Alternatively, the weather window may be increased by increasing the limiting significant wave height for operation. In either case the structural load effects may increase and proper control of the structural response is prerequisite. Lift off, motion through the splash zone and landing of the equipment are especially challenging. Feed back from structural response to the control loop may contribute to reducing the load effects in these phases. The hydrodynamics loads may not be very well known of properly implemented in software used for analysis of the marine operations and resistance formulas may not be adequate if impulsive type actions are encountered.

The purpose of the work is to assess the applicability of USFOS and (possibly) alternative software to simulate selected lift operations. Focus will be placed on code checking of structural response histories. The work is proposed carried out in the following steps:

1) Verify USFOS simulations of lifting operations in flat sea and regular waves. This may comprise both lift off, through the splash zone and landing on sea floor. The environmental conditions shall be varied. Extreme load cases shall be sought. Of particular interest are intense, short duration load pulses caused by wave slamming, wave and current forces in submerged conditions and contact forces during landing on sea floor, this may cause slack in the slings and the wire.
   Check the results with simple hand calculations for steady state conditions in air and in water. Check whether it is possible to start simulations in statically so as to reduce start-up oscillations and cope with some of the challenges identified by Matland in his master thesis work. Investigate whether slack in slings may be simulated.

2) Simulate the same operation as in 1) when motion of the crane mounted on the vessel is simulated. The vessel motion may be modelled by means of transfer functions or using motion spectra. Compare the motion with that for flat sea. Perform repeated simulation (by means of scripting techniques) in irregular seas with different random seeds and

determine characteristic response values on the basis of response statistics. Establish limiting sea states for operation.

3) In collaboration with supervisor select a larger structure and perform simulations as in pt 2) Monitor the load effects with respect to code capacity for selected response quantities.

4) To the extent time permits perform simualation with SIMO/RIFEX on a simple lift operations and compare with USFOS results.

5) Conclusions and recommendations for further work

Literature studies of specific topics relevant to the thesis work may be included.

The work scope may prove to be larger than initially anticipated. Subject to approval from the supervisors, topics may be deleted from the list above or reduced in extent.

In the thesis the candidate shall present his personal contribution to the resolution of problems within the scope of the thesis work.

Theories and conclusions should be based on mathematical derivations and/or logic reasoning identifying the various steps in the deduction.

The candidate should utilise the existing possibilities for obtaining relevant literature.

Thesis format
The thesis should be organised in a rational manner to give a clear exposition of results, assessments, and conclusions. The text should be brief and to the point, with a clear language. Telegraphic language should be avoided.

The thesis shall contain the following elements: A text defining the scope, preface, list of contents, summary, main body of thesis, conclusions with recommendations for further work, list of symbols and acronyms, references and (optional) appendices. All figures, tables and equations shall be numerated.

The supervisors may require that the candidate, in an early stage of the work, presents a written plan for the completion of the work. The plan should include a budget for the use of computer and laboratory resources which will be charged to the department. Overruns shall be reported to the supervisors.

The original contribution of the candidate and material taken from other sources shall be clearly defined. Work from other sources shall be properly referenced using an acknowledged referencing system.

The report shall be submitted in two copies:
- Signed by the candidate
- The text defining the scope included
- In bound volume(s)

- Drawings and/or computer prints which cannot be bound should be organised in a separate folder.
- The report shall also be submitted in pdf format along with essential input files for computer analysis, spreadsheets, MATLAB files etc in digital format.
-

Ownership
NTNU has according to the present rules the ownership of the thesis. Any use of the thesis has to be approved by NTNU (or external partner when this applies). The department has the right to use the thesis as if the work was carried out by a NTNU employee, if nothing else has been agreed in advance.

Thesis supervisor

Prof. Jørgen Amdahl

Deadline: January 15 , 2015

Trondheim, June 10. 2015

Jørgen Amdahl

Preface

This master thesis is a part of the study program Marin teknikk at the Norwegian University of Science and Technology (NTNU). It was carried out during the spring semester of 2015. The problem was selected in May 2014 as a pre-project and continued in the thesis. The reason for choosing this project was that it provided the opportunity to work with both hydrodynamic and structural analysis. It has been rewarding trying to use a program that is not initially designed for doing marine operations, to try out ideas and try to make them work. I would like to thank my supervisor, professor Jørgen Amdahl, for offering me this project and for always being eager to help when showing up at his office.

Trondheim, 2015-10-06

Andreas Andersen

Summary

The offshore oil and gas industry is applying more and more subsea equipment to the deeper fields. One of the challenges of using subsea equipment is the installation process. The installation is very dependent on the weather window, and a better understanding and analysis methods could help to expand the window of operations.

This thesis gives an introduction to the challenges regarding marine operations. The most challenging phases identified were "lift-off from deck", "lowering through the wave zone" and "positioning and landing". The focus of the majority of the thesis fell on the phase "lowering through the wave zone".

To assess USFOS' capability to simulate marine operations, a series of verification studies were done. In theory, USFOS does have the tools to calculate all the necessary forces in a lifting operation through the wave zone.

Two main models were used: a simple model and an advanced model, both of which were taken from a previous master thesis and worked on further. The simple model was a tubular member suspended by two springs. All the verification analyses were run on this model. In addition, a study of limiting sea states on the simple model were performed. The advanced model was used to find the limiting sea state for a more realistic model. The advanced model represents a spool, which was suspended by a single wire and four slings. A spreader beam was used to distribute the forces in the spool.

The verification analyses proved that USFOS indeed was capable of calculating forces in the wire, which is an important limiting factor, as slack forces are not desirable. The weight of the module in air and water had a maximum error of 1%. When drag forces were studied, the error was larger. One lowering velocity of the module generated an error of 40.29%. However, the drag force contribution was only 0.9% of the submerged weight, so it was considered to be irrelevant for cases to be run at a later stage.

The slamming force was harder to check against hand calculations. The reason for this was that the measured forces in the wire were force responses, and not direct forces on the module

itself. A slamming effect was observed, but it was not comparable to hand calculations. By changing the eigenperiod of the system with 50%, new vibrations arose in the module when it was lowered through the wave zone. They showed that USFOS probably was calculating the slamming correctly.

A series of smaller studies were performed to determine the use of the spool wave function and to ensure good results in the upcoming limit studies. A new time step for the simulations was determined to capture the correct forces. The minimum forces were of the highest interest. The effect of damping in wire was checked, and the resulting value appeared to have an impact on the wire force. However, the importance of its impact was uncertain. The studies conducted using the spool wave showed that it was a good method to obtain the minimum wire forces without running a full 3-hour sea state. There was found a difference in the wire force depending on when the module hit the water surface in a spool wave. This confirmed the use of spool wave function as a valid method to obtain the minimum force.

To find the limiting sea states for the simple module, several analyses with different sea states and different seeds were run. From this, statistical models were built, assuming the minimum forces followed a Minimum Value distribution. This was the case for most of the simulations, but simulations that produced both positive and negative minimum values or had some values close to zero and others far away, showed that there may be a different distribution of the results. However, for the simple model there weren't any sea states for which it was necessary to predict the probability of not exceeding the limit force in the wire. The limiting sea states in which the module could operate were sea states with the parameters $H_s = 3\ m, T_p = 5\ s$ and $H_s = 2\ m, T_p = 4\ s$.

Before finding the limiting sea state for the advanced model, a new sensitivity study was performed to ensure that the time interval gave good results and that the use of the spool wave function was still valid. By doing these analyses over again, the best parameters could be found so that the analyses used less computational time. When checked against limiting sea states, 5 out of 8 sea states needed the use of probability paper to evaluate the results. If the limiting probability of exceeding was set to 90%, the limiting sea state were $H_s = 2\ m, T_p = 4\ s$.

Sammendrag

Olje- og gassindustrien bruker mer og mer undervannsutstyr på stadig dypere vann. En av de største utfordringene ved bruk av undervannsutstyr er installasjonsprossesen. Installasjonsprossesen er svært avhengig av værvinduet. En bedre forståelse og analytiske metoder kan bidra til å utvide tidsvinduet for å utføre operasjoner.

Denne tesen gir en innføring i de utfordringer som oppstår ved marine operasjoner. Fasene som regnes som mest utfordrende var "løft av dekk", "senkning gjennom bølgesonen" og "posisjonering og landing under vann". Hovedparten av fokuset i denne tesen falt på fasen "senking gjennom bølgesonen".

For å vurdere USFOS' evne til å simulere marine operasjoner ble en rekke verifikasjonsstudier gjort. USFOS har i teorien verktøyene for å beregne alle de nødvendige kreftene som står oppstår i løpet av en løfteoperasjon gjennom bølgesonen.

To hovedmodeller ble brukt: en enkel modell og en avansert modell. Begge modellene ble hentet fra en tidligere tese, og arbeidet videre på. Den enkle modellen består et rør opphengt ved hjelp av to fjærer. Denne modulen ble brukt til verifikasjonsstudier. I tillegg ble det gjort en studie for å finne den begrensende sjøtilstanden på den enkle modellen. Den avanserte modellen ble brukt til å finne begrensende sjøforhold for en mer realistisk modell. Den avanserte modellen representerer en "spool", som ble opphengt i en enkelt vaier og fire stropper. En sprederbjelte ble brukt til å fordele kreftene på "spoolen".

Verifikasjonsanalysene viste at USFOS var i stand til å beregne viktige krefter i vaieren, som er en viktig begrensende faktor, siden slakk ikke er ønskelig. Vekten i luften og vannet hadde en maksimal feil på 1%. Når motstandskreftene ble studert oppstod noen store forskjeller. En av senkehastighetene til modulen ga en feil på $40,29\%$. Imidlertid er kraftbidraget så lavt som $0,9\%$ av den neddykkede vekt, så dette ble ansett for å være irrelevant for resten av de kommende analysene.

Slammingkraften var vanskeligere å sjekke mot håndberegninger. Grunnen til dette var at den målte kraften i vaieren var en kraftrespons, og ikke en direkte kraft på selve modulen.

Slammingeffekten ble observert, men den var ikke mulig å sammenligne med håndberegninger. Ved å endre egenperioden til systemet med 50% oppstod nye vibrasjoner da modulen ble senket gjennom bølgesonen. Dette viste at USFOS sannsynligvis beregnet slamming riktig.

En rekke mindre studier ble utført med bruk av "spool wave"-funksjonen for å sikre gode resultater i de kommende grensestudiene. Et nytt tidssteg ble bestemt for å fange de riktige kreftene. Det var de minste kreftene i vaieren som var av størst interesse. Effekten av demping i vaieren ble sjekket, og resultatene så ut til å ha en innvirkning på kreftene i vaieren. Omfanget av denne innvirkningen var imidlertid usikker. Studier utført med "spool wave"-funksjonen viste at det var en god måte å oppnå minimumskreftene i vaieren uten å måtte kjøre en fullstendig 3-timers sjø. Det viste seg at vaierkraften var avhengig av når modulen traff vannoverflaten i en "spool"-bølge. Dette bekreftet at bruken av "spool wave"-funksjonen var gyldig for å finne de minste kreftene i vaieren.

For å finne de begrensende sjøtilstander for den enkle modulen ble det kjørt flere analyser med ulike sjøtilstander og ulike frø. På bakgrunn av disse analysene ble det satt opp statistiske modeller, forutsatt at minimumskreftene fulgte en minimumsverdi-fordeling. Dette var tilfellet for de fleste av simuleringene, men noen simuleringer ga både positive og negative minimumsverdier, hadde noen verdier nær null, og oppstod sammen med andre store verdier. Det var med andre ord stor spredning. Dette viste at resultatene nær null kunne ha en annen fordeling i den aktuelle sjøtilstanden. For den enkle modellen var det ingen sjøtilstander som gjorde det nødvendig å forutsi sannsynligheten for å ikke overskride grensekraften i vaieren. Begrensende sjøtilstander der operasjonen kunne utføres hadde parametre $H^S = 3\,m, T_p = 5\,s$ og $H^S = 2\ m, T_p = 4\ s$.

Før den begrensende sjøtilstanden for den avanserte modellen kunne finnes, måtte nye følsomhetsanalyser utføres. Dette ble gjort for å sikre at tidsintervallet ga gode resultater og at anvendelsen av "spool"-bølgen fremdeles var gyldig. Ved å gjøre disse analysene om igjen, kunne de beste parameterne bli funnet slik at analysene tok kortere tid. Da det ble sjekket opp mot begrensende sjøtilstander viste det seg at det måtte brukes sannsynlighetspapir for å evaluere resultatet for 5 av 8 sjøtilstander. Sannsynligheten for å evaluere resultatene. Dersom den begrensende sannsynligheten for å overgå minimumskraften i vaieren ble satt til 90%, ble den

begrensende sjøtilstanden funnet til å ha parametrene $H^S = 2\ m, T_p = 4\ s$.

List of Symbols

η_1	$[m]$	Motion in surge
eta_2	$[rad/m]$	Motion in sway
eta_3	$[m]$	Motion in heave
eta_4	$[rad/m]$	Motion in roll
eta_5	$[m]$	Motion in pitch
eta_6	$[rad/m]$	Motion in yaw
s	$[m]$	Point of motion
s_3	$[m]$	Point of motion in heave
ζ	$[m]$	Wave profile
ζ_a	$[m]$	Wave height
ω	$[rad/s]$	Wave frequency
β	$[rad]$	Angle of wave attack
$H(\omega)$	$[m]$	Transfer function
t	$[s]$	Time
η_{3R}	$[m]$	Relative heave motion
$\ddot{\eta}_{3R}$	$[m/s^2]$	Relative heave acceleration
F_{snap}	$[N]$	Snap load
m_{module}	$[kg]$	Mass of module
F_{line}	$[N]$	Force in hoisting line/cable
W_0	$[kg]$	Weight of object in air
F_B	$[N]$	Buoyancy force
F_C	$[N]$	Steady force due to current
F_I	$[N]$	Inertia force
F_{wd}	$[N]$	Wave damping force
F_d	$[N]$	Drag force
F_w	$[N]$	Wave excitation force
F_s	$[N]$	Slamming force
F_e	$[N]$	Water exit force
F_0	$[N]$	Mean force
F_{dyn}	$[N]$	Dynamic force
F_3	$[N]$	Force in heave
A_{33}^{2d}	$[kg/m]$	2-D Added mass in heave from heave motion
A_{33}	$[kg]$	Added mass in heave from heave motion

ρ	$[kg/m^3]$	Density
Ω	$[m^3]$	Volume of submerged cylinder
V	$[m/s]$	Velocity
g	$[m/s^2]$	Gravitational acceleration
R	$[m]$	Radius of cylinder
C_s	$[-]$	Slamming coefficient
$B_{33}^{(1)}$	$[Ns/m]$	Linear damping coefficient
$B_{33}^{(2)}$	$[Ns/m]$	Quadratic damping coefficient
M	$[kg]$	Mass of ship
$\ddot{\eta}$	$[m/s^2]$	Acceleration
v_3	$[m/s]$	Particle velocity in z-direction
$\dot{v_3}$	$[m/s^2]$	Particle acceleration in z-direction
h	$[m]$	Distance between surface and bottom of cylinder
ϕ	$[-]$	Wave potential
u_z	$[m/s]$	Velocity in z-direction
a_z	$[m/s^2]$	Acceleration in z-direction
P_{dyn}	$[Pa]$	Dynamic pressure
k	$[-]$	Wave number
C_L	$[-]$	Lift coefficient on cylinder
D	$[m]$	Diameter of cylinder
C_m	$[-]$	Mass coefficient
C_D	$[-]$	Drag coefficient
u_c	$[m/s]$	Current velocity
v_r	$[m/s]$	Relative velocity
l	$[m]$	Length of cylinder
S_n	[]	Wave spectrum value
H_s	$[m]$	Significant wave height
T_p	$[m]$	Peak period
γ	$[-]$	Preakness factor
ω_p	$[rad]$	Spectral peak frequency
σ	[ ]	Standard deviation
X	[ ]	Realization
μ	[ ]	Mean value
Υ	[ ]	Euler's constant
x_i	[ ]	Individual smallest value
$F_{I,max}$	[ ]	Cumulative density function for extreme values
$F_{I,min}$	[ ]	Cumulative density function for minimum values
n	[ ]	number of observations
u^m	[ ]	Random number

λ	$[m]$	Wave length
E	$[Pa]$	Young's modulus
σ_y	$[Pa]$	Yield stress
ρ_w	$[kg/m^3]$	Water density
k_w	$[N/m]$	Wire stiffness
t_end	$[s]$	Time of end of acceleration
C_2	$[-]$	Peak factor
v^l_{const}	$[m/s]$	Constant lowering velocity

Contents

List of Figures

List of Tables

Chapter 1

Introduction

As the offshore oil and gas industry is moving into deeper and deeper waters to find oil, the use of subsea modules becomes more common. The understanding of forces and responses in marine operations is important to be able to install and maintain the modules. The overall goal is to increase the time window in which marine operations can be done safely.

In this thesis, the use of a program called USFOS to do crane lift simulations will be investigated. This program is not usually used for this, as its main purpose is to calculate loads and capacities in fixed marine structures, such as jacket platforms. However, the program can calculate hydrodynamic forces and responses in hanging structures. By using this, it should be possible to simulate crane operations in USFOS.

1.1 Scope

Initially, all the critical phases of the operation with their corresponding critical sea states were intended to be simulated. However, familiarizing with the program and developing good simulations took up most of the time, so the lowering through the wave zone ended up being the only operation that was studied. In collaboration with the supervisor, the code capacity check was considered less important to do if the time didn't allow for it. It was also anticipated that the verification analyses could be tested against another simulation program,

e.g. SIMO. However, time did not allow for this to be done.

In summary, this thesis covers:

- An introduction to loads and mechanisms that are important to consider when performing simulations of marine operations for the different phases.
- An introduction to probability calculations needed to determine the characteristic response.
- A brief introduction to USFOS and its different functions which enable it to simulate marine operations.
- Thorough verification of the simple model to establish the applicability of using USFOS.
- Studies of the use of the spool wave functions for doing marine operations in USFOS.
- Limit studies of the simple model and the advanced model
- An overview of models used in simulations

Chapter 2

Typical Subsea Equipment

In this chapter, the subsea equipment that is typically installed by a side-hanging crane is briefly described.

2.1 Typical Models

Typical subsea modules were found to be (AkerSolutions, 2014f):

- Tie-in connections
- Manifolds
- Subsea trees
- Power- and processing modules
- Suction anchors

2.1.1 Tie-in Connection

The typical tie-in connection is a spool which connects the different modules together within short distances. The module consists of a rigid pipe as shown in figure 2.1a. It is often referred to as a "spool."

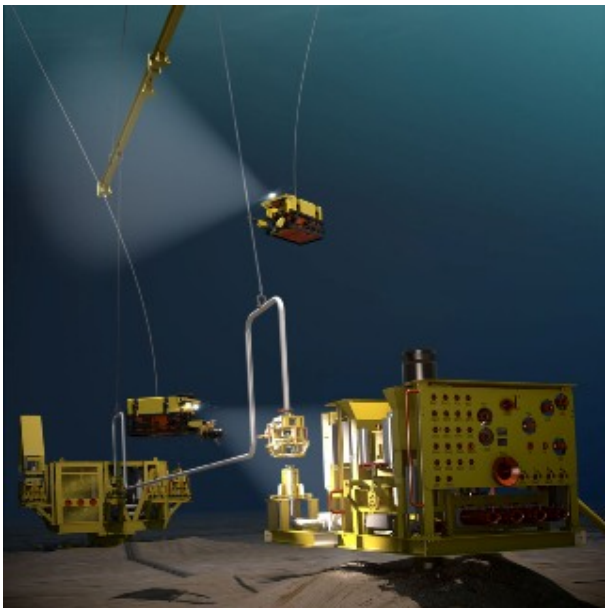

(a) Tie-in connection systems illustration (AkerSolutions, 2014g)

2.1.2 Manifolds

Manifolds are often in system with each other, and are protected by a tubular frame. The protective frame can be independent of the manifolds and can be used to protect other systems, see figure 2.2c. Together, they make a highly complex module. The modules can vary in size, see figure 2.2a and 2.2b.

(a) Small manifolds system from AkerSolutions (AkerSolutions, 2014e)

(b) Deepwater cluster manifolds from AkerSolutions (AkerSolutions, 2014b)

(c) Satellite protection structure from AkerSolutions (AkerSolutions, 2014d)

Figure 2.2: Pictures of different manifolds and protection modules

2.1.3 Subsea Tree

A subsea tree is a collection of control valves. The structure can be in connection with a protective frame, see figure 2.3.

(a) Subsea tree from AkerSolutions (AkerSolutions, 2014a)

(b) Unprotected subsea tree (Unknown, 2014b)

Figure 2.3: Different subsea trees

2.1.4 Power and Processing Modules

These are large subsea modules containing power- and processing equipment inside a protective frame. See figure 2.4

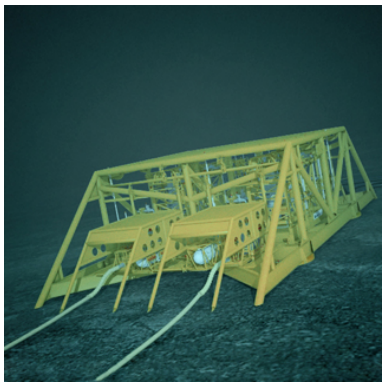

Figure 2.4: Subsea production and power module (AkerSolutions, 2014c)

2.1.5 Suction Anchor

A suction anchor is used to fasten the subsea modules and can also be used as an anchor for different kinds of surface floaters. One example of a suction anchor is the cylinder which sits under the module, which fastens it to the seabed, see figures 2.5

(a) A typical suction anchor (EniNorge, 2014)

(b) A frame with subsea anchors (Unknown, 2014a)

Figure 2.5: Different subsea anchors

The structures shown in this section are highly complex in terms of modeling and analysis, maybe with the exception of the tie-in connections. The interaction between the members of the structures creates dynamic forces that are hard to predict. The regulations and guidelines provided by classification societies such as Det Norske Veritas GL (DNVGL) are very conservative in many cases. (Kimiaei, Jiajing, & Yu, 2014) showed that the guidelines from (DNV, 2011b) could be overestimating the Dynamic Amplification Factor (DAF) by 51% for a flat frame structure compared to numerical analysis.

Chapter 3

Loads in subsea lifts

DNV-RP-H103 divides lifting operations into two categories (DNV, 2011b):

- A ***light lift*** is when the object is very small compared to the crane vessel. The weight is less than 1-2% of the displacement of the crane vessel. The motion of the crane tip is not affected by the lifted object.
- A ***heavy lift*** is when the object is more than 1-2% of the crane vessels displacement. Coupled dynamics must be considered.

According to (DNV, 2011b) chapter 3, the typical phases of a subsea lift are:

- lift-off from deck and maneuvering the object clear of the transportation vessel
- lowering through the wave zone
- further lowering down to sea bed
- positioning and landing.

Further, (DNV, 2014) states that the important loads to consider in a subsea operation are:

- Weight and center of gravity
- Weight of rigging
- Special loads

  - tugger line loads
  - guide line loads
  - wind loads
  - hydrostatic loads
  - hydrodynamic loads
- Skew loads
  - sling length inaccuracies
  - fabrication tolerances of lift points
  - deflections of lifted object
  - crane hook geometry
  - multi hook lifting
  - doubled slings
  - difference in sling elongations

In this thesis, the focus will be on the light lifting operations. This means that the crane boom can be treated as a stiff structure (DNV, 2011b). The motion of the crane tip is thus governed by the crane vessel's Response Amplitude Operator (RAO).

3.1 Lift-off from Deck

When lifting a module off the deck of a transport vessel or a barge, the relative motions between the crane vessel and the transport vessel can lead to snap loads and impact loads.

3.1.1 The Relative Motions between Two Ships

The position s at any point (x, y, z) of the ship can be written as (Faltinsen, 1990):

$$s = (\eta_1 + z\eta_5 - y\eta_6)\mathbf{i} + (\eta_2 - z\eta_4 + x\eta_6)\mathbf{j} + (\eta_3 + y\eta_4 - x\eta_5)\mathbf{k} \tag{3.1}$$

where η_i are the motions in surge, sway, heave, roll, pitch and yaw. **i**, **j** and **k** are unit vectors along the x-, y- and z-axis.

The vertical motions of the ship are of most interest. If the ship is assumed to be stationary under the operation, the vertical displacement s_3 at any point can be written as:

$$s_3 = \eta_3 + y\eta_4 - x\eta_5 \tag{3.2}$$

If a harmonic wave is assumed with the profile

$$\zeta(x, y, t) = \zeta_a sin(\omega t - kxcos(\beta) - kysin(\beta)) \tag{3.3}$$

where ζ_a = wave amplitude, ω = wave frequency and β = angle of wave attack.

The different motions are then given by:

$$\eta_i = |H(\omega)|_i \zeta \qquad \text{where i = 3,4,5} \tag{3.4}$$

where $|H(\omega)|_i$ is the RAO for the ship in the different degrees of freedom.

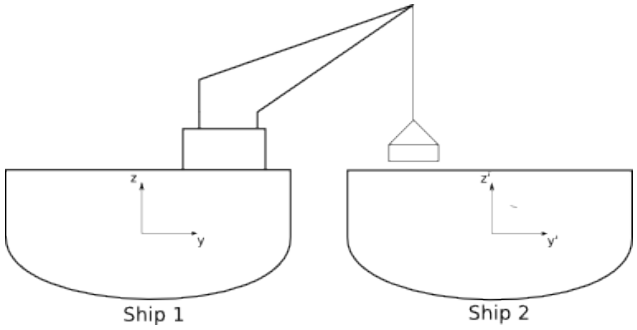

Figure 3.1: Lift off operation from separate vessels

The relative motions between two ships can be calculated by using two coordinate systems, see figure 3.1. For Ship 1, the wave elevation at the center can be written as:

$$\zeta(a,b,t) = \zeta_a sin(\omega t - a\ kcos(\beta) - b\ ksin(\beta)) \tag{3.5}$$

and for Ship 2:

$$\zeta(x',y',t') = \zeta_a sin(\omega t') \tag{3.6}$$

The relation between the wave elevations is:

$$\omega t' = \omega t - a\ kcos(\beta) - b\ ksin(\beta)$$

Where a and b is the distance between the ships' centers. The motions are now:

$$\eta_i^{ship\ 1} = |H(\omega)|_i^{Ship\ 1} sin(\omega t) \tag{3.7}$$

$$\eta_i^{ship\ 2} = |H(\omega)|_i^{Ship\ 2} sin(\omega t - a\ kcos(\beta) - b\ ksin(\beta)) \tag{3.8}$$

The relative motion between the two ships is then:

$$\eta_{3R} = \left(\eta_3^{ship\ 1} + y_{crane\ tip}\ \eta_4^{ship\ 1} - z_{crane\ tip}\ \eta_5^{ship\ 1}\right) - \left(\eta_3^{ship\ 2} + y_{module\ pos}\ \eta_4^{ship\ 2} - z_{module\ pos}\ \eta_5^{ship\ 2}\right) \tag{3.9}$$

From this, the relative acceleration for the crane and the module can be derived. This way, the snap loads that may occur can be calculated using Newton's 2. law:

$$F_{snap} = m_{module}\ \ddot{\eta}_{3R} \tag{3.10}$$

From the equations for the motions of the ships it is apparent that their respective RAOs are what make their motions different. This means that two ships with near equal RAO will have an equal response to the incoming waves, which is beneficial for doing e.g. crane operations safely. The phase difference between the time where the waves hit the two ships will vary with

the heading of the ships and the distance between them. In head sea ($\beta = 0$ $[deg]$), the phase difference plays a small role in the relative motion. However, in beam sea ($\beta = 45$ $[deg]$), the effect from the phase difference is much greater. The placement of the module on the transportation ship relative to the placement of the crane on the crane ship influences the phase difference.

3.2 Lowering through the Wave Zone

According to (DNV, 2011b), an object lowered into or lifted out of water will be exposed to a number of forces. In general, these forces are:

$$
\begin{aligned}
F_{line} &= \text{force in hoisting line/cable} \\
W_0 &= \text{weight of object (in air)} \\
F_B &= \text{buoyancy force} \\
F_C &= \text{steady force due to current} \\
F_I &= \text{inertia force} \\
F_{wd} &= \text{wave damping force} \\
F_d &= \text{drag force} \\
F_w &= \text{wave excitation force} \\
F_s &= \text{slamming force} \\
F_e &= \text{water exit force}
\end{aligned}
$$

where the force $F_{line}(t)$ in the hoisting line is the sum of the means of the forces F_0 and F_{dyn} due to the motion of the crane tip and the wave excitation on the object.

3.2.1 Slamming

The vertical slamming force including the hydrostatic forces can be expressed as (Faltinsen, 1990):

$$F_3 = \frac{d}{dt}(A_{33}V) + \rho g \Omega \tag{3.11}$$

Where Ω is the submerged volume and A_{33} is the high-frequency added mass in heave.

If the vertical velocity is assumed to be constant, the dynamic part of the equation 3.11 can be rewritten to:

$$\frac{d}{dt}(A_{33}^{2D}(t)V) = \frac{dA_{33}^{2D}}{dh}V^2 \tag{3.12}$$

By introducing a slamming coefficient (C_s):

$$\frac{dA_{33}^{2D}}{dh}V^2 = 0.5\rho 2 C_s R V^2 \tag{3.13}$$

The slamming coefficient for cylinder is found experimentally by using figure 3.2

(DNV, 2011b) presents the equation of motion of lifted objects subjected to the combination of buoyancy, inertia, wave exitation, slamming and drag damping forces:

$$\begin{aligned}(M + A_{33})\ddot{\eta} = B_{33}^{(1)}(v_3 - \dot{\eta}) + B_{33}^{(2)}(v_3 - \dot{\eta})|(v_3 - \dot{\eta})| \\ +(\rho V + A_{33})\dot{v_3} + \frac{dA_{33}^{\infty}}{dh}(\dot{\zeta} - \dot{\eta})^2 + \rho g V(t) - Mg + F_{line}(t)\end{aligned} \tag{3.14}$$

where

$$\begin{aligned} B_{33}^{(1)} &= \text{the linear damping coefficient} \\ B_{33}^{(2)} &= \text{the quadratic damping coefficient} \\ v_3 &= \text{Water particle velocity} \\ F_{line} &= \text{force in hoistion line} \end{aligned}$$

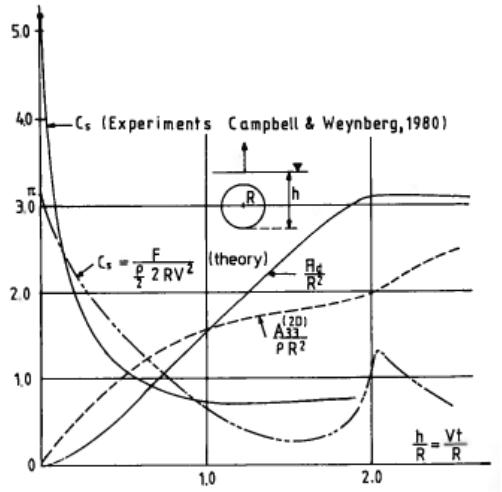

Figure 3.2: Slamming and added mass coefficients for cylindrical structures. Retrieved from (Faltinsen, 1990)

3.3 Loads on Different Geometries

There are different types of geometry to consider. For simplicity, the module can be defined as either a square or a set of cylinders. The reason for doing this is that analyzing complex structures such as a subsea tree or a production module (see figures 2.3 and 2.4) involves Computational Fluid Dynamics (CFD) or model testing to be able to determine the hydrodynamic coefficients. (Ø ritsland, Lehn, & Reitan, 1986) present key data for some complex geometries such as added mass, linear and quadratic damping at a 2 second period of oscillation.

3.3.1 Slender Cylinders

On a cylinder in cross stream, the force can be calculated using Morrison's equation:

$$dF = \rho \frac{\pi D^2}{4} C_m a_x dz + 0.5 \rho C_d u|u| dz \tag{3.15}$$

where D is the diameter, C_m is the mass coefficient and C_d is the drag coefficient. C_d and C_m can be found in (DNV, 2011a). C_d varies when the cylinder is moved towards the seabed. If

the current is taken into account, the equation becomes

$$dF = \rho \frac{\pi D^2}{4} C_m a_x dz + 0.5 \rho C_d (u + u_c)|(u + u_c)|dz$$

Chapter 4

Stochastic Theory

4.1 Wave Spectrum

To describe the waves that are used in a irregular sea state a sea spectrum is used. Commonly used in Norway is the Joint North Sea Wave Observation Project (JONSWAP). The spectrum describes the energy of the wave in a certain frequency range.

$$S_n(\omega) = \frac{5}{32\pi} H s_s^2 T_p \left(\frac{\omega_p}{\omega}\right)^5 e^{-\frac{5}{4}\left(\frac{\omega_p}{\omega}\right)^5} (1 - 0.287 ln(\gamma)) \gamma^{e^{-\frac{\left(\frac{\omega}{\omega_p}-1\right)^2}{2\sigma^2}}} \tag{4.1}$$

where:

$$\sigma = \begin{cases} 0.7 & for \quad \omega \leq \omega_p \\ 0.5 & for \quad \omega \geq \omega_p \end{cases} \tag{4.2}$$

and

$$\omega_p = \frac{2\pi}{T_p} \tag{4.3}$$

Hs significant wave height.

Tp spectral peak period .

γ peakiness factor .

4.2 Minimum Value

The type I Extreme Value model Cumulative Density Function (CDF) is given as (Bury, 1978):

$$F_{I,max}(X_i;\mu,\sigma) = exp\left[-exp\left(-\frac{x_e-\mu}{\sigma}\right)\right] \tag{4.4}$$

where: x_e is the extreme value of the realization of x, μ is the mean value and σ is the standard deviation.

Using the method of moment to determine μ and σ:

The moment function of the reduced variable $Z_i = \frac{X_i-\mu}{\sigma}$ is given by:

$$M(t; f_{I,max}) = \int_{-\infty}^{\infty} exp(tz) f_{I,max}(z)dz \tag{4.5}$$

where $f_{I,max}$ is the probability density function and t is the order. Further,

$$\mu = \sigma + \Upsilon\mu \tag{4.6}$$

where Υ = Euler's constant = 0.57722 giving:

$$\mu = \sigma + 0.057722\mu \tag{4.7}$$

and

$$\sigma = \frac{\pi}{\sqrt{6}}\mu \tag{4.8}$$

The type I smallest extremes are:

$$min(x_i) = -max(-x_i) \tag{4.9}$$

where x_i is individual smallest value, giving

$$F_{I,min}(X_e;\mu,\sigma) = 1 - exp\left[-exp\left(\frac{x_e-\mu}{\sigma}\right)\right] \tag{4.10}$$

with corresponding

$$\mu = \sigma - 0.057722\mu \tag{4.11}$$

and

$$\sigma = \frac{\pi}{\sqrt{6}}\mu \tag{4.12}$$

4.2.1 Probability Paper

"The method of probability plotting provides a convenient check of the distributional assumptions $F_{I,max}$. In addition, this method detects "outlying" observations and furnishes preliminary parameters estimates." (Bury, 1978)

To make a probability plot the CDF has to be linearized:

$$ln\left(-ln[F_{I,min}(x_i;\mu,\sigma)-1]\right) = -\frac{\mu}{\sigma} + \frac{x_i}{\sigma} \tag{4.13}$$

This makes the axes:

$$\begin{aligned} Y &= ln\left(-ln[F_{I,min}(x_i;\mu,\sigma)-1]\right) \\ X &= x_i \end{aligned} \tag{4.14}$$

$F_{I,min}$ is replaced with its expected value $i/(n+1)$, where $i = [1,2,...,n]$ and n is the number of observations. The sample of x_i has to be sorted.

When checking whether the lowest force is exceeded, the probability paper can be transformed back to an S-curve, where the y-axis is in the range from 0 to 1. The values for exceeding a given force are then read:

$$F(x) = P(X \leq x) \Rightarrow P(X > x) = 1 - F(x) \tag{4.15}$$

4.3 Monte Carlo Simulation

By running Monte Carlo simulations on the Minimum Value distribution ($F_{I,min}$) an uncertainty band can be obtained within a given probability. This means that the "Monte Carlo simulation implies that realizations of each source variable X_i are "sampled" from the corresponding distribution function $F_i(x_i)$." (Bury, 1978). By inverting

$$u^m = F(x) \Rightarrow x = F^{-1}(u^m) \tag{4.16}$$

Where u^m is a uniform random set of numbers between 0 to 1, a statistical equivalent random set of realization of x is obtained. The $F_{I,min}$ can be then be inverted to:

$$x = \mu + \sigma ln\left[ln(1 - u^m)\right] \tag{4.17}$$

By running multiple Monte Carlo simulations and plotting the results on the probability paper and removing the values outside a given confidence level, a confidence interval or error bound is obtained corresponding to the sample.

Chapter 5

USFOS

According to (SINTEF, 2001), "USFOS is a numerical tool for ultimate strength and progressive collapse analysis at space frame structures. The formulation includes nonlinear geometry and nonlinear material properties. The basic idea of the program is to use only one finite element per physical element of the structure, i.e. to use the same finite element discretization as in linear, elastic analysis."

USFOS was developed by SINTEF Marintek and NTNU through a joint industry project. USFOS AS was established in 2003 by prof. Jørgen Amdahl, dr. Tore Holmås, dr. Øyvind Helland and dr. Ernst Eberg. The marketing and sales are done by DNV software. (USFOS, n.d.-b)

"The USFOS program has been in commercial use since 1985 by oil companies and engineering consultants all over the world. The program has proved significant cost savings in areas such as inspection planning, lifetime extension and integrity assessment of ageing structures, and in fire protection assessment for new designs. It is verified through participation in extensive benchmark activities both in Europe and USA, through comparison with experiments and through extensive scientific publication."(USFOS, n.d.-b)

5.1 Hydrodynamics

All the basic hydrodynamic calculation methods and theory are presented in (USFOS, 2010).

5.1.1 Waves

Airy waves theory can be applied for infinite, finite and shallow water depth in USFOS. The wave profile can be given by:

$$\phi = \frac{gh}{w} e^{-kz} cos(wt - kx) \tag{5.1}$$

where g is the gravitational acceleration, h is the wave amplitude, ω is the circular wave frequency and k is the wave number.

The deep water assumption holds when: $\frac{d}{\lambda} \geq 0.5$, where λ is the wave length and d is the water depth.

The hydrodynamics on the free surface ($z = 0$) can be calculated using extrapolated Airy theory, see figure 5.1

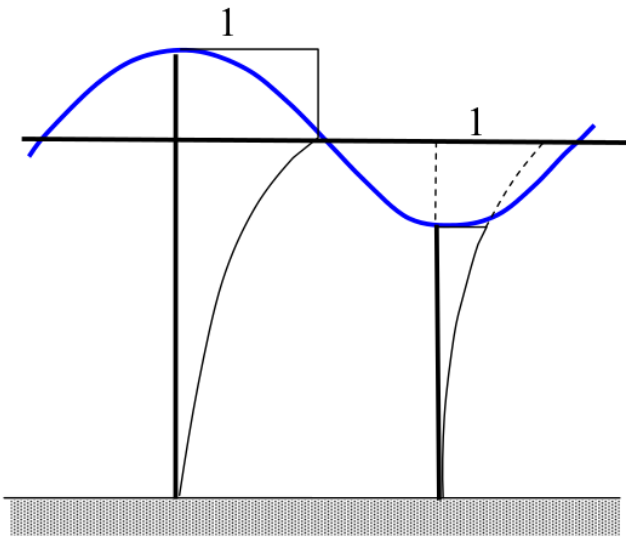

Figure 5.1: Extrapolated Airy wave. Retrieved from (USFOS, 2010)

5.1.2 Slender Cylinders

Hydrodynamic forces on slender members are calculated with use of Morrison's equation. The theory can be found in section 3.3.1. Both the drag (C_d) and mass (C_m) coefficients can be specified for individual elements or by depth. The default values of the coefficients are $(C_d) = 0.7$ and $(C_m) = 2.0$.

5.1.3 Slamming

To account for slamming forces USFOS, corrects the drag term in Morrison's equation with respect to the graph obtained by Campbell and Weinberg. See figure 3.2 and 5.2. It uses the von Karman method, which means that it doesn't account for wet surface rising around the cylinder as it hits the water. See section 3.2 for more extensive theory on slamming.

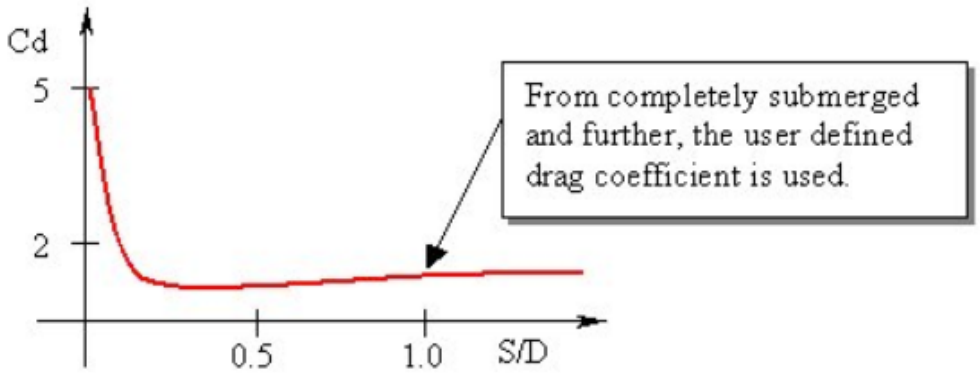

Figure 5.2: C_d based on instant surface/diameter ratio, up to 1. Retrieved from (USFOS, n.d.-a)

5.2 Irregular Sea

USFOS used JONSWAP spectrum to simulate irregular waves. H_s, T_p, γ, T_{lim}^{lower}, T_{lim}^{upper}, number of different frequency and seed was the different parameters needed to bed set. By changing the seed number the sea state parameters is kept the same but a different sea was generated.

5.3 Spool Wave Function

The Spool wave command in USFOS takes out one of the largest waves in a given sea state within a time interval. The order of the largest wave is chosen by the user. This shortens the analyses by only running a few hundred seconds, instead of a full 3 hour sea state/storm. Inputs to the "spool wave" command were:

- Length of the sea state.
- Time before largest wave.
- End time of the simulation
- Which of the five largest waves the simulation should be run over.

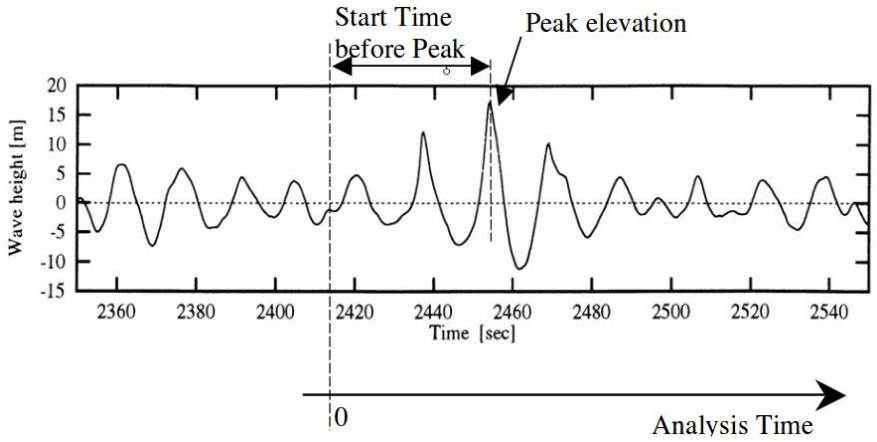

Figure 5.3: Spool wave illustration. Retrieved from (USFOS, 2014)

To ensure the right values were selected, a series of smaller sensitivity studies were done.

The following questions arose:

- How long should the time before peak be so that the module has the right response before the peak hits?
- For how long should the simulations run? The largest force/response could occur after the peak.
- When should the module be lowered in a Spool Wave to capture the minimum/maximum forces?

- Does the minimum/maximum force in the wire occur at the peak?

5.4 Running Analyses

USFOS can be run in two ways: through the terminal or the graphical user interface Xact. Xact is where the model and simulations of the work are displayed. Xact also contains plotting tools, the ability to see the node and element numbers or generate a animation of a dynamic simulation.

USFOS requires two input files. A model file and a head file, both with file extension ".fem". The model file contains specifications of the node coordinates, materials, geometry, boundary condition and loads. The head file tells USFOS what kind of analyses should be run. They can be static, dynamic or a combination. In this file the hydrodynamic properties like wave, drag and mass coefficients are specified, as well as which elements to consider in the analyses. These saved effects can be found in the dynamic plot function in Xact or extracted by the simple program "Dynres", which can be run with USFOS as a postprocessing tool.

The two input files create two new results files. The ".raf" is the simulation file that can be imported to Xact. The ".res" is the result file which contains the results for each calculated step. This file also contains the error information if USFOS fails to run or crashes under an analysis.

5.4.1 Multiple Runs and Scripting

Using the Linux operating system or corresponding programs in Windows, USFOS can be scripted to run multiple analyses. This way, more of the computer's power can be used, and the user can easily run multiple analyses without submitting each one manually by making a script that makes different input files based on the user's specifications. These may be different wave heights, lengths of the analyses or seed numbers. Each different case is then run with different input files in series or parallel, depending on the capacity of the computer.

Chapter 6

Models

The two models used in this thesis can be classified as a "simple model" or an "advanced model". The simple model was used to verify and get familiar with the program. The advanced model represented a Tie-in connection or commonly know as a Spool, with a spreader beam to distribute the load on the spool. Both these models where taken from (Matland, 2014) and worked on further.

6.1 Simple Model

The simple model consists of a tubular member with two springs acting as lifting wires, see figure 6.1a. The dimensions and properties for the module and water are given in table 6.1. The global axis system has its origin in the bottom left node, see figure 6.1b. In addition, the structural damping (Rayleigh damping) was set to $\alpha_1 = 0.01$ and $\alpha_2 = 0.01$. The spring damping was set to be 10^5 $[Ns^2/m]$. More on reasonable wire damping choices can be found in section 7.1.2.

Table 6.1: Technical data for the simple model

Parameter	Symbol	Value	Unit
Length	L	45	[m]
Diameter	D	1	[m]
Thickness	t	0.4	[m]
Density	ρ_s	7890	[kg/m^3]
E-modulus	E	2.1×10^{11}	[Pa]
Yield stress	σ_y	3.30×10^8	[Pa]
Water density	ρ_w	1024	[kg/m^3]
Wire stiffness	k	1.69×10^6	N/m

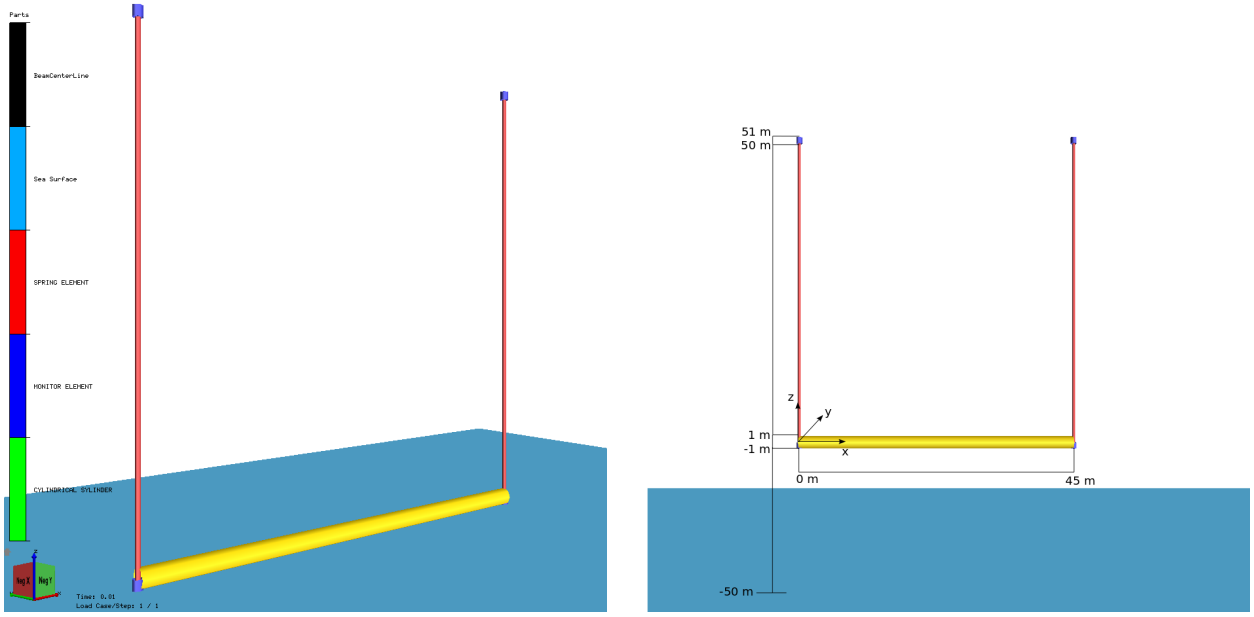

(a) Simple model (b) Simple model with coordinate system

Figure 6.1: Simple model

The model was used for estimating:

- Drag
- Weight in air and water
- Slamming
- When the maximum/minimum force in 3 hour sea state occurred
- Use of the spool wave function in USFOS

6.2 Advanced Model

The model was kept the same as in (Matland, 2014), the only changes done were applying the soft start function and adding the spool wave function to the input files. The technical specifications can be seen in table 6.2.

Table 6.2: Technical data for the advanced model, retrieved from (Matland, 2014)

Spool	Value	Unit
Outer steel diameter	0.3239	$[m]$
Wall thickness	0.0127	$[m]$
Coating thickness	0.003	$[m]$
Cross-sectional area *	0.0124	$[m^2]$
Total cross-sectional area **	0.0155	$[m^2]$
Modulus of elasticity	210	$[GPa]$
Yield stress	550	$[MPa]$
Material density	7850	$[kg/m^3]$
Inner fluid density	1100	$[kg/m^3]$
Spreader bar		
Modulus of elasticity	210	$[GPa]$
Yield stress	355	$[MPa]$
Material density	7850	$[kg/m^3]$
Main part		
Outer diameter	0.6604	$[m]$
Wall thickness	0.0254	$[m]$
Cross-sectional area	0.0506	$[m^2]$
Length	30	$[m]$
Connections		
Outer diameter	0.4064	$[m]$
Wall thickness	0.0159	$[m]$
Cross-sectional area	0.0195	$[m]$
Length	1.33	$[m]$
Wire data		
Outer diameter	0.08	$[m]$
Wall thickness	0.03	$[m]$
Elastic modulus	8.80E+010	$[Pa]$
Cross-sectional area	4.71E-3	$[m^2]$
Initial length	10	$[m]$
Stiffness	4.15E9	$[N/m]$

* Area of cross section without coating
** Area of cross section with coating

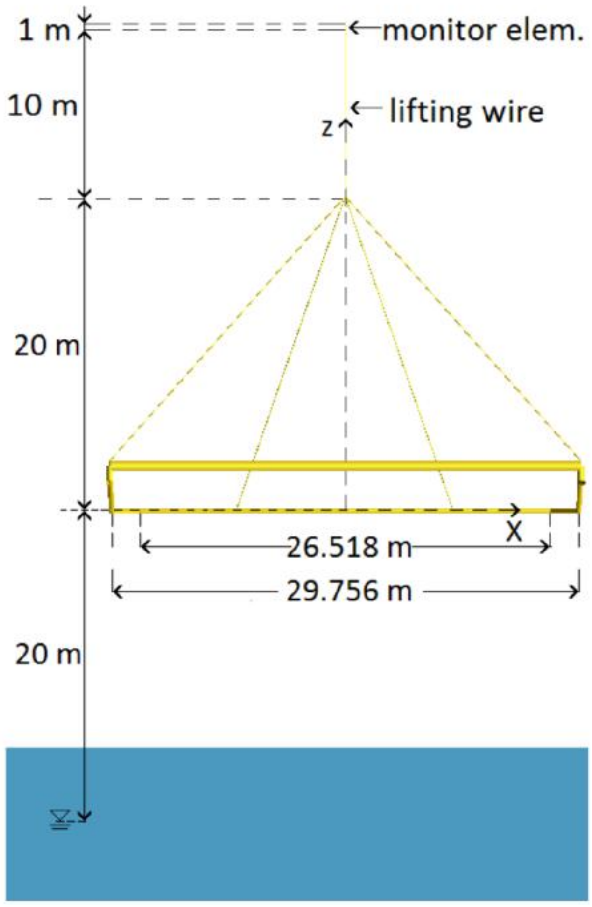

(a) Spool model in x-z plane

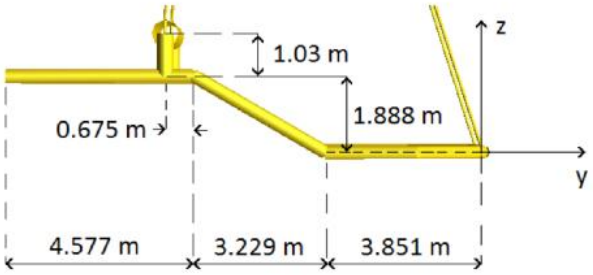

(b) Spool model in y-z plane

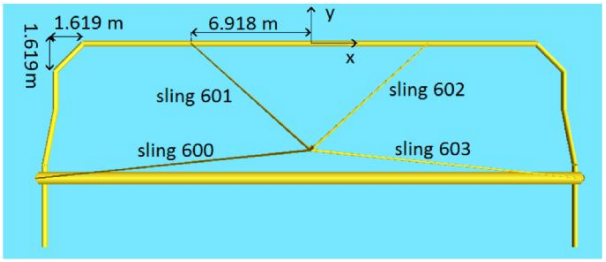

(c) Spool model in x-y plane

Figure 6.2: Advanced model retrieved from (Matland, 2014)

6.3 Wire Modeling

To be able to model a wire element a spring system needed to be modeled. The reason for this is that USFOS could increase the length of the spring with a given time history.

The spring needed to be connected to the beam elements. For analysis purposes a monitor element was placed at the top of the spring. The monitor element has a very high stiffness so it doesn't contribute to the motions of the module. From the monitor element the forces could be read.

The spring element was defined by using a tension spring material (TensSpri) in USFOS. Here the spring stiffness could be defined as well as the time history of its elongation. The geometry of the element from this time on does not matter in the analyses. From the same nodes between the monitor elements a spring damping element was modeled. This was defined by setting a material to the function (MREF), which is used for non-linear damping. The parameters were set to 0 in all dofs. The (spriDamp) parameters could then be assigned to an element. This parameter can assign damping to elements in a chosen dof. The damping was only assigned to work in the axial direction. The damping from the water was calculated and added separately by USFOS.

The elongation history of the spring element could be chosen from three types of S-curves or a user defined history. The different types of S-curves were linear curve, S-curve in power of 2 and S-curve in power of 3. The elongation of the spring was the initial length of the spring element (distance between the monitor element and the module) multiplied by a user defined factor. The initial choice was an S-curve with power of 3 was to prevent initial vibrations when the analysis started. The effect of using a linear S-curve is shown in (Matland, 2014).

6.3.1 Soft Start

Problems with lowering the module with constant velocity arised due to large accelerations in the beginning, which lead to large forces at the start of the analyses. There are no built-in time history functions in UFSOS to elongate the spring element, with the ability to start softly and then maintaining a constant velocity. The S-curve function generated a soft start, but did not provide an accurate way to control the lowering velocity of the module. One solution was to set a linear length increment of the wire element and run the first part of the simulation in quasi static mode, only solving $kx(t) = F(t)$ for the motion. However, when

introducing a spring element into the system, simulations could only be run in dynamic mode. The solution was to use a user defined time point history for the length increment. By transforming equation 6.1 for acceleration to displacement, a soft start was obtained with the constant lowering velocity. The system now accelerated and decelerate slowly until it had reached the desired lowering velocity.

The chosen formula for the acceleration where:

$$a = \frac{(t_{end} \times t - t^2)}{C_2} \tag{6.1}$$

Where t_{end} is the time when $a = 0$ again and C_2 is the peak factor. C_2 is preferably larger than t_{end} to avoid a high peak value. t_{end} for a constant lowering velocity was found by:

$$v^l_{const} = \int a dt = t_{end} \left(\frac{t^2}{2C_2} - \frac{t^3}{3C_2} \right) \tag{6.2}$$

By assuming the acceleration is equal to zero when $t = t_{end}$:

$$v^l_{const} = \frac{1}{6C_2} t^3_{end} \tag{6.3}$$

Based on the required lowering velocity and peak factor the acceleration time became:

$$t_{end} = (6C_2 v^l_{const})^{\frac{1}{3}} \tag{6.4}$$

The displacement of the wire was then described as:

$$S = \int v dt = \begin{cases} \frac{1}{24} t^4 & 0 < t \leq t_{end} \\ t \times v^l_{const} & t > t_{end} \end{cases} \tag{6.5}$$

Based on the equations 6.3, 6.4 and 6.5, a MATLAB script was made that generated a string of displacement points in time based on lowering speed, peak factor, initial length and total lowering length. see ... The MATLAB-generated acceleration can be seen in figure 6.3

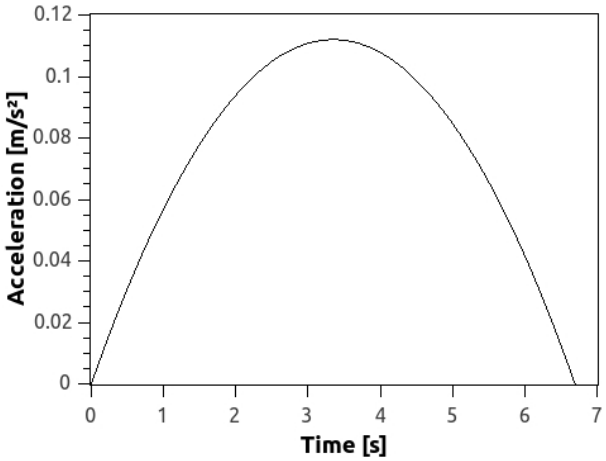

Figure 6.3: Start acceleration

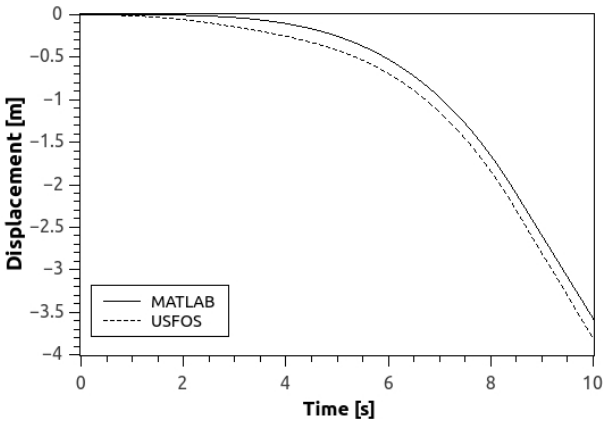

Figure 6.4: Difference in displacement from USFOS and theory

The small difference in the displacement from MATLAB and USFOS seen in figure 6.4 is due to activation of the deadweight in the first five seconds. This lead to an initial displacement of the wire in the results from USFOS. The resulting effect on start forces in the wire can be seen in figure 6.5

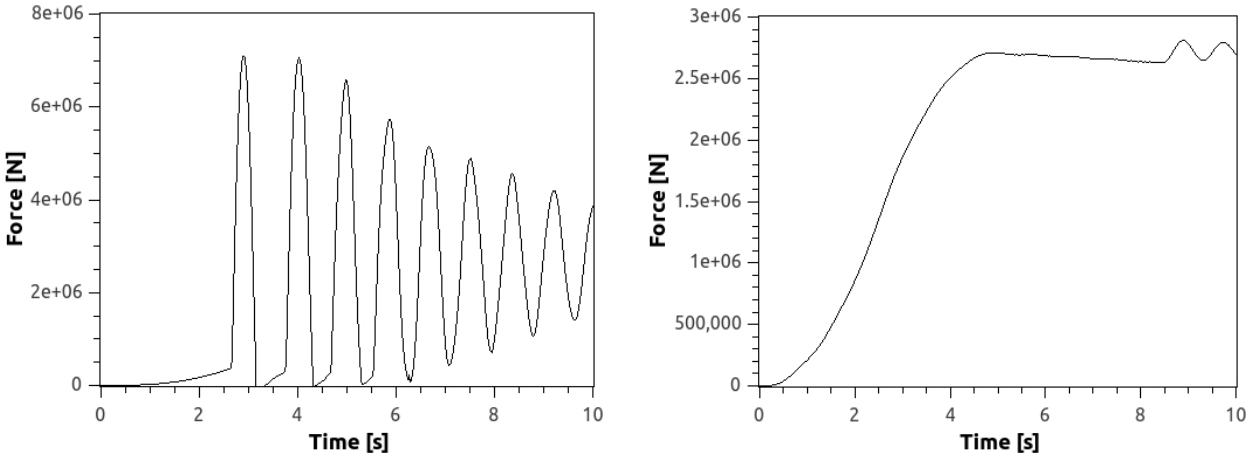

(a) Start forces without soft acceleration (b) Start forces with soft acceleration

Figure 6.5: Comparison of start forces in wire with and without soft start

6.4 Ship Motion

The ship motions were defined by transfer functions which were taken from (Matland, 2014). The transfer functions were for sea with an incoming heading of 45°. The functions described some sort of ship, but the details of the ship were not provided nor known by the supervisor, who provided it to (Matland, 2014). The relevant plot over the motions heave, pitch and roll can be seen in figures 6.6. For the advanced model, the crane tip was located at $(0, 38, 72)$ $[m]$ from the ship's center of gyration. By using the formula 3.1 and basic geometry, it was found that the heave motions affected the crane tip motions the most. Hence larger wave periods were more likely to lead to slack in the wire.

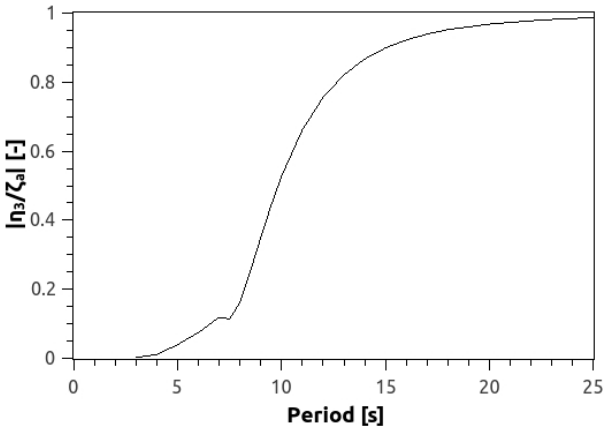

(a) Transfer heave

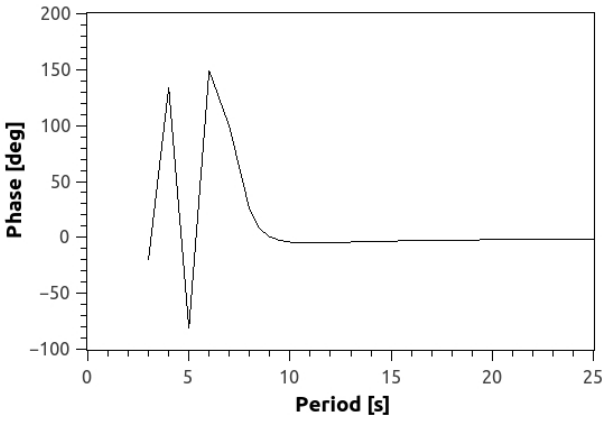

(b) Phase angle heave

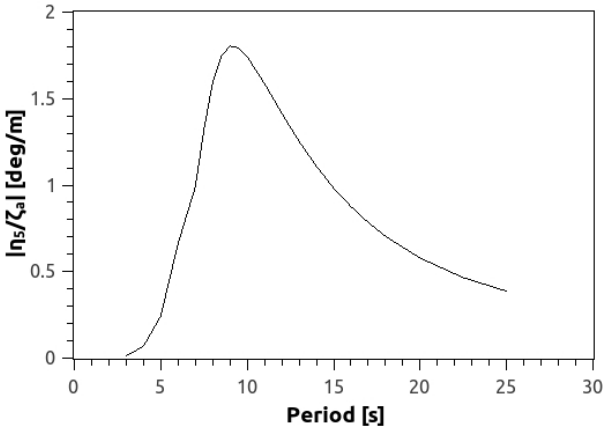

(c) Transfer pitch

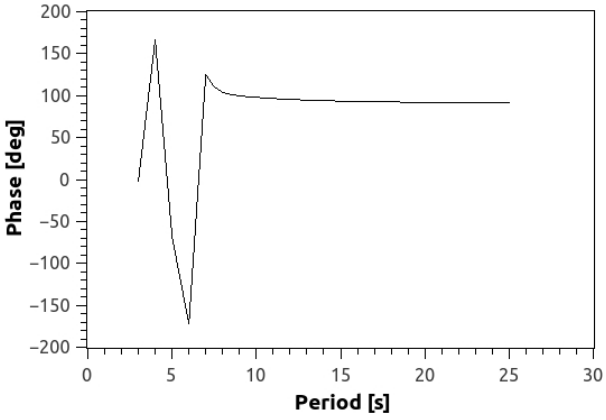

(d) Phase angle pitch

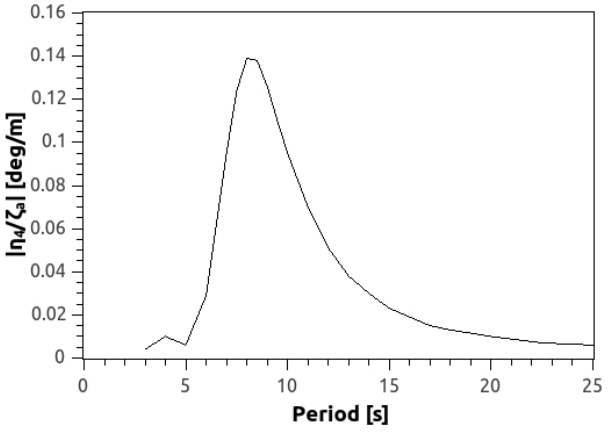

(e) Transfer roll

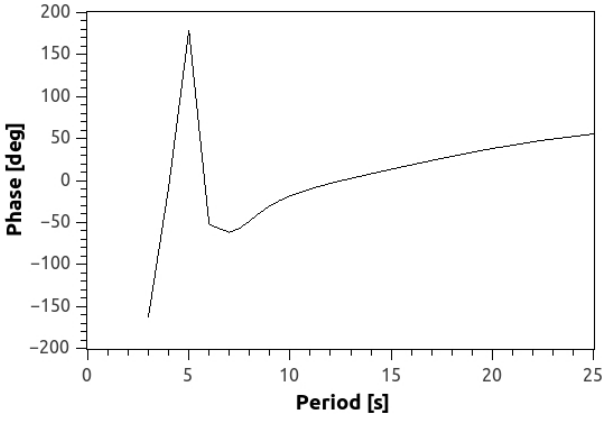

(f) Phase angle roll

Figure 6.6: Ships transfer functions and phases

6.5 Sea state

Based on the report (Eik & Nygaard, 2003) the spectral peak period (T_p) given a significant wave height (H_s) over 43 years were:

H_s	SPECTRAL PEAK PERIOD																		SUM
	0-3	3-4	4-5	5-6	6-7	7-8	8-9	9-10	10-11	11-12	12-13	13-14	14-15	15-16	16-17	17-18	18-19	19-20	<20	
0-1	21	179	529	859	977	889	701	503	337	217	135	82	49	29	17	10	6	4	5	5550
1-2	5	141	959	2762	4683	5644	5411	4430	3245	2193	1399	855	507	294	167	94	53	29	36	32909
2-3	0	9	168	956	2604	4359	5230	4964	3980	2819	1822	1099	629	346	185	97	50	25	25	29368
3-4	0	0	9	127	634	1629	2633	3053	2777	2109	1398	835	461	239	118	56	26	12	9	16126
4-5	0	0	0	8	88	397	955	1460	1593	1349	941	566	303	148	67	29	12	5	3	7924
5-6	0	0	0	0	7	66	268	594	838	836	639	397	210	97	41	16	6	2	1	4019
6-7	0	0	0	0	0	6	49	177	352	445	393	263	141	63	25	9	3	1	0	1928
7-8	0	0	0	0	0	0	5	36	111	192	209	159	90	40	15	5	1	0	0	863
8-9	0	0	0	0	0	0	0	5	25	64	93	85	54	25	9	3	1	0	0	363
9-10	0	0	0	0	0	0	0	0	4	16	33	39	29	15	6	2	0	0	0	145
10-11	0	0	0	0	0	0	0	0	0	3	9	15	14	8	3	1	0	0	0	55
11-12	0	0	0	0	0	0	0	0	0	0	2	5	6	4	2	1	0	0	0	20
12-13	0	0	0	0	0	0	0	0	0	0	0	1	2	2	1	0	0	0	0	7
13-14	0	0	0	0	0	0	0	0	0	0	0	0	1	1	0	0	0	0	0	2
14-15	0	0	0	0	0	0	0	0	0	0	0	0	0	0	0	0	0	0	0	1
SUM	25	329	1667	4712	8993	12991	15255	15222	13262	10243	7075	4403	2495	1312	657	322	158	78	81	99280

Table 6.3: Joint frequency table retrieved from (Eik & Nygaard, 2003)

In collaboration with the supervisor, the chosen T_p corresponding to H_s should be a short and a long T_p. Based on table 6.3 the T_p was chosen so it would have at least 100 occurrences over 43 years. The chosen values for the sea state can be seen in table 6.4. When using these values in the JONSWAP spectrum, the γ parameter was set to 3 for the simple model and 3.3 for the advanced model.

H_s	T_p
1	4 and 12
2	4 and 16
3	5 and 16
4	7 and 15
5	7 and 15

Table 6.4: Chosen $T_p|H_s$

Chapter 7

Simple Model Analyses

7.1 Sensitivity Studies

7.1.1 Time Interval

The time interval used in the studies was established at an early stage to ensure correct results. In the verification of the model, the time interval from (Matland, 2014) $dt = 0.01\ s$ was used, as the module was lowered in flat sea or hanging still. However when ship motion and waves were introduced, a new study was necessary.

The module was hanging still in the water surface and the sea state parameters were $H_s = 4\ m$, $T_p = 8\ s$ and $\gamma = 3$. The spool wave function was used to ensure a large wave was hitting the module. Based on figures 7.1a and 7.1b, the new time interval was 0.009 or less.

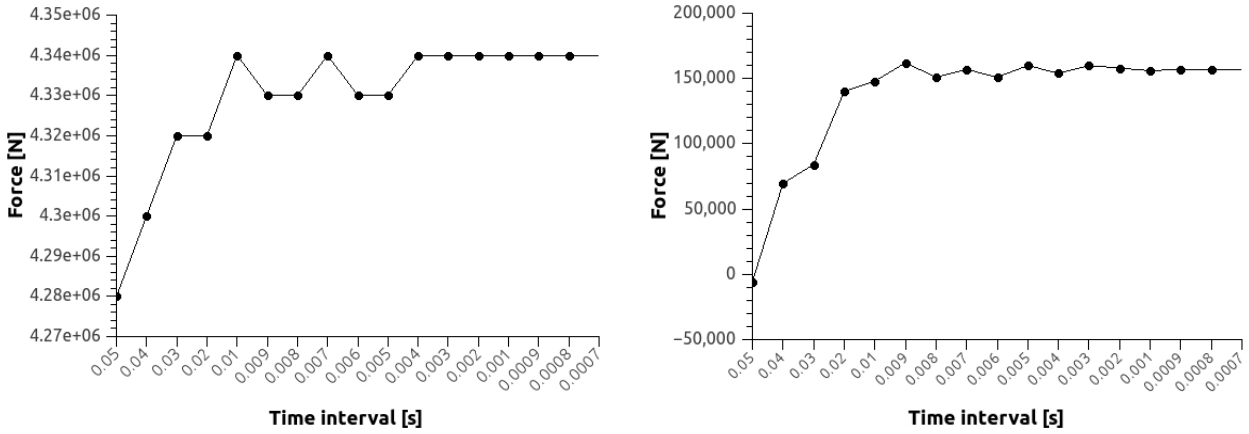

(a) Maximum force in wire

(b) Minimum force in wire

Figure 7.1: Time interval studies for simple model

7.1.2 Effect of Wire Damping

The damping coefficient for the damping element was not found in any literature. There is, however, damping in the wire due to the fibers. However, the magnitude was not known. Therefore, a study of the effect the wire damping had on the force in the element was conducted. This was done by lowering the module with the spool wave function and various sea states with different values for the damping coefficient, see table 7.1.

With a damping value of 10^5, the damping gave a contribution to the resulting wire force. Therefore, this value was used in the simple model simulations.

Table 7.1: Maximum and minimum forces in wire when subjected to different wire damping

Damping value [N/s]	Maximum force in wire [N]	Maximum force in wire [N]
$Hs = 1\ m, Tp = 3\ s$		
1	2.71E+6	1.92E+6
10	2.71E+6	1.92E+6
100	2.71E+6	1.92E+6
1000	2.71E+6	1.92E+6
10000	2.70E+6	1.94E+6
100000	2.62E+6	2.03E+6
1000000	2.63E+6	2.13E+6
$Hs = 2\ m, Tp = 4\ s$		
1	3.06E+6	1.78E+6
10	3.06E+6	1.78E+6
100	3.06E+6	1.78E+6
1000	3.06E+6	1.78E+6
10000	3.06E+6	1.80E+6
100000	2.95E+6	1.95E+6
1000000	2.81E+6	2.04E+6
$Hs = 4\ m, Tp = 8\ s$		
1	4.64E+6	-2.54E+3
10	4.64E+6	-2.52E+3
100	4.64E+6	-2.30E+3
1000	4.64E+6	-4.04E+2
10000	4.60E+6	-3.03E+3
100000	4.34E+6	1.60E+5
1000000	3.92E+6	1.07E+6
$Hs = 10\ m, Tp = 12$ s		
1	1.31E+7	-6.55E+4
10	1.38E+7	-5.59E+4
100	1.67E+7	-6.91E+4
1000	1.39E+7	-8.39E+4
10000	1.11E+7	-1.38E+5
100000	1.07E+7	-6.80E+5
1000000	1.26E+7	-5.20E+6

7.1.3 Time Before and After Peak when Using the Spool Wave Function

A study was first conducted to determine the minimum duration required to develop the largest wave when using the spool wave function. It was found that 70 s were needed to obtain the correct value for the largest wave.

The study was taken further to find how much motion had to be induced to the system before the peak wave hit the module. The study was conducted with the module hanging in the water surface. The parameters in the JONSWAP spectrum were set to $H_s = 1\ m$, $T_p = 2\ s$ and $\gamma = 3$, and the simulation was set to run for 500 s in total.

The simple model needed to run for 250 s before reaching peak wave. See figures 7.9. The times when the maximum/minimum forces occur were the same for all the analyses, see table 7.2. However, the maximum/minimum forces did not occur at the peak wave. This raised the question of the validity of using the spool wave function for still-hanging structures. See subsection 7.1.4 for further discussion.

Table 7.2: Results of length of spool wave function

Time before [s]	$Force_{max}$ [N]	Time [s]	$Force_{min}$ [N]	Time [s]
100	2770631.4	176.936	1902063	177.456
150	3494753	243.704	1223758	244.2
200	3510556	293.704	1215634	294.192
250	3514123	343.704	1212458	344.192
300	3512376.4	393.704	1214758	394.192
350	3510716.2	443.704	1212854.4	444.192
400	3511037	493.704	1213645	494.192

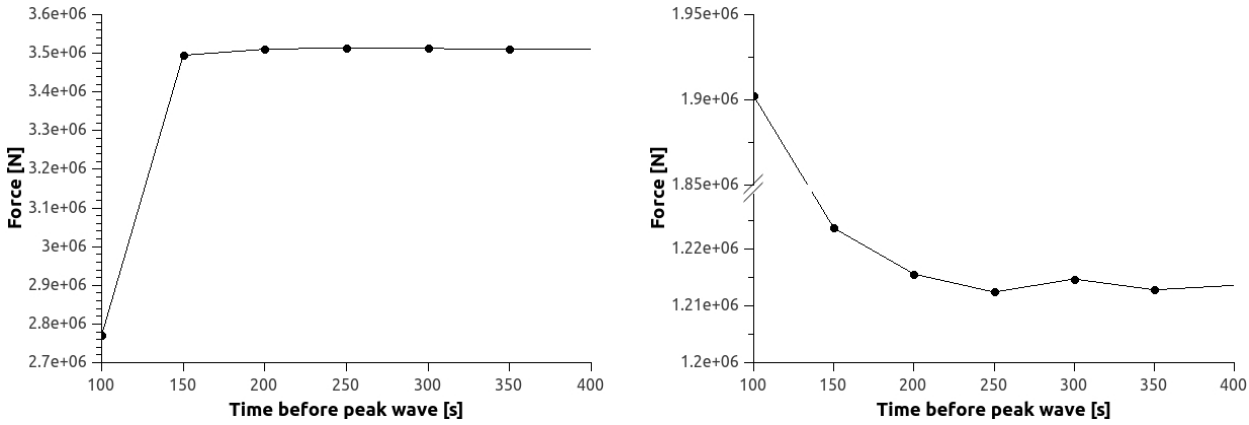

(a) Maximum force in wire (b) Minimum force in wire

Figure 7.2: Time to start before peak wave with moving ship

7.1.4 Maximum/Minimum Forces in a 3-Hour Sea State

The objective of the study was to confirm if the spool wave function gave lower or equal minimum forces compared to the full 3-hour simulation. If so, the spool wave was more conservative and would be considered used further. The results are shown in table 7.3

To compare the use of the spool wave function instead of a full 3-hour sea state, the module was set to be lowered. The simple model was placed so that half of the module was submerged.The idea was that this would be the worst place for the module to hang. If the module were to have descending motion, there would have had to be done a lot of simulations where the module started to be lowered at different times in a 3-hour sea state. This was considered to be too time consuming.

By running eight full 3-hour sea state and eight "spool wave" simulation over the 5 largest waves in the spectrum, a comparison between the maximum/minimum forces in the wire could be made. This showed the whether running the spool wave function was a valid method to determine the maximum/minimum force in a 3-hour sea state.

The same sea state parameters were chosen for both the full 3-hour and spool wave simulations. The chosen sea state was $H_s = 1\ m$, $T_p = 2\ s$ and $\gamma = 3$, with eight different seed numbers.

Table 7.3: Maximum and minimum forces in wire in 3 hour sea state and the spool wave

Seed nr	Full 3 hour		Spool				Diff	
	max [N]	min[N]	max[N]	Order[N]	min[N]	Order[N]	max[N]	min[N]
10	3.54×10^6	1.24×10^6	3.4×10^6	2	1.32×10^6	2	2.13%	6.866%
20	3.59×10^6	1.10×10^6	3.59×10^6	3	1.11×10^6	3	0.02%	0.22%
30	3.55×10^6	1.25×10^6	3.33×10^6	3	1.41×10^6	4	6.21%	12.75%
40	3.56×10^6	1.23×10^6	3.38×10^6	4	1.29×10^6	4	5.03%	4.91%
50	3.58×10^6	1.25×10^6	3.41×10^6	1	1.35×10^6	4	4.66%	8.03%
60	3.49×10^6	1.26×10^6	3.46×10^6	2	1.28×10^6	4	0.84%	1.85%
70	3.53×10^6	1.27×10^6	3.32×10^6	2	1.27×10^6	4	5.91%	0.23%
80	3.47×10^6	1.20×10^6	3.42×10^6	2	1.32×10^6	2	1.47%	10.01%

Sometimes the spool wave function gave valid results, but the error depended on the sea state. It was also observed that the maximum and minimum forces only occur twice within 200 seconds, meaning that running only one of the peak waves would not capture both the maximum and minimum in the wire.

Further, the same analyses were run with different lowering times to investigate whether the time of the module hitting the surface relative to the peak would produce more conservative results.

7.1.5 When to lower the module when using spool wave function

The parameters in the JONSWAP spectrum were set to $H_s = 1$, $T_p = 2$ and $\gamma = 3$. The module was lowered with a constant velocity of 0.5 $[m/s]$.

Table 7.4: A selection of lowering start times with moving ship

Start lowering time [s]	$Force_{max}$ [N]	Time [s]	$Force_{min}$ [N]	Time [s]
100	2786231	107.1	1307166	281.4
200	3021765	220.4	1307637	281.4
225	3062622	247.8	1132882	251.7
250	3103507	253.4	1285533	282.6

The lowest minimum force was of interest, as the slack condition was considered to be the limiting factor in choosing a sea state in which the operation could be done. When 225 s was used as the lowering start point, the maximum and minimum force occurred right before and after the peak wave, see table 7.4, figures 7.3b and 7.9b.

Table 7.5: Comparing the spool wave to full 3-hour analyses

Seed nr	Full 3 hour	Spool	
	min[N]	min[N]	Order[N]
10	1.24×10^6	1.132×10^6	1
20	1.10×10^6	1.268×10^6	1
30	1.25×10^6	1.293×10^6	1
40	1.23×10^6	1.173×10^6	1
50	1.25×10^6	1.264×10^6	1
60	1.26×10^6	1.185×10^6	1
70	1.27×10^6	1.081×10^6	1
80	1.20×10^6	1.132×10^6	1

The minimum force in the wire in the conservative case occurred at 251.7 s, which is 1.7 s after the spool wave hits the module. Knowing this, the simulations could be shortened down to 260 s to save computational time. The same start time is also found for simulations without ship motion.

Again, the lowest force in the wire was considered to be the most concerning force, so the 225 s option was taken as the conservative case. Comparing the results with the full 3-hour analysis to the results from running the spool wave function with order 1 showed that the minimum force could not always be obtained by running the spool wave function. This can be seen in table 7.5. However, the error produced by using the spool wave function is small, and is still considered valid throughout this thesis.

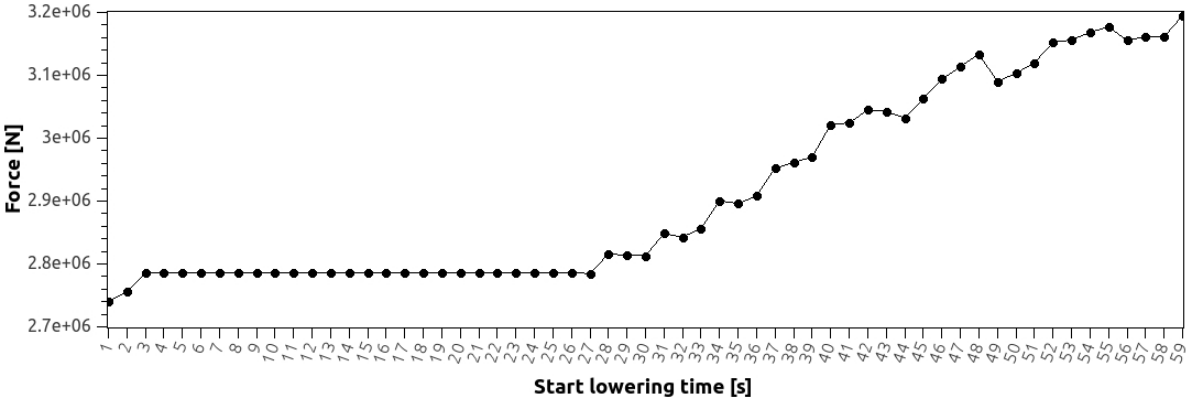

(a) Maximum force in wire

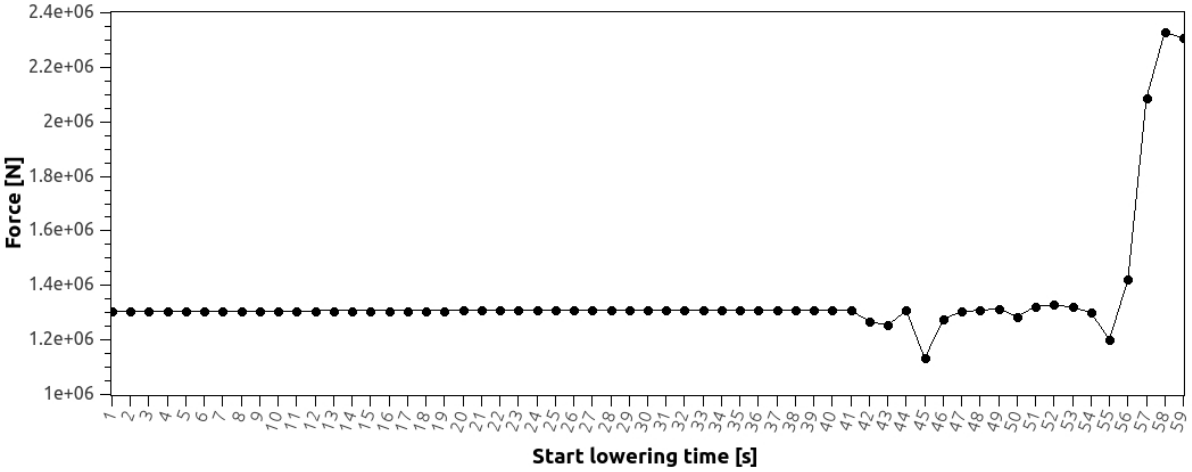

(b) Minimum force in wire

Figure 7.3: Time to start lowering with moving ship

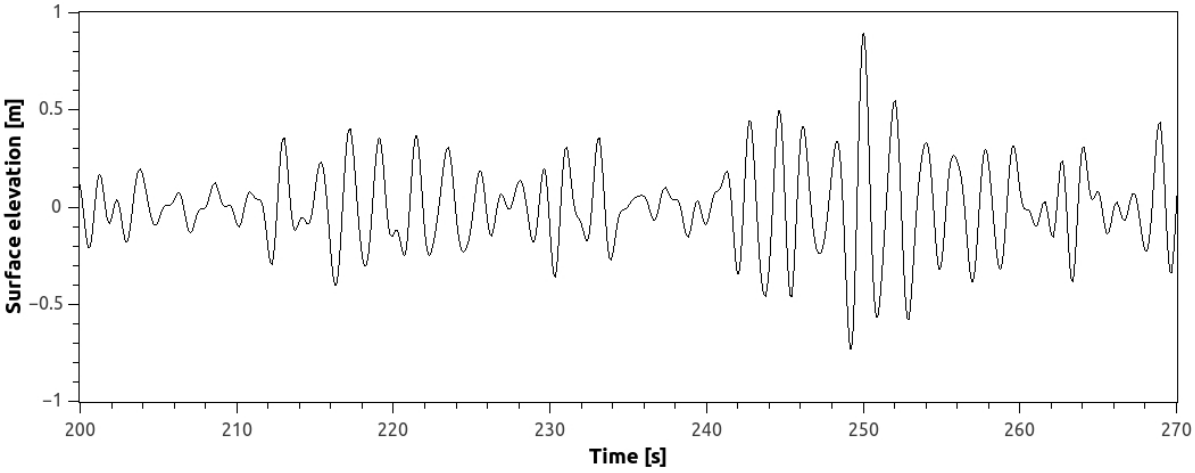

(a) Surface elevation

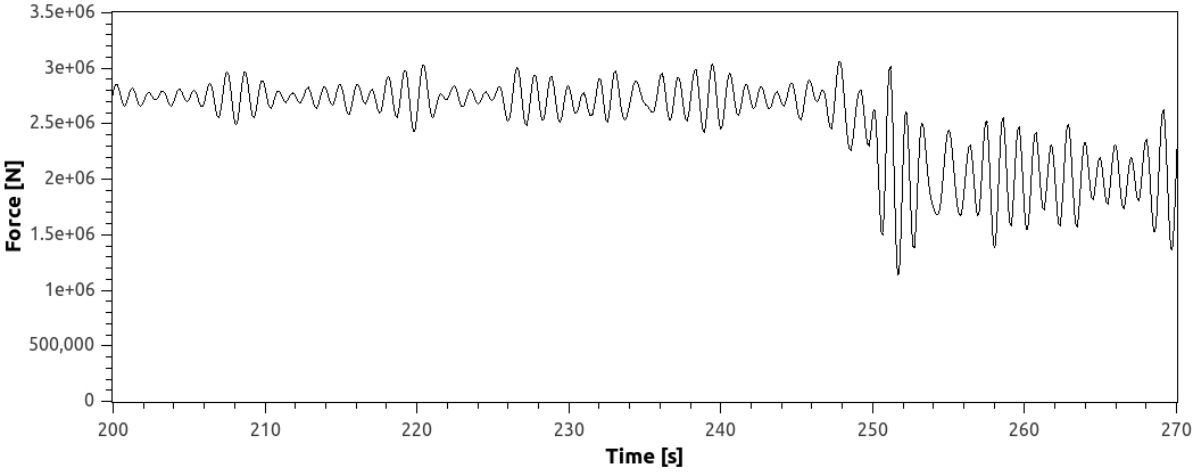

(b) Force in wire

Figure 7.4: Surface elevation with corresponding force in wire

7.2 Verification of Simple Model

Some verifications of USFOS' capabillity to simulate marine operations were performed. This was done by simulating the simple model in different situations and comparing the results with hand calculations. How the forces act in the wire and how it was used to read the results its shown in 7.5. The results were obtained with the lowering displacement of the module to be an S-curve or with constant lowering speed. The soft start application was discovered at a later point see section 6.3.1. By using the S-curve for lowering displacement, the module lowering velocity was constantly changing, see figure 7.6. Using constant lowering speed created unwanted responses in the beginning, see figure 7.7b. The small decreasing force in the "in air" condition shown in figure 7.5 appears because of the change in velocity. The same for is the case for the "fully submerged" condition.

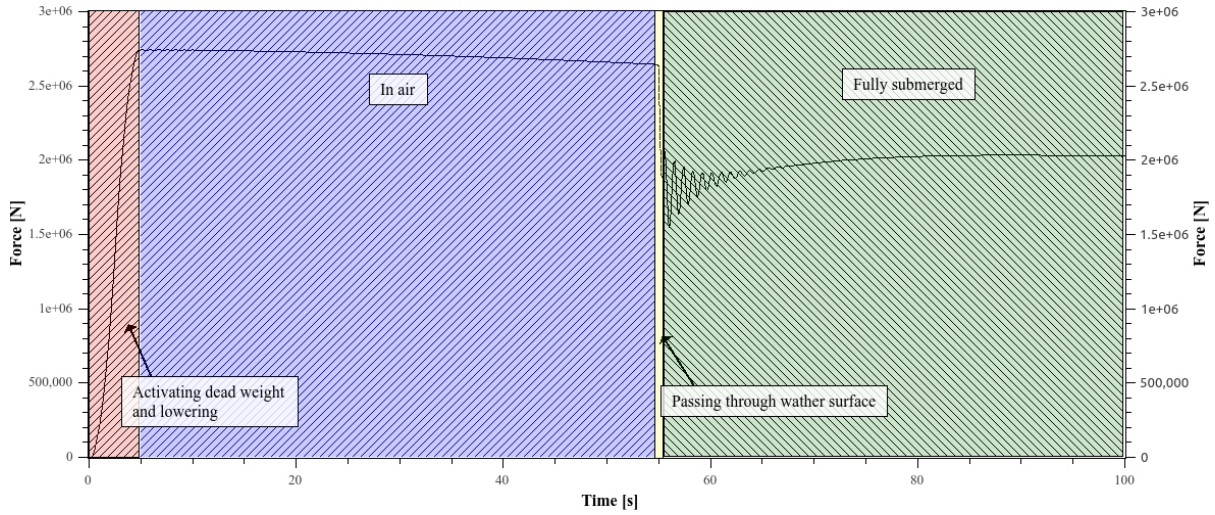

Figure 7.5: Force in monitor element

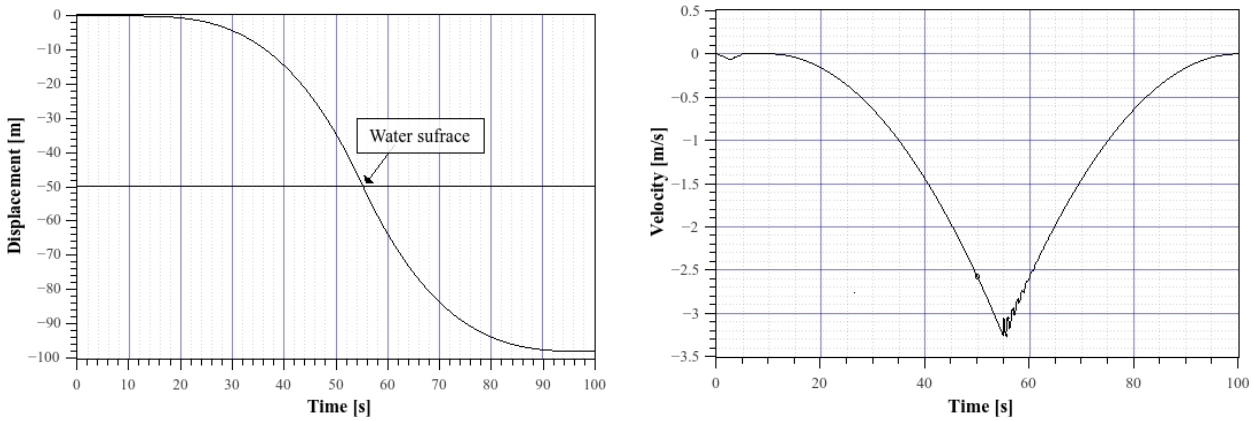

(a) Displacement of module (b) Velocity of module

Figure 7.6: Displacement and velocity of module lowered in verification simulations

7.2.1 Weight

The weight in air was found by reading the force from the "in air" condition seen in figure 7.5, or by running the simulation with the module hanging still in the air. The submerged weight was found by hanging the module in water with no lowering velocity, or by doing the simulation without drag, see figure 7.7a. The calculated hydrodynamic forces were limited to the pipe only. The rest of the model was set to having no hydrodynamic properties.

The weight in air has an error of 0 when hanging still. When it's lowered with different velocities, the error was between 0 and 0.63%. When the module was hanging still submerged, the error was as small as 0.03%. There was a larger error when the module was lowered, however this was also very low. The error was in the range of $0.31 - 0.82\%$.

Table 7.6: Weight in air and water, with module hanging still

Force in single wire	USFOS	Hand calculations
In air [N]	2.74×10^6	2.74×10^6
In water [N]	2.03×10^6	2.03×10^6

7.2.2 Drag

In drag simulation the velocity was set to be constant. As mentioned, this created large responses at the beginning of the simulation. However, the last part of the simulation,

[90-100] s, could be used, see figure 7.7a.

The module was fully submerged from the start of the simulation, and the drag forces were taken as the difference between results of simulations with and without drag contributions. This was done by setting $C_d = 0$ and $C_m = 0$ in the simulations. USFOS was then only calculating the buoyancy force acting on the module. Next C_d and C_m was set to 1 and 2 respectively. In principle, the module was passing through water with constant lowering velocity, and therefore the Morrison 3.15 equation could be applied to calculate the forces acting on the module.

The simulations were done with different lowering velocities, as a difference was discovered a in USFOS' results compared to hand calculations. As the lowering velocities increased, so did the difference between the theoretical and experimental results, see table 7.7.

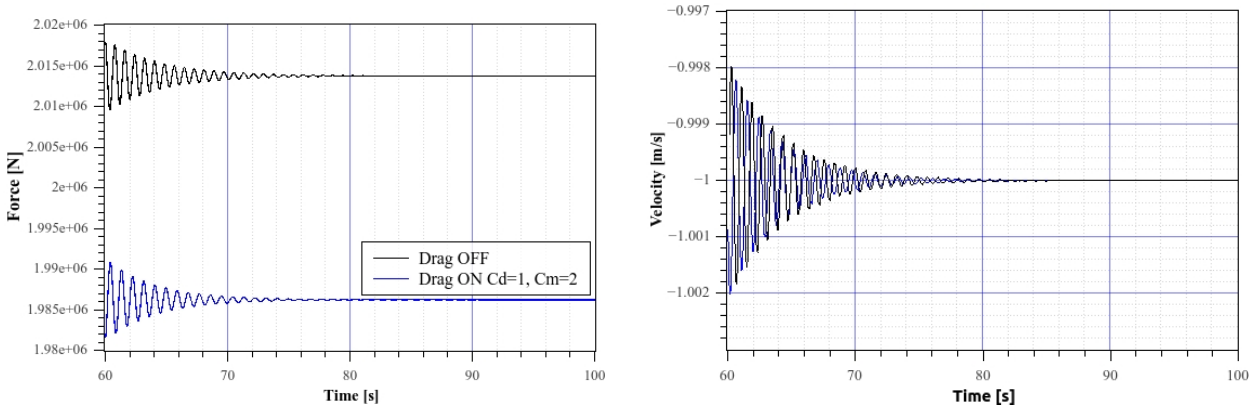

(a) Force in end of simulation

(b) Velocity in simulation

Figure 7.7: Force and velocity of module lowered in drag simulations

Table 7.7: Results from drag simulations

Theory velocity [m/s]	Theory Drag [N]	Experimental Drag [N]	Difference [N]	Error %
0.20	1.85E+03	1.82E+03	3.00E+01	1.63
0.25	2.88E+03	2.56E+03	3.26E+02	11.30
0.31	4.50E+03	3.65E+03	8.58E+02	19.05
0.45	9.53E+03	6.81E+03	2.72E+03	28.57
0.63	1.80E+04	1.18E+04	6.20E+03	34.43
1.00	4.61E+04	2.75E+04	1.86E+04	40.29

As the largest difference was only 0.9% of the weight in water, the error was considered to be insignificant.

7.2.3 Slamming

The slamming effect was difficult to determine. There was a slamming effect, but the magnitude was inconclusive. This was because of the way the forces were detected in the model. The forces detected in the monitor element were force responses, and not the direct force from the sea on the module. This can be seen in figure 7.8b. The impact of slamming on the wires' minimum force was very small compared to simulations without slamming. The simulations were run with a constant lowering velocity of 1 m/s.

Based on the slamming force described in 3.2.1, the total force and the slamming force alone are presented in figure 7.8a

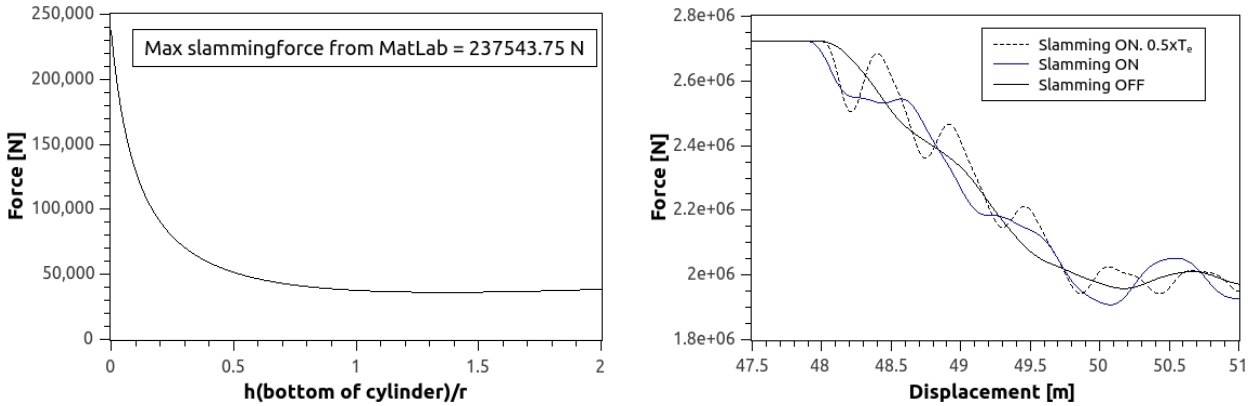

(a) Slamming calculated in MATLAB (b) Slamming from USFOS

Figure 7.8: Calculated slamming and slamming from USFOS

A different simulation was done to confirm USFOS' capability to calculate the slamming force by changing the eigenperiod of the model. This way the oscillations observed when the module was passing through the water surface should change. This was done by changing the spring stiffnesses k_{wire1}, k_{wire2} in the model and reducing the eigenperiod T_e with 50%, see figure 7.8b.

The eigenperiod for the module is:

$$0.5 \times T_e = 2\pi\sqrt{\frac{(k_{wire1} + k_{wire2})}{m}} \tag{7.1}$$

$$T_e = 2\pi\sqrt{\frac{4 \times (k_{wire1} + k_{wire2})}{m}} \tag{7.2}$$

7.2.4 Regular Sea

A series of simulations with regular sea were performed to check which regular sea state limits the operations by inducing slack. This was checked by seeing if the minimum force was zero or negative for the respective case. The parameters were varied between a short and a long period to increasing H_s. A T_p corresponding to H_s was chosen by consulting table 6.3 in the same way as done in section 6.5. The ship was assumed to have motions.

All the analyses done for regular waves did not lead to the forces reaching their limit in e.g. slack, not even by setting $H_s = 11\ m$ and $Tp = 10\ s$. It was therefore concluded that Airy waves were not good to use for simulating regular waves in marine operations.

Table 7.8: Minimum forces in wire in regular waves

Sea parameters	Minimum force in wire
$H_s = 1\ m, T_p = 4\ s$	1.931×10^6
$H_s = 1\ m, T_p = 12\ s$	1.945×10^6
$H_s = 2\ m, T_p = 4\ s$	1.936×10^6
$H_s = 2\ m, T_p = 16\ s$	1.846×10^6
$H_s = 3\ m, T_p = 5\ s$	1.895×10^6
$H_s = 3\ m, T_p = 16\ s$	1.577×10^6
$H_s = 4\ m, T_p = 7\ s$	1.849×10^6
$H_s = 4\ m, T_p = 15\ s$	1.287×10^6
$H_s = 5\ m, T_p = 8\ s$	1.810×10^6
$H_s = 5\ m, T_p = 15\ s$	9.941×10^6
$H_s = 6\ m, T_p = 10\ s$	1.179×10^6
$H_s = 7\ m, T_p = 10\ s$	1.051×10^6
$H_s = 7\ m, T_p = 13\ s$	1.587×10^6

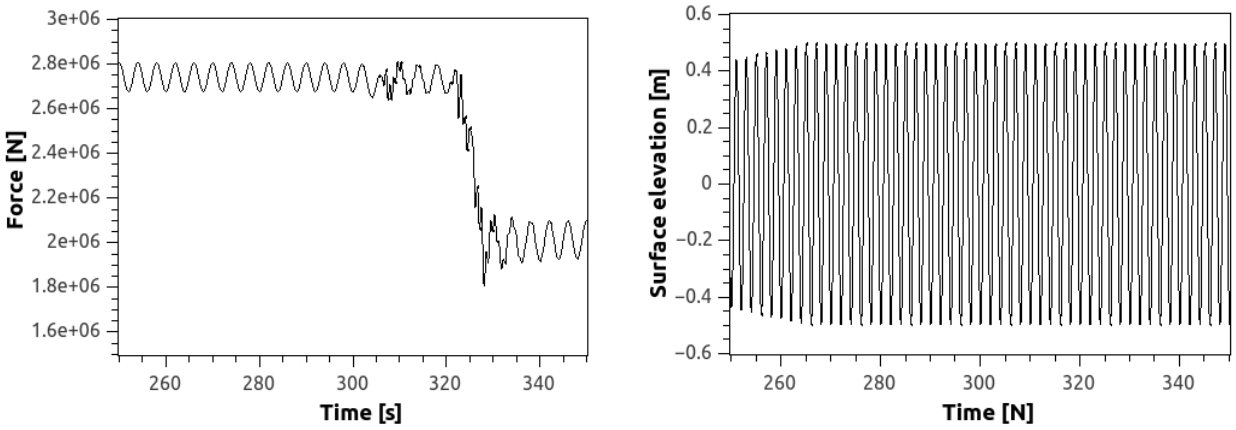

(a) Force in wire

(b) Force in wire

Figure 7.9: Surface elevation with corresponding force in wire

7.3 Limiting Sea State

Based on the results from section 7.1.4 and 7.1.5, the model was run with the spool wave function over the largest wave in the sea state with 30 different seeds. The resulting wire forces in the two cases, the ship with and without motion, were compared after simulating with the chosen sea states from section 6.5.

The limit of the wire force was considered to be $F_{wire\ limit} = 2030424\ N \times 0.1 = 203042\ N = 2.03 \times 10^5\ N$, which is 10% of the submerged weight of the module. 10% of submerged weight as a limit was found in (DNV, 2011b). The minimum/maximum value of the minimum force in the wire is presented in table 7.9. See appendix A.1 for all the results plotted in probability papers.

Table 7.9: The highest and lowest minimum force in the wire

Analysis	F_{min}^{hig} [N]	F_{min}^{low} [N]	Under limit
With ship motion			
$H_s = 1$, $T_P = 4$	1820941	1639810	No
$H_s = 1$, $T_P = 12$	1456244	681137	No
$H_s = 2$, $T_P = 4$	1617378	1350683	No
$H_s = 2$, $T_P = 16$	322864	-124948	Maybe
$H_s = 3$, $T_P = 5$	1470335	1057236	No
$H_s = 3$, $T_P = 16$	-157232	-230108	Yes
$H_s = 4$, $T_P = 7$	768214	-87205	Maybe
$H_s = 4$, $T_P = 15$	-186355	-295966	Yes
Without ship motion			
$H_s = 1$, $T_P = 4$	1954674	1814386	No
$H_s = 1$, $T_P = 12$	1940349	1890457	No
$H_s = 2$, $T_P = 4$	1889466	1477637	No
$H_s = 2$, $T_P = 16$	1957356	1798022	No
$H_s = 3$, $T_P = 5$	1900272	1462947	No
$H_s = 3$, $T_P = 16$	1951508	1522992	No
$H_s = 4$, $T_P = 7$	1890500	1428143	No
$H_s = 4$, $T_P = 15$	1901006	1155525	No

There were two sea states in which the results could be over the limit. See figure 7.10 and 7.11. For sea state $H_s = 2\ m$, $T_P = 16\ s$ one value was over the limit, while the rest were negative. The conclusion is that this sea state creates too low forces in the wire. The other sea state, $H_s = 4\ m$, $T_P = 7\ s$, was more interesting. Most of the results were under the limit, see the probability paper in figure 7.11a. Only 9 out of 30 simulations gave results above the limit. Since there were negative values from the simulation, the minimum probability is indeterminable. 4 out of 30 results were inside the 95% confidence interval. The same was observed for every analysis that had negative values.

By removing the minimum values under 10^3 N, the probability of exceeding the limit became readable, see figure 7.14. 14 remaining values was not enough to give a good estimation of the minimum force in the wire.

Reasons for the bad probability papers when there are values under 10^3 N could be that USFOS has a numerical difficulty handling low or negative values for this case. It could also be that the lowest values have a different probability distribution than the rest of the results,

which seemed to be the case for simulations where $H_s = 2\ m$, $T_P = 16\ s$.

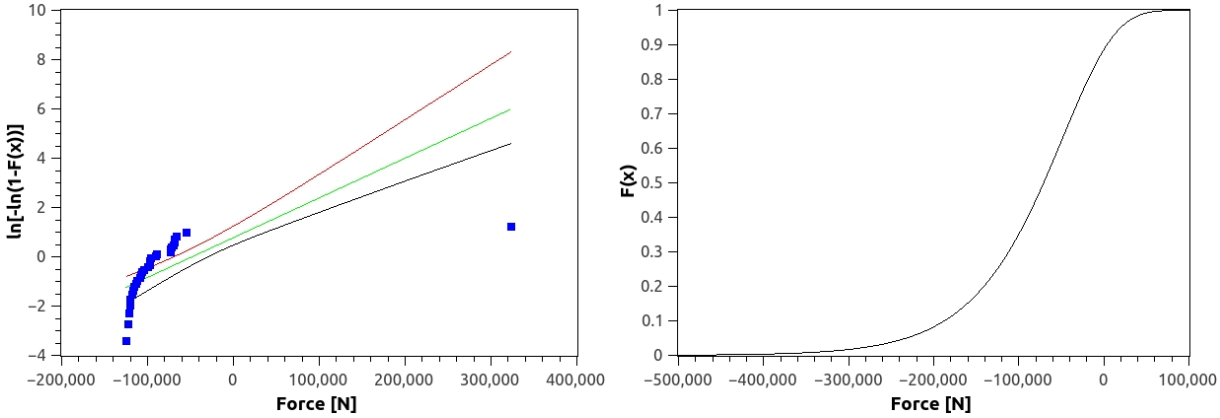

(a) Probability paper (b) S-curve

Figure 7.10: Results for sea state $H_s = 2$, $T_p = 16$ with ship motion

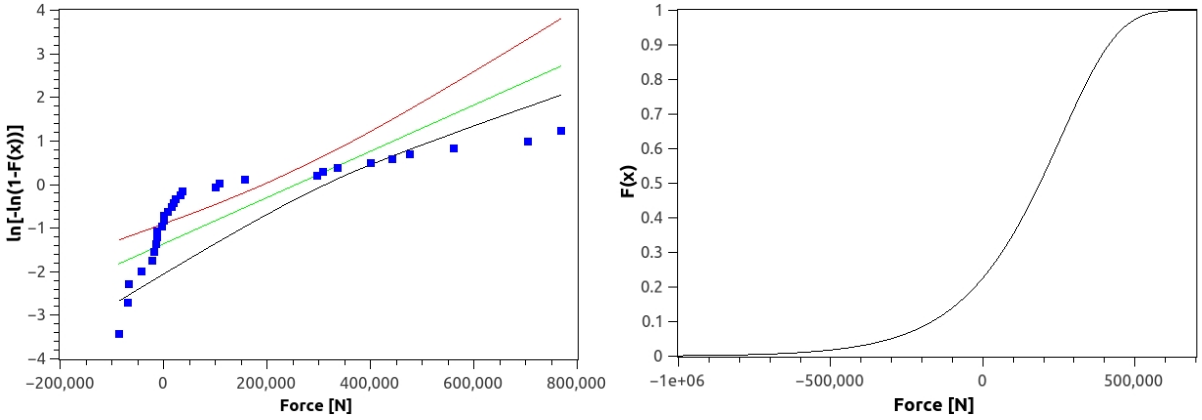

(a) Probability paper (b) S-curve

Figure 7.11: Results for sea state $H_s = 4$, $T_p = 7$ with ship motion

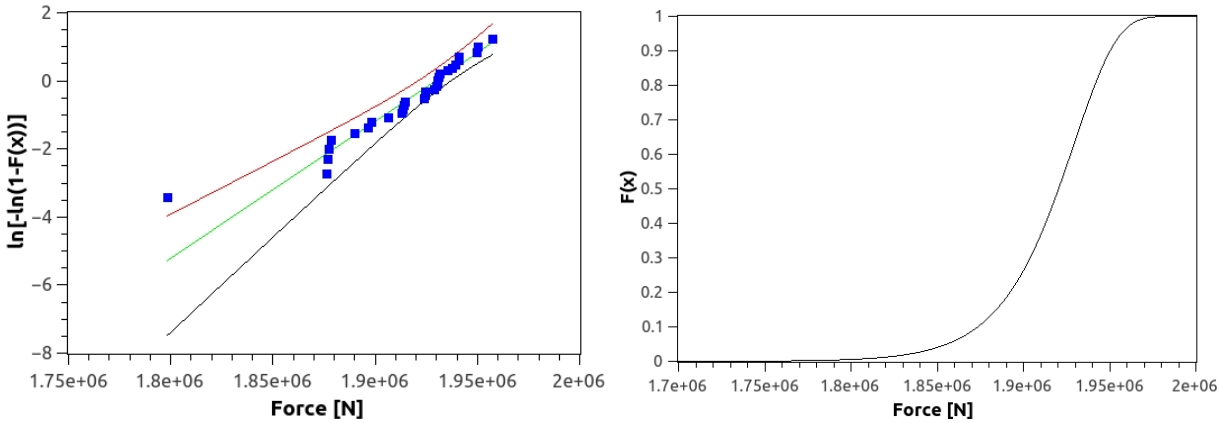

(a) Probability paper (b) S-curve

Figure 7.12: Results for sea state $H_s = 2$, $T_p = 16$ without ship motion

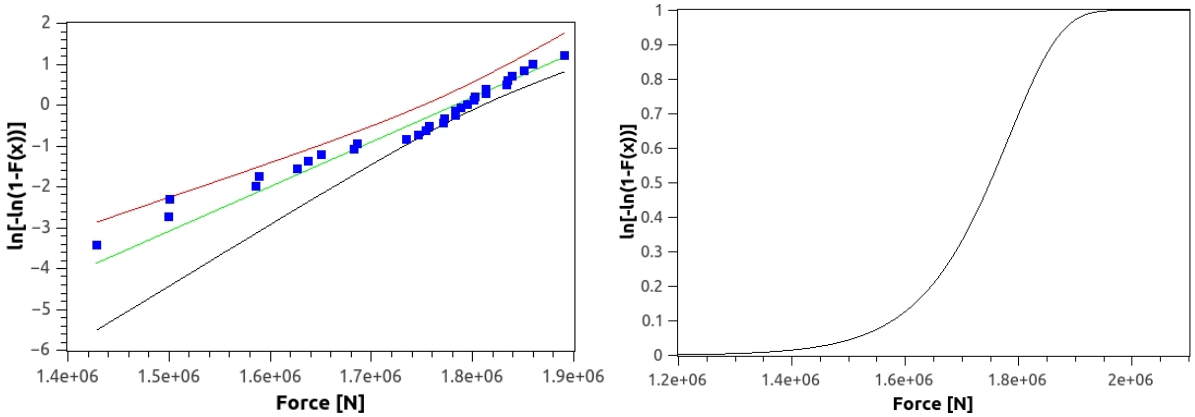

(a) Probability paper (b) S-curve

Figure 7.13: Results for sea state $H_s = 4$, $T_p = 7$ without ship motion

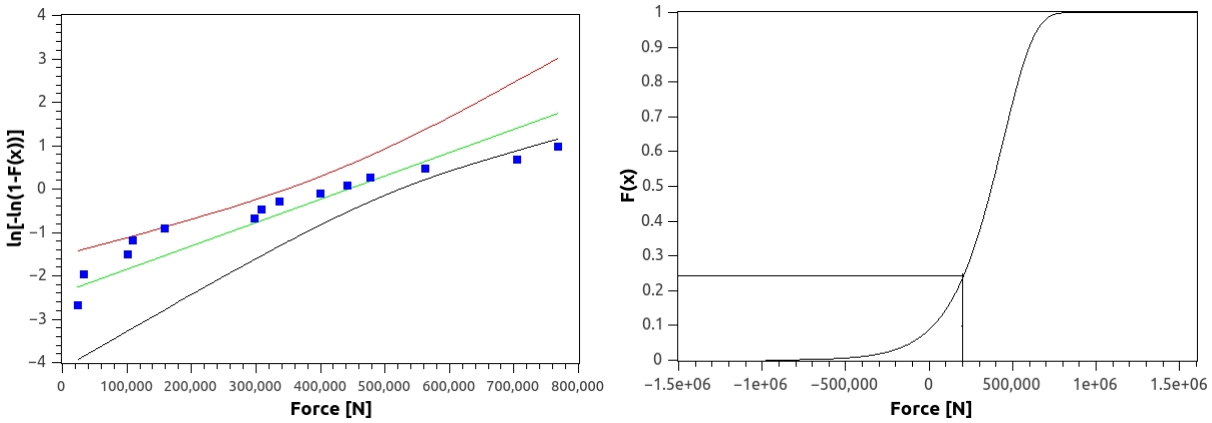

(a) Probability paper (b) S-curve

Figure 7.14: Results for sea state $H_s = 4$, $T_p = 7$ with ship motion and results above 10^3

With and Without Ship Motion

Comparing the minimum force in the wire with and without ship motions showed the highest factor of difference was 3261.371 and the lowest was 0.002. The sea states that gave values under the limit or negative values produced the largest factor of difference. The other sea states produced an average difference of less than 1. However, as the factor of difference between with and without ship motion in the same sea state is so large, there is no clear correlation between the results in these two cases. See table 7.10

Table 7.10: Factors of difference with and without ship motion in same sea state

Analysis	Lowest factor	Average factor	Highest factor
$H_s = 1$, $T_P = 4$	0.033	0.074	0.131
$H_s = 1$, $T_P = 12$	0.327	0.682	1.824
$H_s = 2$, $T_P = 4$	0.002	0.151	0.259
$H_s = 2$, $T_P = 16$	-35.939	-20.733	5.006
$H_s = 3$, $T_P = 5$	0.130	0.367	0.656
$H_s = 3$, $T_P = 16$	-13.115	-10.449	-8.592
$H_s = 4$, $T_P = 7$	-426.355	186.805	3261.371
$H_s = 4$, $T_P = 15$	-10.266	-7.505	-5.811

Chapter 8

Advanced model

Before starting with the limit studies of the advanced model, a series of sensitivity analyses had to be done. As for the simple model, when the model had more elements the analyses started to take longer time. Therefore, choosing a good time interval and proper length of the spool wave function could reduce the computation time significantly. The advanced model was also larger and higher, so the time when it hit the wave surface had to be re-examined.

By hanging the module still over and under water, the forces in the wire and slings were found. See figure 8.1 and table 8.1.

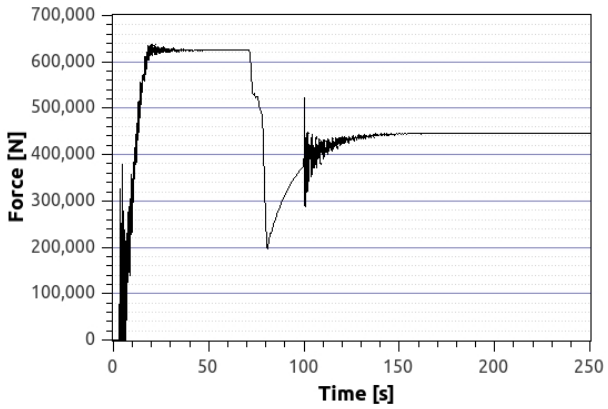

Figure 8.1: Force in wire

Table 8.1: Initial weights and forces

	F_{air} [N]	$F_{submerged}$ [N]
Wire	6.225×10^5	4.4704^5
Slings		
600	2.8882×10^5	2.3217×10^5
601	1.0444×10^5	5.4387×10^4
602	1.0828×10^5	5.7147×10^4
603	2.8764×10^5	2.3073×10^5

8.1 Sensitivity Studies

8.1.1 Time Interval

The original simulations done in (Matland, 2014) used a time interval of 0.05 s. Based on the results in table 8.2, a time interval of 0.08 s seemed sufficient. However, when using the spool wave function and lowering the model in the worst case, some of the simulations crashed. So an interval of 0.01 was chosen until the module was lowered, and then the time interval was set to 0.005 s.

Table 8.2: Time interval study. Advance model

Time interval [s]	F_{max}^{wire} [N]	F_{min}^{wire} [N]
0.01	647763.7	163076.03
0.008	648622	163133.5
0.005	649007.93	162937.01
0.003	649211.1	162997.93

8.1.2 Time Before and After Peak when Using the Spool Wave Function

First, the same analyses as for the simple model were run. This was done to determine how long before the peak wave the simulation needed begin to capture the lowest force in the wire. This was necessary because of the different dynamics of the system. However, the same time before peak, 250 s, was used. When checking for the worst place to lower the module over a peak wave, the time of the minimum force occurred close to the peak. Hence the end time

of the simulation was set to 260 s.

8.1.3 When to Lower the Module when Using the Spool Wave Function

Since the module had a different geometry and the wire length was different, a new study had to be done. A sea state with $H_s = 2$ and $T_p = 4$ was chosen.

The module now had to start being lowered at 175 s, see figure 8.2

It was discovered that having the module hit the waves 15 s before the peak and being fully submerged 5 s before the peak wave gave the lowest force in the wire. This is illustrated in figure 8.3

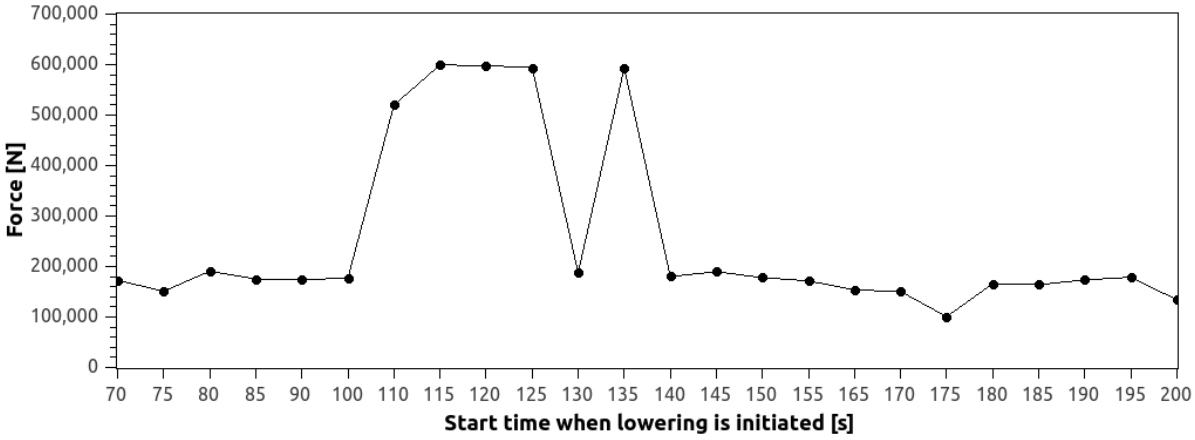

Figure 8.2: Minimum force in wire with different start time

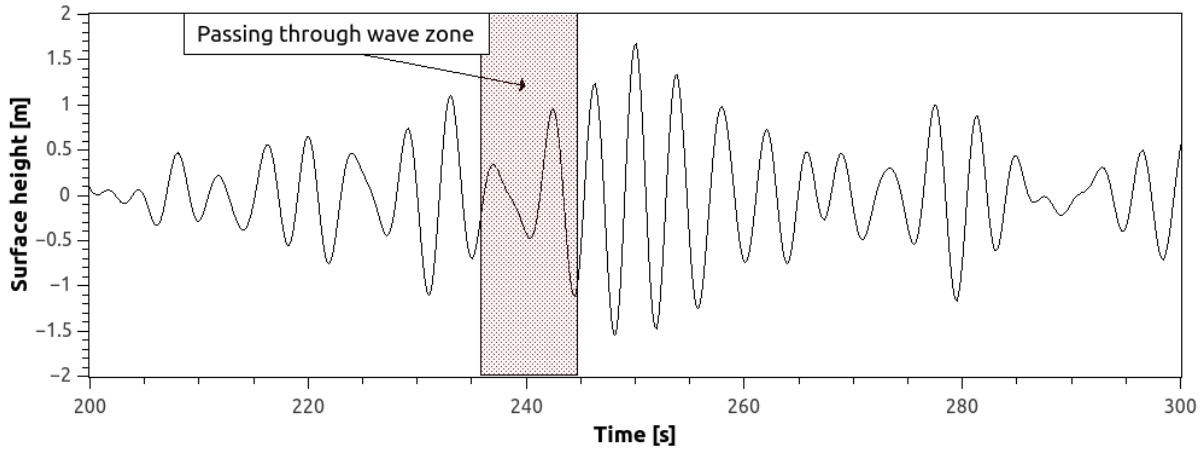

(a) Surface elevation

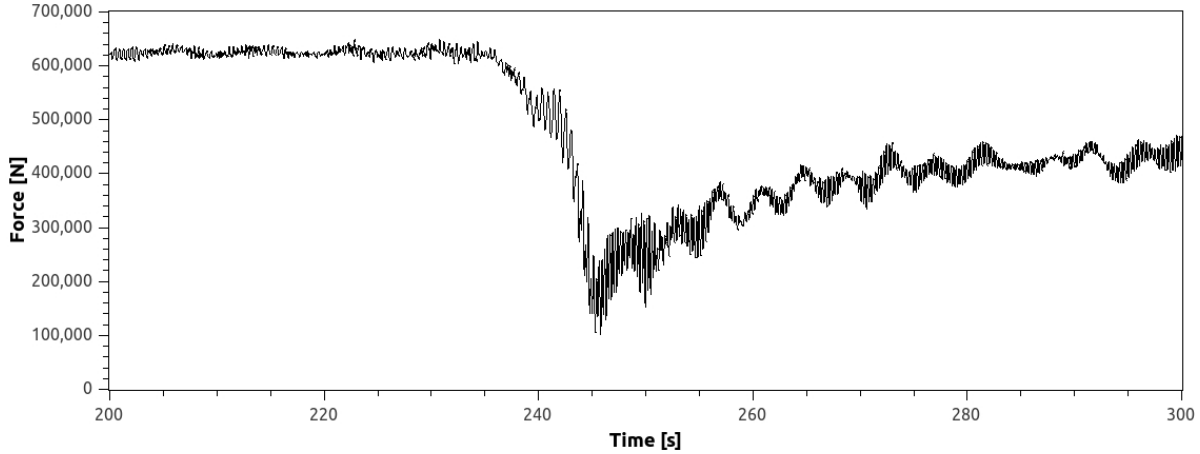

(b) Force in wire

Figure 8.3: Surface elevation with corresponding force in wire

8.2 Limiting Sea State

From the maximum and minimum of the minimum forces in the wire or the slings in the different sea states, a preliminary evaluation could be done. In table 8.4, the result from each sea state and forces in the wire and slings are classified as “yes”, “no” or “possibly”. The sea states denoted “yes” indicates that none of the 30 different seeds in a sea state produced a force exceeding the limit force. For sea states denoted “no”, the opposite was the case: All of the 30 different seeds in the sea state produced a force exceeding the limit force. The sea states containing the limiting forces were classified as “possibly”. These were then checked and verified by checking the probability paper for the given sea state and the S-curve to see if the minimum force could occur.

Based on $F_{submerged}$ from table 8.1, the limiting forces became $F_{submerged} \times 0.1$:

Table 8.3: Limit forces for Advanced module

	F_{lim} [N]
Wire	4.4704[4]
Slings	
600	2.3217×10^4
601	5.4387×10^3
602	5.7147×10^3
603	2.3073×10^4

Table 8.4: Results from preliminary exceedence check

		Slings			
Analyses	Wire	600	601	602	603
With ship motion					
$H_s = 1\ m, T_p = 4\ s$	No	No	No	No	No
$H_s = 1\ m, T_p = 12\ s$	No	Possibly	No	No	No
$H_s = 2\ m, T_p = 4\ s$	No	Possibly	No	No	Possibly
$H_s = 2\ m, T_p = 16\ s$	Possibly	Possibly	Possibly	Possibly	Possibly
$H_s = 3\ m, T_p = 5\ s$	Possibly	Possibly	No	No	Possibly
$H_s = 3\ m, T_p = 16\ s$	Possibly	Possibly	Possibly	Possibly	Possibly
$H_s = 4\ m, T_p = 7\ s$	Yes	Yes	Yes	Yes	Yes
$H_s = 4\ m, T_p = 15\ s$	Yes	Possibly	Possibly	Yes	Yes

All the sea states containing a wire or a sling that had the highest minimum force under the limit could be disregarded (indicated by "yes"). As was the case for the analyses containing $H_s = 4\ m$, the parameters $H_s = 1\ m, T_p = 4\ s$ produced forces over the limit in both the wire and the slings, so this was considered to be a safe sea state to conduct the operation (indicated by "no").

As for the other sea states, by checking the probability plots found in appendix B.1 describing the forces in the wire, all the sea states above $H_s = 3\ m, T_p = 16\ s$ could be disregarded. Hence too many of the results were under the limit.

After checking the forces in the slings for the remaining sea states, the sea states that needed to be further investigated were $H_s = 1\ m, T_p = 12\ s$, $H_s = 2\ m, T_p = 4\ s$, $H_s = 2\ m, T_p = 16\ s$ and $H_s = 3\ m, T_p = 5\ s$, see appendix B.3 for relevant S-curves. Equation 4.15 was used to calculate the probability of not exceeding the limit force.

Table 8.5: Probability of not exceeding limiting force in percent

Analyses	Wire	600	601	602	603
$H_s = 1\ m, T_p = 12\ s$	6.02	-	-	-	-
$H_s = 2\ m, T_p = 4\ s$	-	6.35	-	-	5.92
$H_s = 2\ m, T_p = 16\ s$	15.05	19.40	9.70	10.37	19.06
$H_s = 3\ m, T_p = 5\ s$	13.38	12.71	-	-	11.61

If the acceptable limiting probability is set to be 90% of exceeding the limiting value, the remaining sea state was $H_s = 2\ m, T_p = 4\ s$, see table 8.5. Hence the limiting sea state for this case was $H_s = 2\ m, T_p = 16\ s$.

Table 8.5 also shows that the wire and slings with corresponding element numbers 600 and 603, were the ones most prone to experience slack.

Chapter 9

Conclusion

The scope of this thesis was to assess the applicability of USFOS with respect to simulations of marine operations. One of the phases that is recognized as the most challenging when doing a marine operation was selected: lowering through the wave zone.

Two models were used in the process. A simple model consisting of a tubular member suspended by two springs, and an advanced model, representing a more realistic subsea module.

The wire elements had to be modeled as spring elements, as this was the only way to incorporate wire elongation in the simulations. There were some problems when the elongation was modelled as either an S-curve or a linear curve. There was either an uncontrollable lowering velocity or large forces in the beginning of the simulation, as the wire elongation was set to follow a linear displacement. The solution was to make user-defined points for the displacement history. This was done by expressing the displacement by deriving a function for acceleration that didn't create sudden accelerations in the simulations. This way, the module started with a soft motion and maintained the desired constant lowering velocity for the rest of the simulation.

The verification of the model showed that USFOS solves the equilibrium equations correctly. For drag, the difference between the hand calculations and the results from USFOS increased with increasing lowering velocity. However, the drag's contribution on the resulting force in

the wire was so small that it could be neglected.

When investigating slamming, USFOS gave no values corresponding directly to the hand calculations. This was because the force measured in the monitor element at the top of the spring was a response force. There was no way of obtaining the direct forces acting on the module while it passed through the water surface in USFOS. However, a difference in the response forces was observed when slamming calculations were turned on and off. By reducing the eigenperiod by 50%, a different vibration pattern was obtained when the module passed through the water surface. Because of this, it was concluded that USFOS takes account for the slamming effect.

A series of sensitivity studies were performed for both models. The most important finding was that the spool wave function could be used for finding the minimum forces in the wire or slings. This means that the analyses could be reduced from a full 3-hour analysis to an analysis with a duration of only 260 s. This saved considerable computational time. However, the spool wave function didn't give the minimum values for all the cases. Compared to a full 3-hour analysis with the module hanging still in the water surface, there were a few cases where the spool wave function gave a relative difference in wire force of 10%. However, the limiting studies showed by use of probability plot that the minimum values obtained were inside the 95% confidence interval. It was only when the results were negative or relatively close to zero that the results seemed to have another distribution.

Negative forces were observed in the monitor element. A tension spring element was used for the wire, so there shouldn't be negative forces in the monitor element. These forces occur because of errors in the numerical method of USFOS. These cases should probably have represented slack in the wire. However, there were no values that indicated that snap load was reached.

All the analyses done for regular waves did not lead to the forces reaching their limit in e.g. slack, not even by setting $H_s = 11\ m$ and $Tp = 10\ s$. It was therefore concluded that Airy waves were not suitable for simulating regular waves in marine operations.

By finding the minimum values in different sea states with different seeds, a statistical model

for predicting the minimum value could be developed. It was based on a transformed Gumbel distribution. In most of the cases it was not necessary to use the probability paper to determine if the module would experience slack. However, it was a good way to see if the results were inside a confidence interval or error bound. For the advanced model in the limiting studies, 5 out of 8 cases had to be checked against the probability papers.

There was an attempt to simulate the "lift off deck" phase, but there was no possibility to include two ships, and the author was not able to make two independent members in USFOS interact with each other.

Chapter 10

Further Work

Only the "lowering through wave zone" phase was studied in this thesis. Even if the "lift off deck" phase can't be simulated, the lowering processes under water and hitting the surface seem more likely to work in USFOS.

Testing the results of USFOS against another program like SIMO should be done. This is considered by the author to be one of the most conclusive ways to determine the applicability of USFOS in simulation of marine operations.

USFOS has the possibility to define shadow members or different hydrodynamic diameters of the tubular members. This could be used for doing a much more complex model, where there is interaction between the members and the added mass coefficients have to be set manually for each member.

Investigation of USFOS' ability to calculate slack should be done. Negative forces were observed in the tension spring (wire element), even though it has no capacity to take up forces in compression. There were also no signs of any snap loads in the response forces induced in the system, even though it experienced negative forces and there probably was slack.

Further investigation of using the spool wave function to find the maximum/minimum force in a full 3-hour sea state is recommended. If the spool wave function is confirmed to be

valid to use, considerable computational time could be saved. This would provide a good argument for using USFOS to simulate marine operations.

Bibliography

AkerSolutions. (2014a). *AkersSolutions subsea tree.* Retrieved 2014-10-14, from http://www.akersolutions.com/Global/Subsea/Subseaproducts/Productimagesanddocuments/Subseatrees/subseatreetranby320.jpg

AkerSolutions. (2014b). *Deepwater cluster manifolds.* Retrieved 2014-10-14, from http://www.akersolutions.com/Global/Subsea/Subseaproducts/Productimagesanddocuments/Manifolds/deepwaterclustermanifold320x320.jpg

AkerSolutions. (2014c). *Power and processing figure.* Retrieved 2014-10-14, from http://www.akersolutions.com/Global/Subsea/Subseaproducts/Productimagesanddocuments/Powerprocessingboosting/AkerSolutions_Power_and_processing_320.jpg

AkerSolutions. (2014d). *Satellite protection structure.* Retrieved 2014-10-14, from http://www.akersolutions.com/Global/Subsea/Subseaproducts/Productimagesanddocuments/Manifolds/viljeprotstructure320.jpg

AkerSolutions. (2014e). *Small manifolds system.* Retrieved 2014-10-14, from http://www.akersolutions.com/Global/Subsea/Subseaproducts/Productimagesanddocuments/Manifolds/manifoldsstructures320x320.jpg

AkerSolutions. (2014f). *Subsea Products overview.* Retrieved 2014-10-14, from http://www.akersolutions.com/en/Global-menu/Products-and-Services/Subsea-technologies-and-services/Subsea-production-systems-and-technologies/

AkerSolutions. (2014g). *Tie-in connection systems figure.* Retrieved 2014-10-14, from http://www.akersolutions.com/Global/Subsea/Subseaproducts/

Productimagesanddocuments/Tieinconnectionstooling/VCSinternet320x320.jpg

Bury, K. V. (1978). Statistical models in applied science, Karl V. Bury, Wiley, London, 1975, Prico: £14.00, No. of pages 625, ISBN 0-471-12590-3. *International Journal for Numerical Methods in Engineering*, *12*(6), 1054. Retrieved from http://dx.doi.org/10.1002/nme.1620120617 doi: 10.1002/nme.1620120617

DNV. (2011a). DNV-OS-H101: Marine Operations, General. (October).

DNV. (2011b). DNV-RP-H103: Modelling and Analysis of Marine Operations. (April).

DNV. (2014). DNV-OS-H205 Lifting Operations (VMO Standard - Part 2-5). (April).

Eik, K. J., & Nygaard, E. (2003). Statfjord Late Life Metocean Design Basis. , 57. Retrieved from http://www.ivt.ntnu.no/imt/courses/tmr4195/introduction/Example_Metocean_Design_Basis.pdf

EniNorge. (2014). *Suction anchors.* Retrieved from http://www.eninorge.com/Global/Bilder/Goliat/665_installasjonHammerfest/install5.jpg

Faltinsen, O. M. (1990). *SEA LOADS ON SHIPS AND OFFSHORE STRUCTURES*. Cambridge University press.

Kimiaei, M., Jiajing, X., & Yu, H. (2014). Comparing the Results of a Simplified Numerical Model With DNV Guidelines for Installation of Subsea Platforms. , 1–8.

Matland, A. (2014). Simulation of Marine Lifting Operations with Focus on Structural Response Control. (June). Retrieved from http://www.diva-portal.org/smash/record.jsf?pid=diva2:746619

Ø ritsland, O., Lehn, E., & Reitan, O. E. (1986). Hydrodynamic Forces on Subsea Modules. Model Test Results. *NTNF Reasearch Programme Marine Operations. Marintek report 5 532013 03*.

SINTEF. (2001). USFOS Getting Started.

Unknown. (2014a). *Single suction anchor.* Retrieved 2014-10-14, from http://subseaworldnews.com/wp-content/uploads/2013/04/Bladt-Industries-Announces-Successful-Loadout-of-12-Suction-Anchors-Norway.jpg

Unknown. (2014b). *Unprotected subsea tree.* Retrieved 2014-10-14, from http://www.offshore-technology.com/projects/gyrfalcon/images/gyrfalcon3.jpg

USFOS. (n.d.-a). *No Title.* Retrieved 2014-12-15, from http://www.usfos.no/examples/usfos/hydrodynamics/slam1/index.html

USFOS. (n.d.-b). *No Title.* Retrieved 2014-12-17, from http://usfos.no/

USFOS. (2010). USFOS Hydrodynamics.

USFOS. (2014). *Usfos Commands. Overview and Description* (Tech. Rep.).

Appendix A

Results Simple Model Limit Sea States

A.1 With ship motions

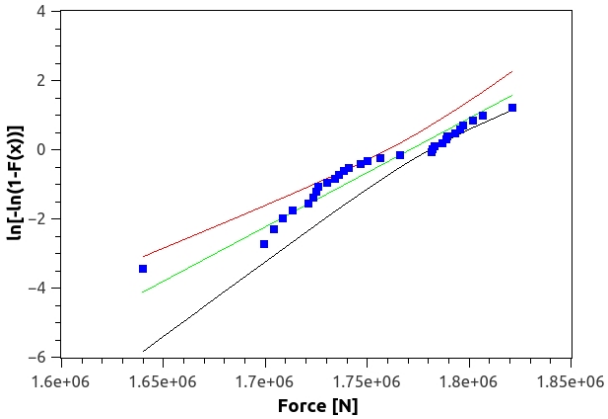

$H_s = 1, T_p = 4$

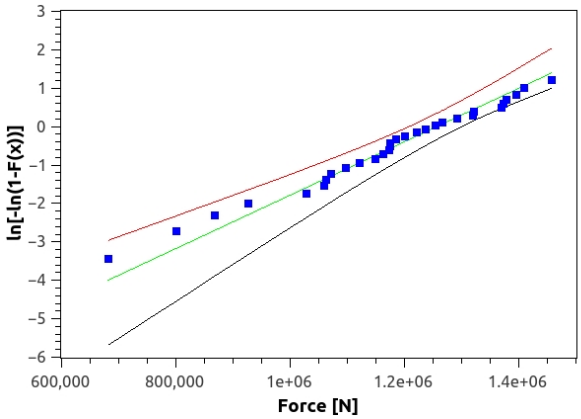

$H_s = 1, T_p = 12$

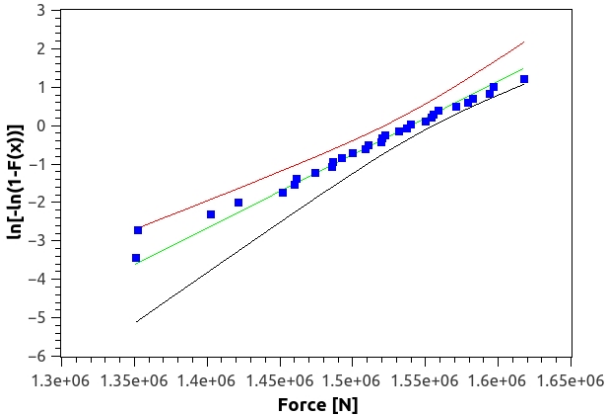

$H_s = 2, T_p = 4$

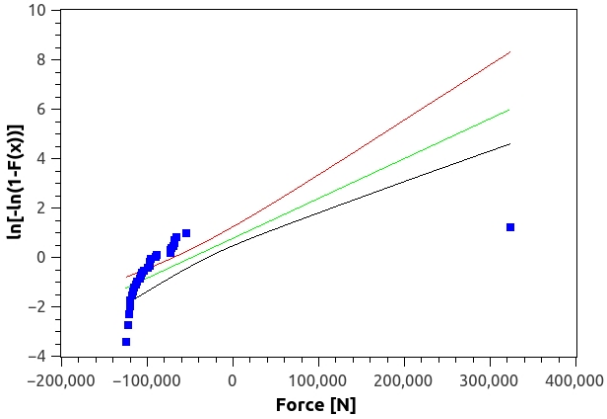

$H_s = 2, T_p = 16$

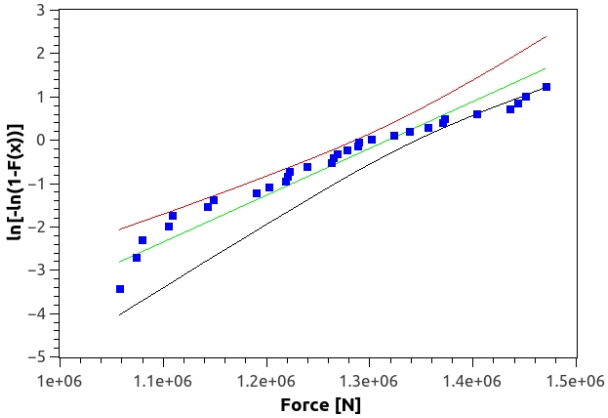

$H_s = 3, T_p = 5$

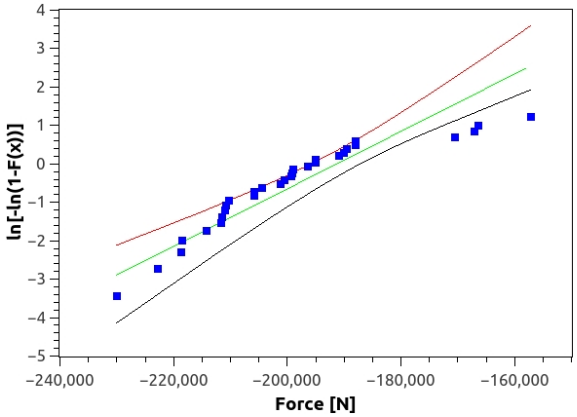

$H_s = 3, T_p = 16$

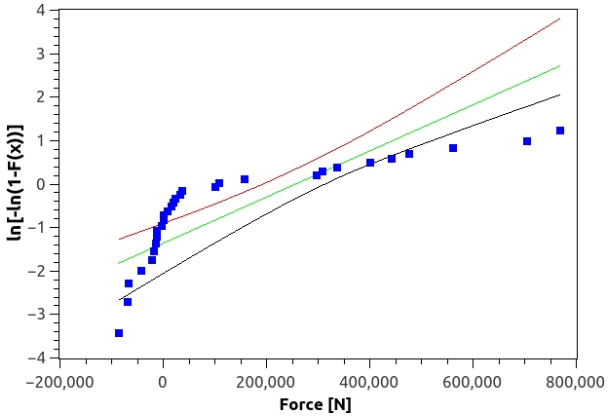

$H_s = 4, T_p = 7$

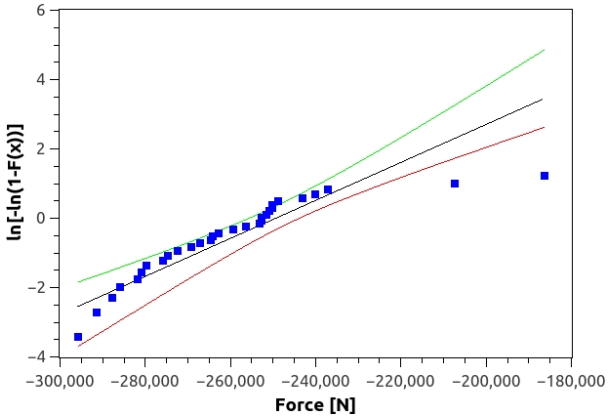

$H_s = 4, T_p = 15$

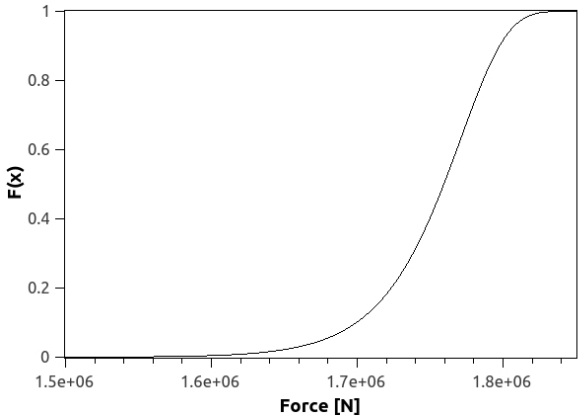

$H_s = 1, T_p = 4$

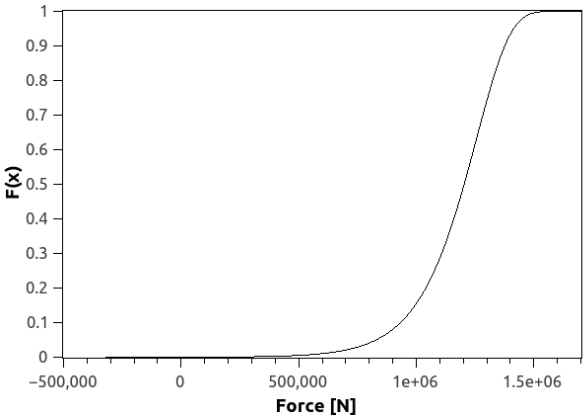

$H_s = 1, T_p = 12$

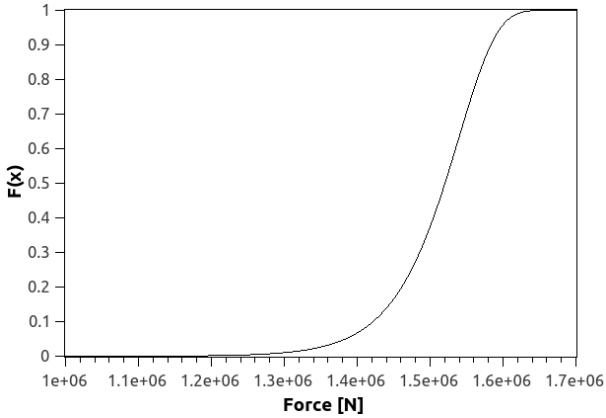

$H_s = 2, T_p = 4$

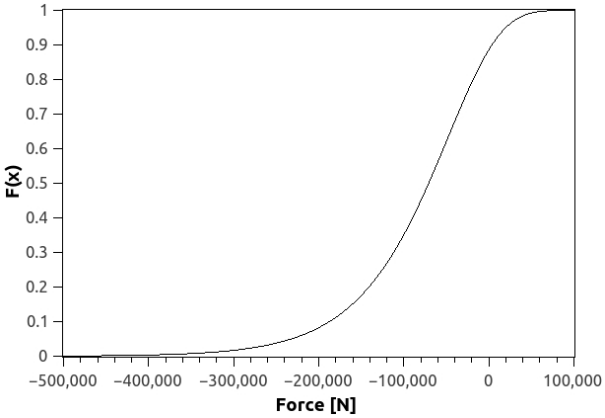

$H_s = 2, T_p = 16$

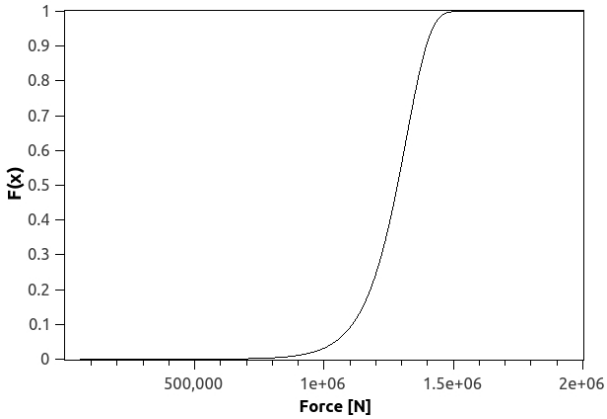

$H_s = 3, T_p = 5$

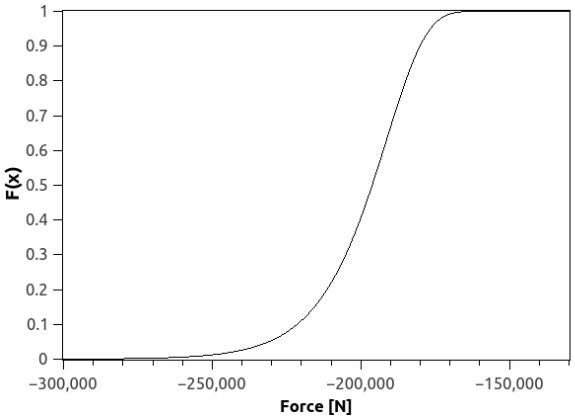

$H_s = 3, T_p = 16$

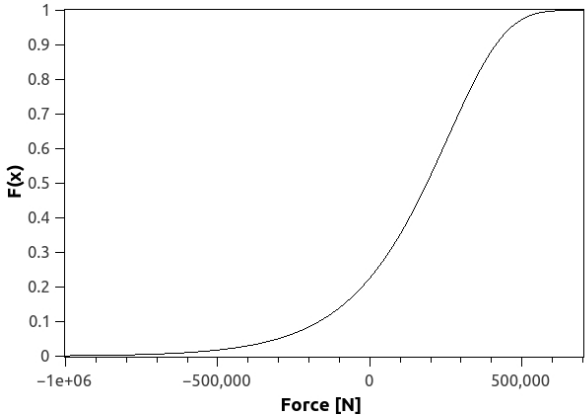

$H_s = 4, T_p = 7$

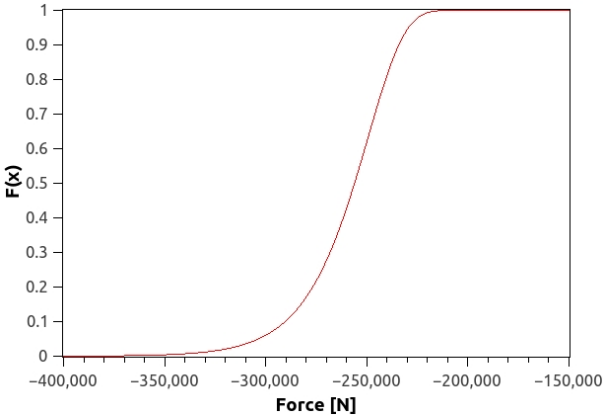

$H_s = 4, T_p = 15$

A.2 Without ship motions

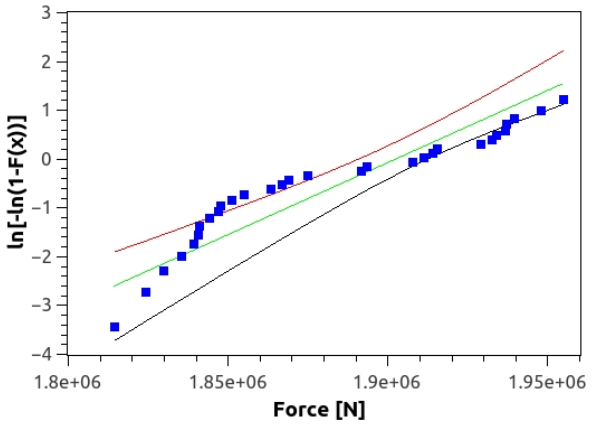

$H_s = 1, T_p = 4$

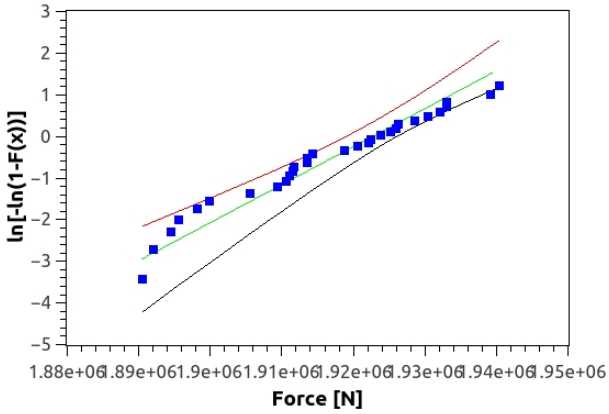

$H_s = 1, T_p = 12$

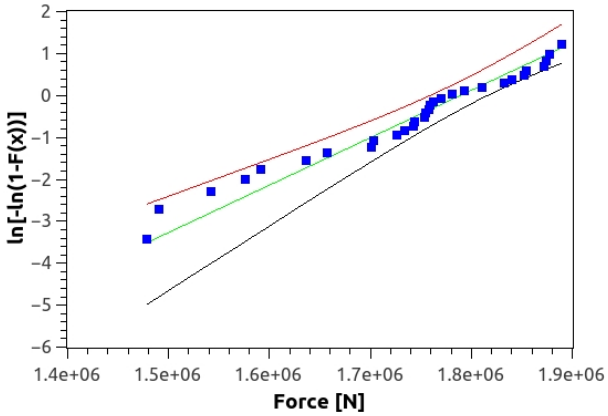

$H_s = 2, T_p = 4$

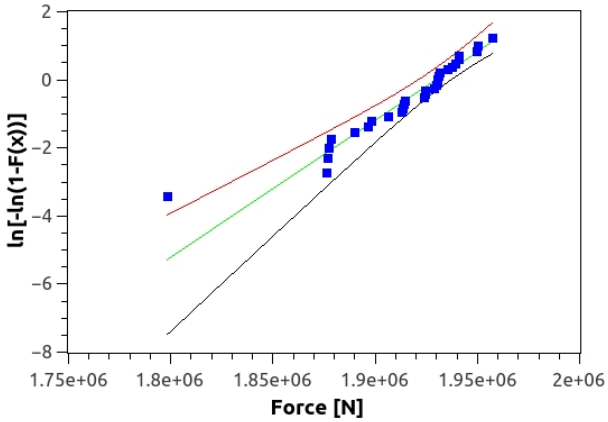

$H_s = 2, T_p = 16$

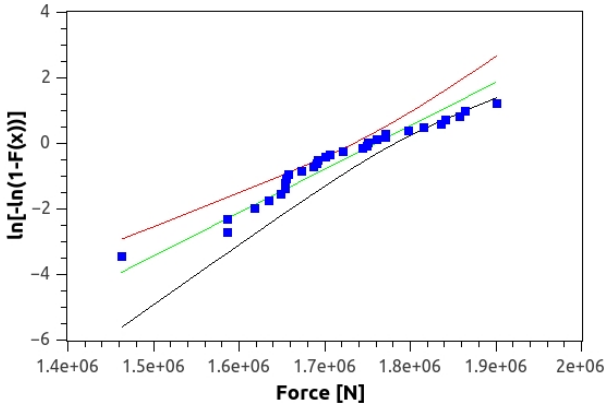

$H_s = 3, T_p = 5$

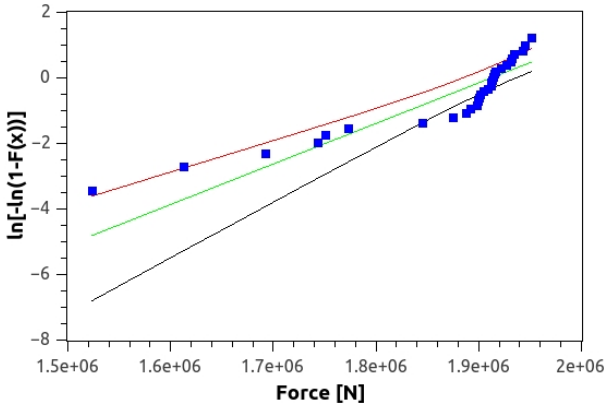

$H_s = 3, T_p = 16$

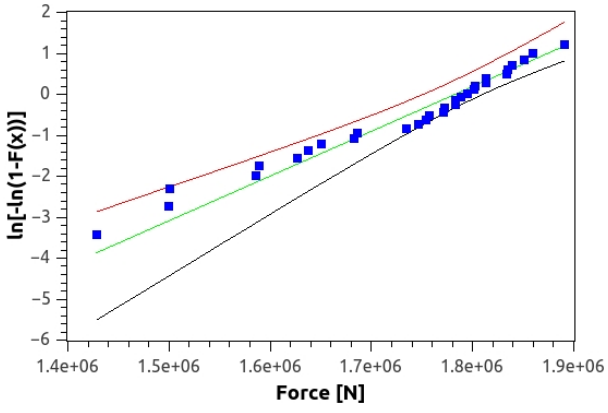

$H_s = 4, T_p = 7$

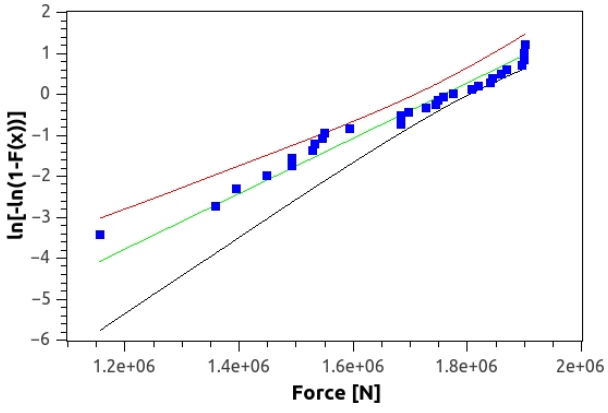

$H_s = 4, T_p = 15$

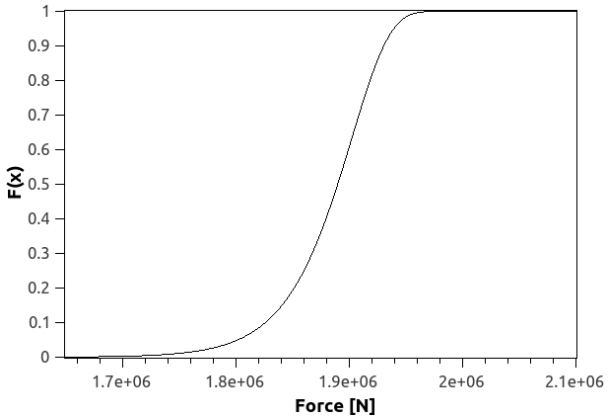

$H_s = 1, T_p = 4$

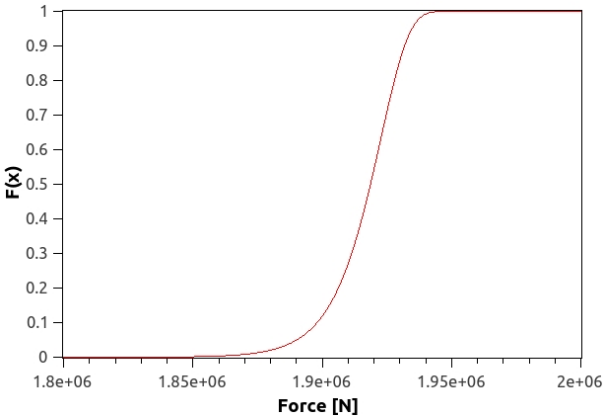

$H_s = 1, T_p = 12$

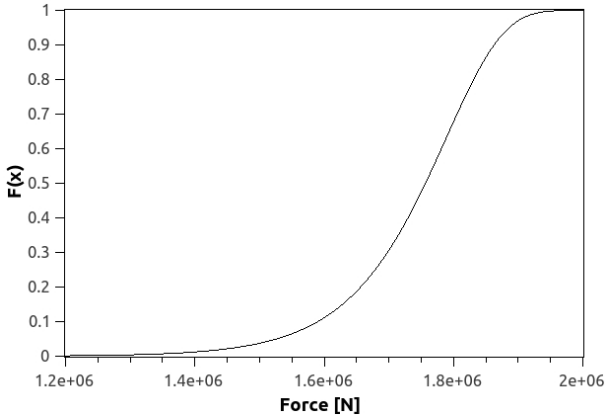

$H_s = 2, T_p = 4$

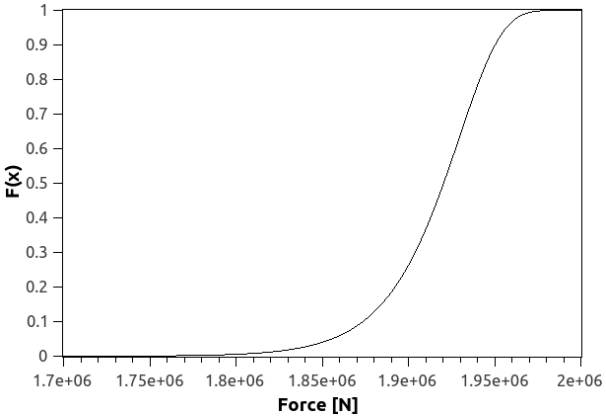

$H_s = 2, T_p = 16$

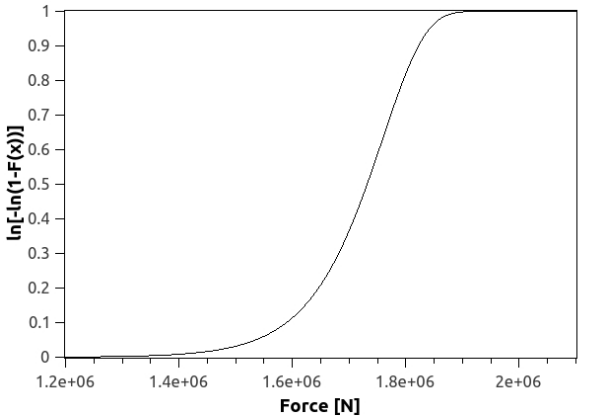

$H_s = 3, T_p = 5$

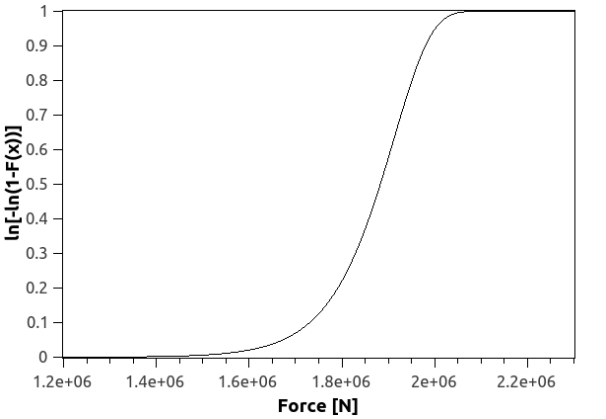

$H_s = 3, T_p = 16$

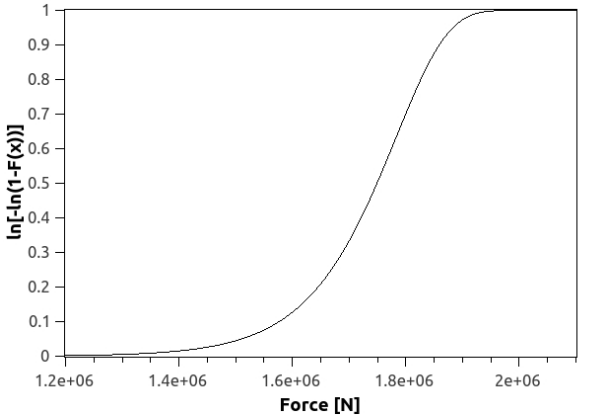

$H_s = 4, T_p = 7$

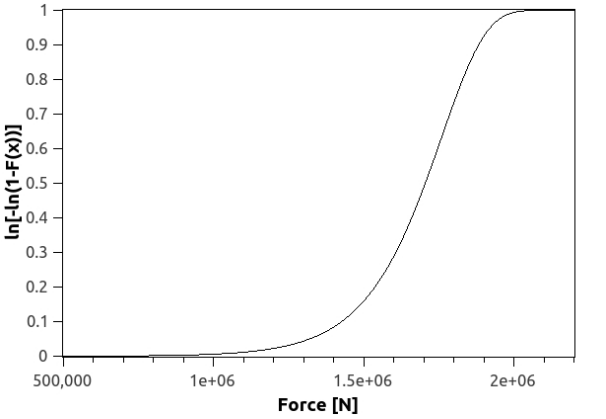

$H_s = 4, T_p = 15$

Appendix B

Results Advanced Model Limit Sea States

B.1 Probability paper for Wire Forces

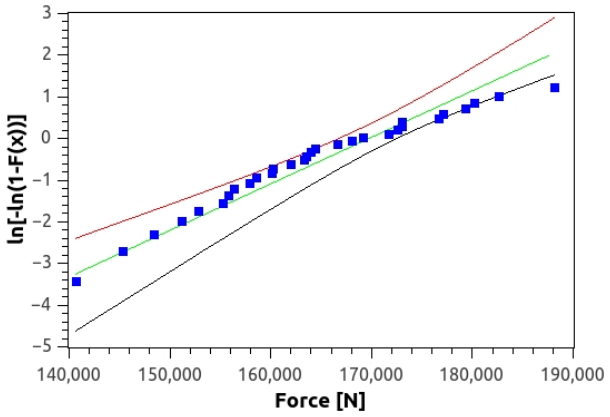

$H_s = 1, T_p = 4$

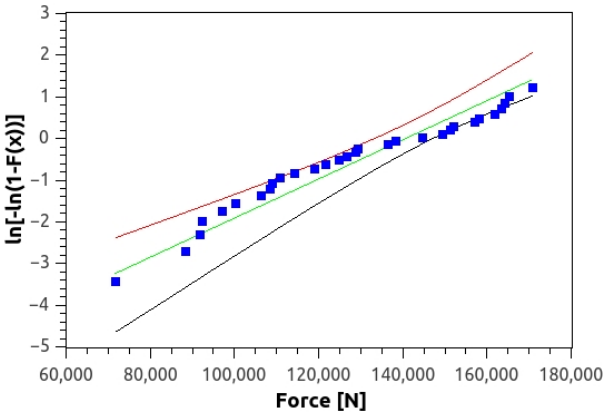

$H_s = 1, T_p = 12$

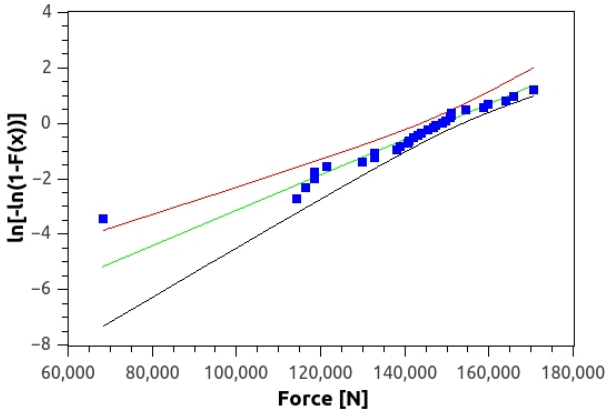

$H_s = 2, T_p = 4$

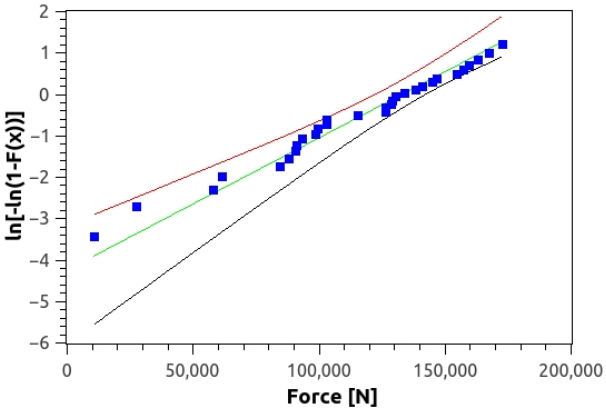

$H_s = 2, T_p = 16$

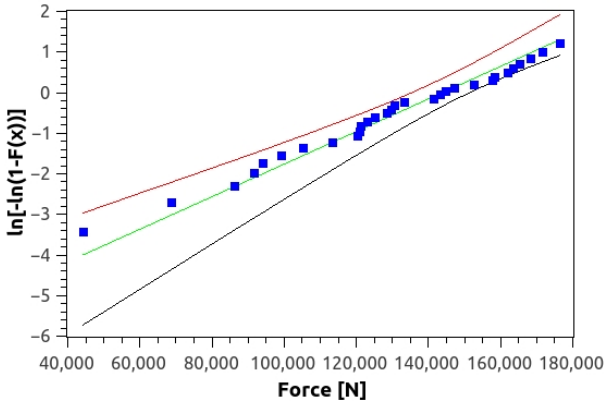

$H_s = 3, T_p = 5$

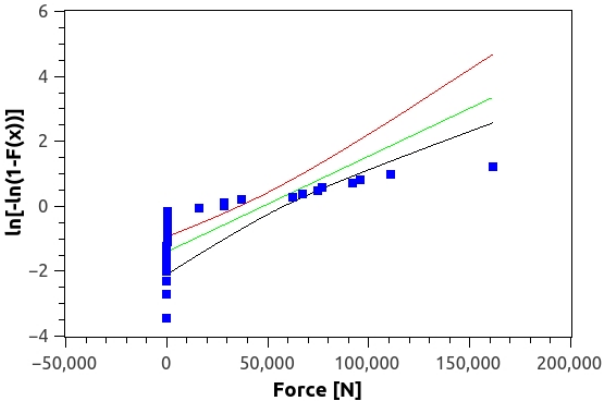

$H_s = 3, T_p = 16$

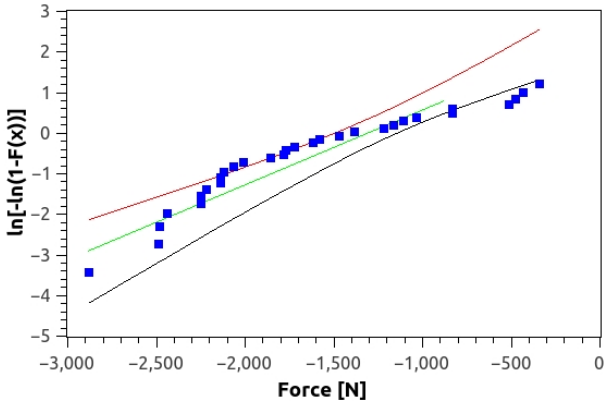

$H_s = 4, T_p = 7$

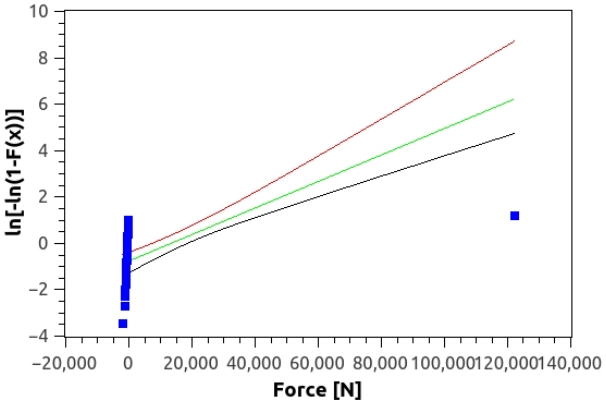

$H_s = 4, T_p = 15$

B.2 Probability paper for Sling Forces

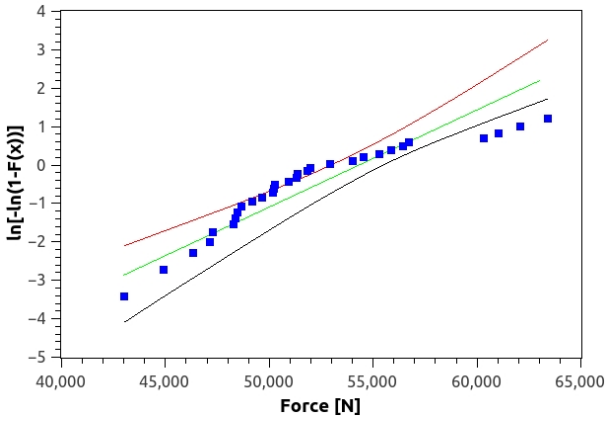

$H_s = 1$,$T_p = 4$, Element 600

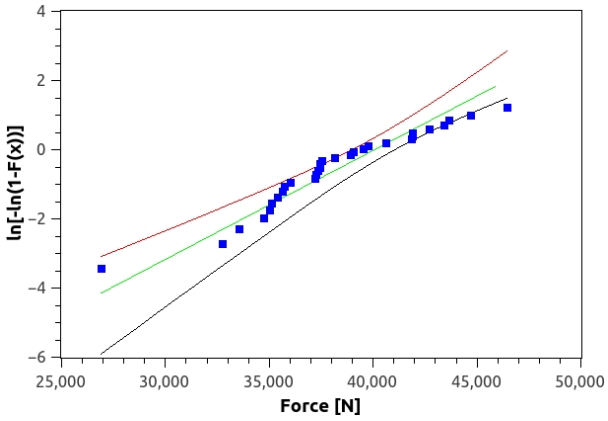

$H_s = 1$,$T_p = 12$, Element 600

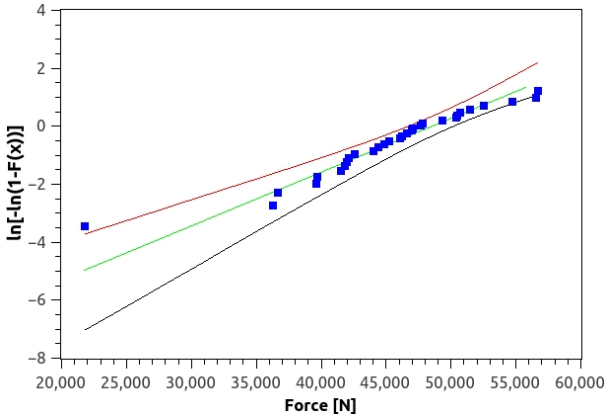

$H_s = 2$,$T_p = 4$, Element 600

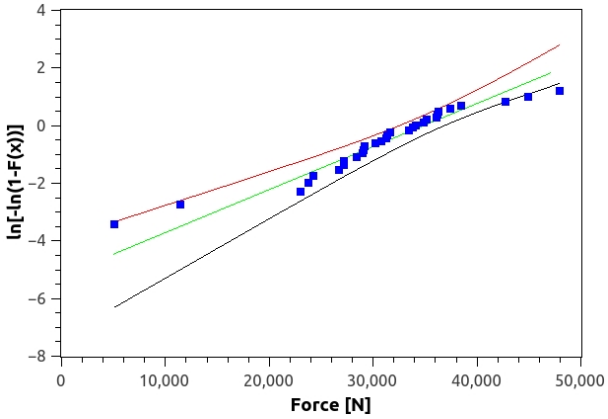

$H_s = 2$,$T_p = 16$, Element 600

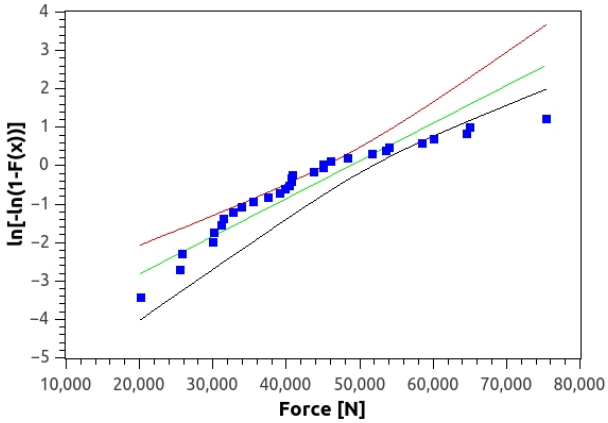

$H_s = 3$,$T_p = 5$, Element 600

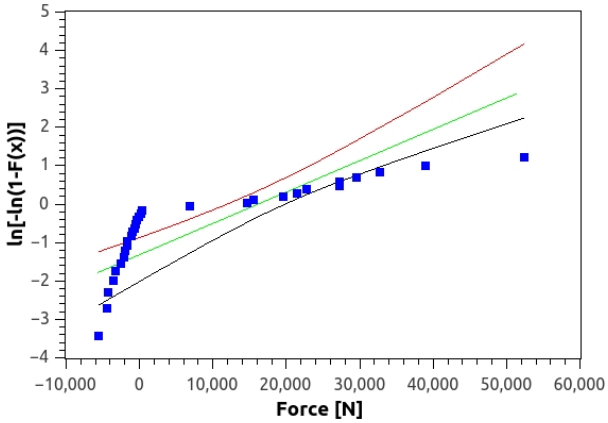

$H_s = 3$,$T_p = 16$, Element 600

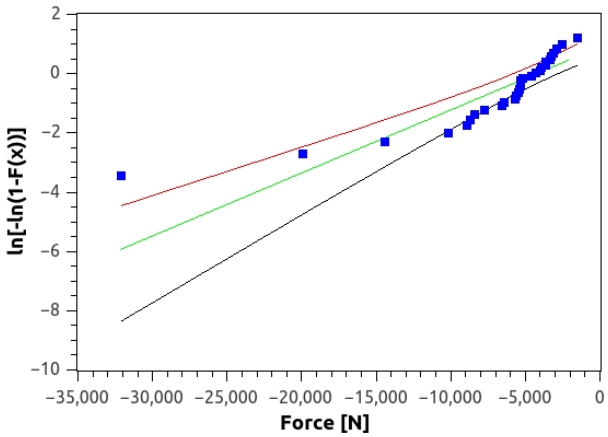

$H_s = 4$,$T_p = 7$, Element 600

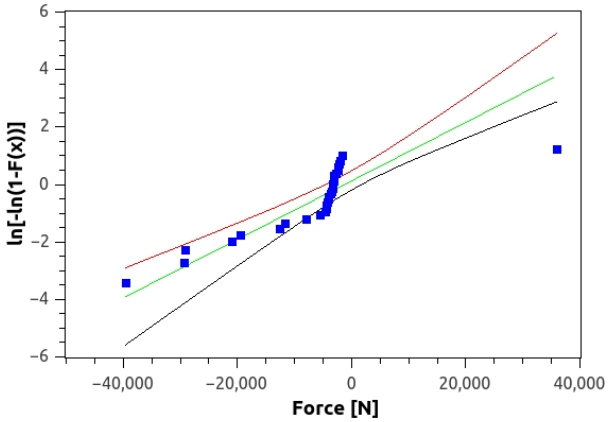

$H_s = 4$,$T_p = 15$, Element 600

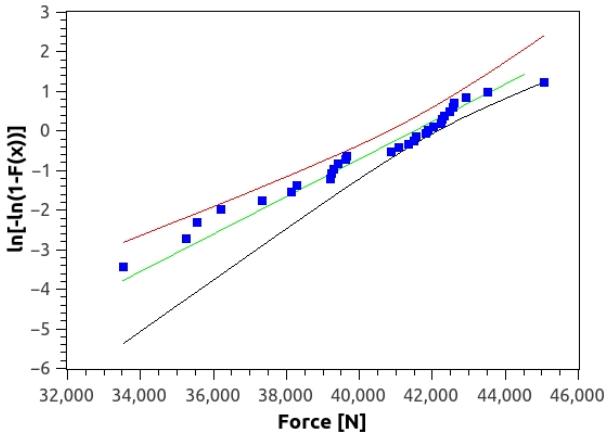

$H_s = 1$,$T_p = 4$, Element 601

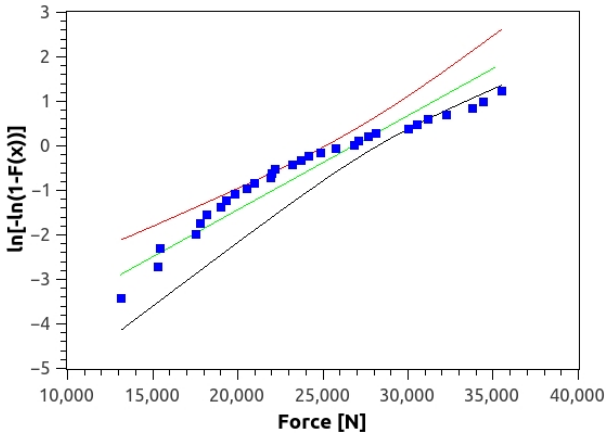

$H_s = 1$,$T_p = 12$, Element 601

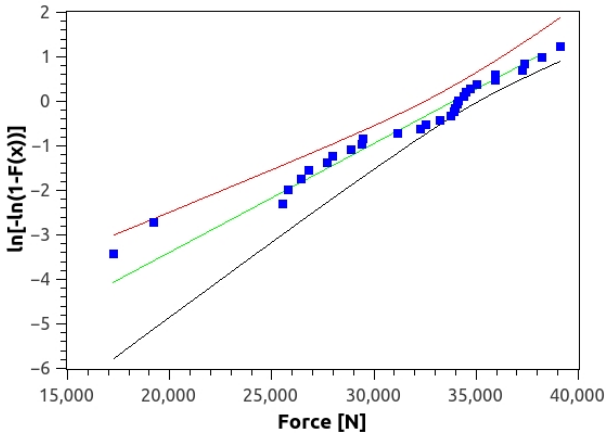

$H_s = 2$,$T_p = 4$, Element 601

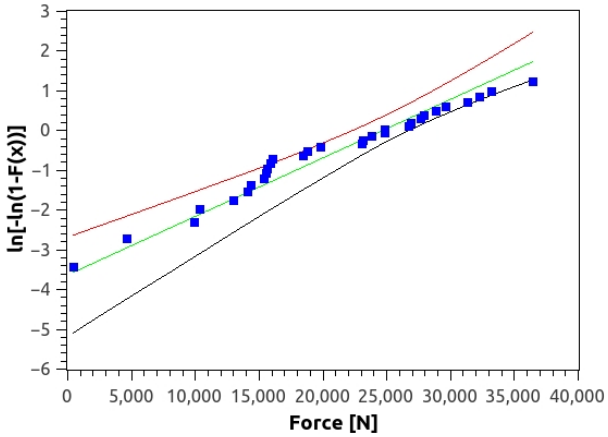

$H_s = 2$,$T_p = 16$, Element 601

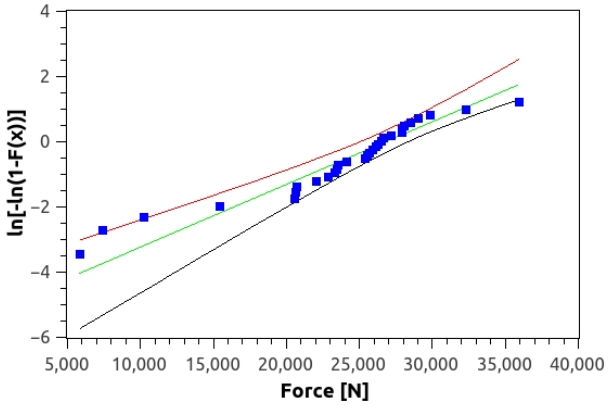

$H_s = 3$,$T_p = 5$, Element 601

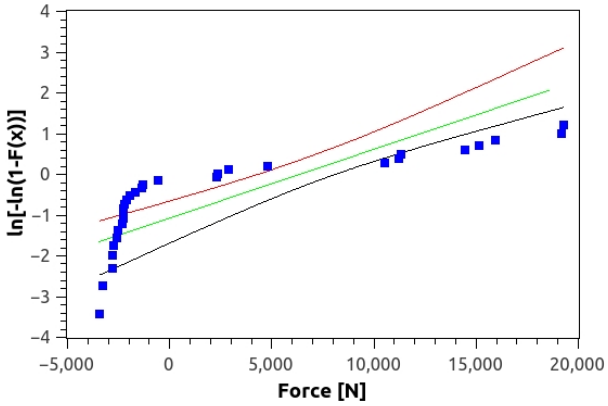

$H_s = 3$,$T_p = 16$, Element 601

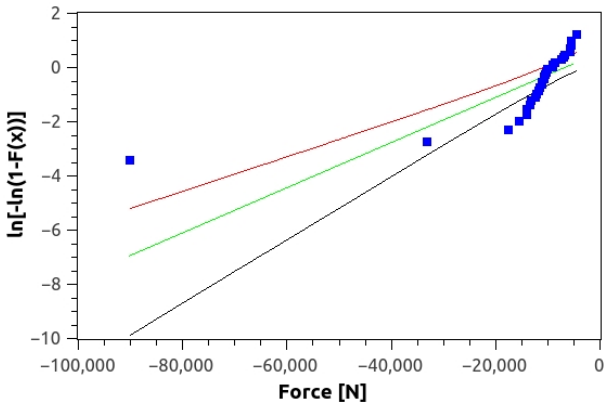

$H_s = 4$,$T_p = 7$, Element 601

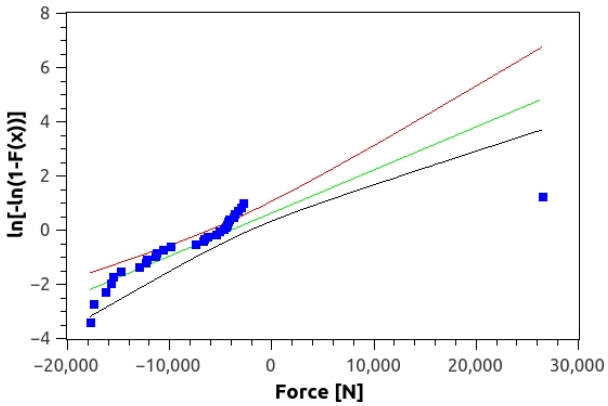

$H_s = 4$,$T_p = 15$, Element 601

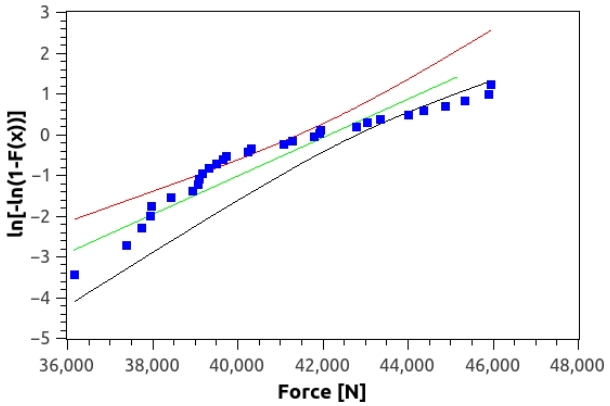

$H_s = 1$,$T_p = 4$, Element 602

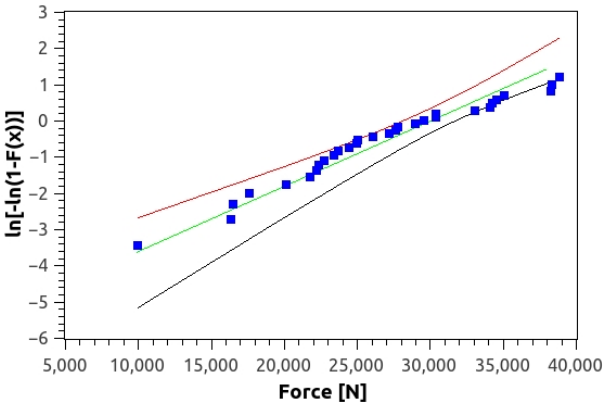

$H_s = 1$,$T_p = 12$, Element 602

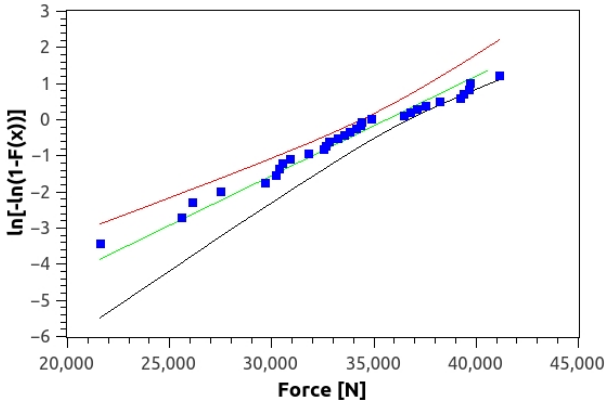

$H_s = 2$,$T_p = 4$, Element 602

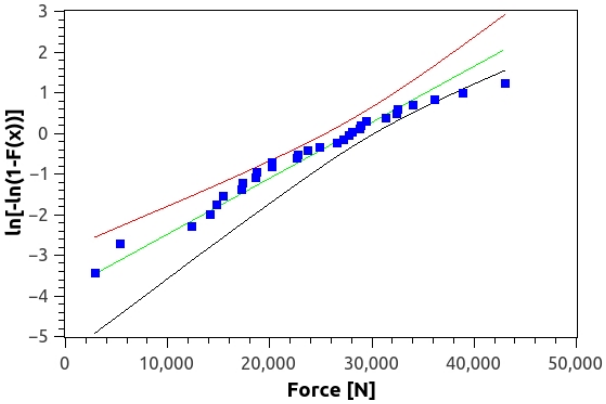

$H_s = 2$,$T_p = 16$, Element 602

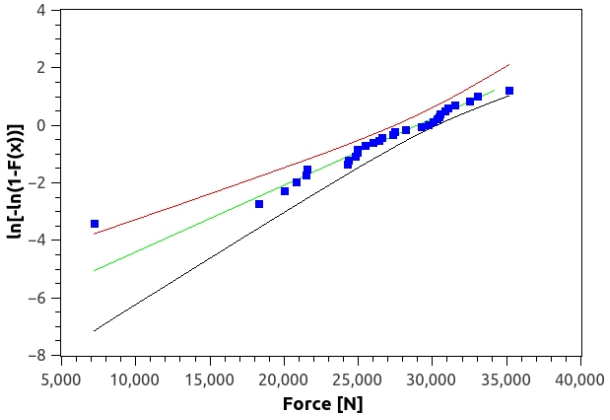

$H_s = 3$,$T_p = 5$, Element 602

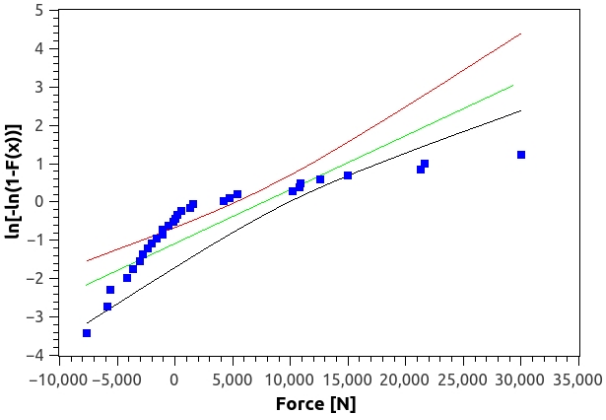

$H_s = 3$,$T_p = 16$, Element 602

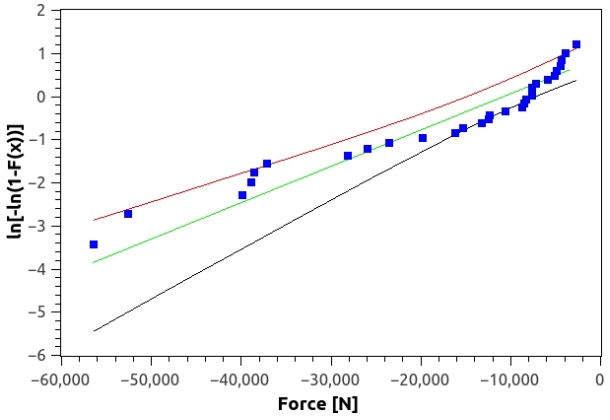

$H_s = 4$,$T_p = 7$, Element 602

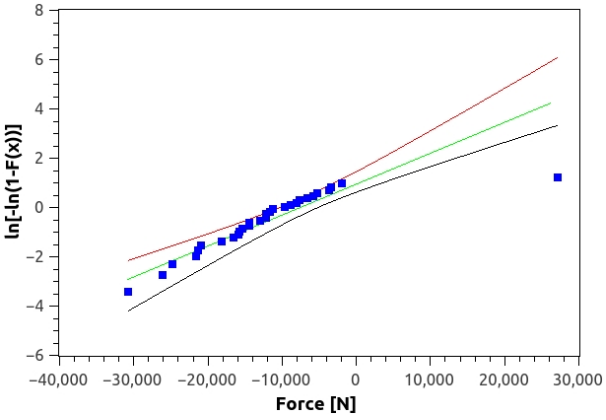

$H_s = 4$,$T_p = 15$, Element 602

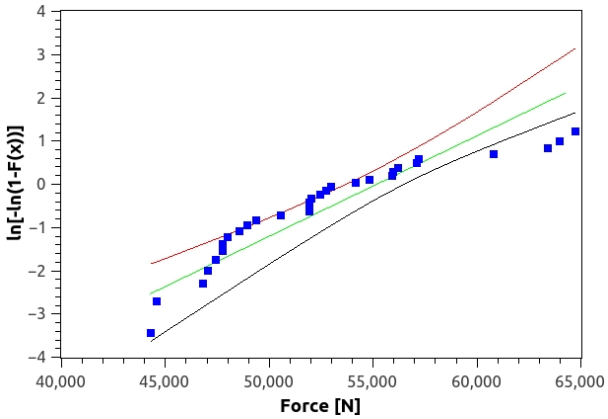

$H_s = 1$,$T_p = 4$, Element 603

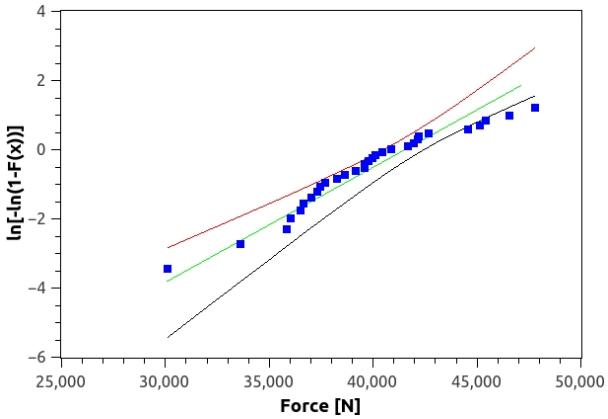

$H_s = 1$,$T_p = 12$, Element 603

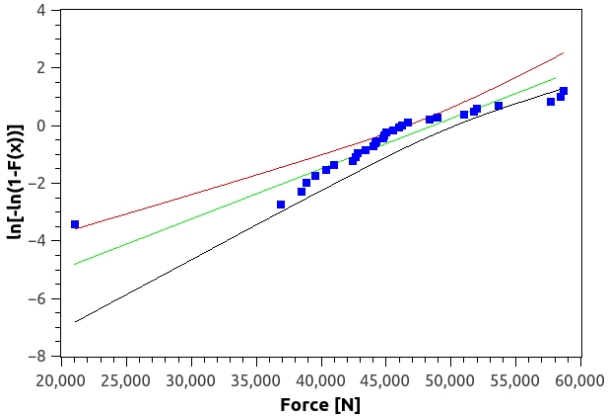

$H_s = 2$,$T_p = 4$, Element 603

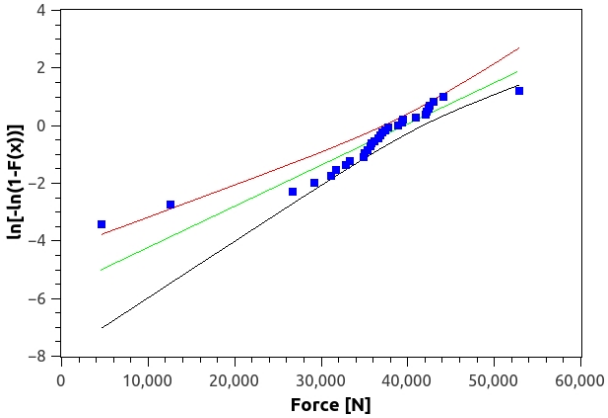

$H_s = 2$,$T_p = 16$, Element 603

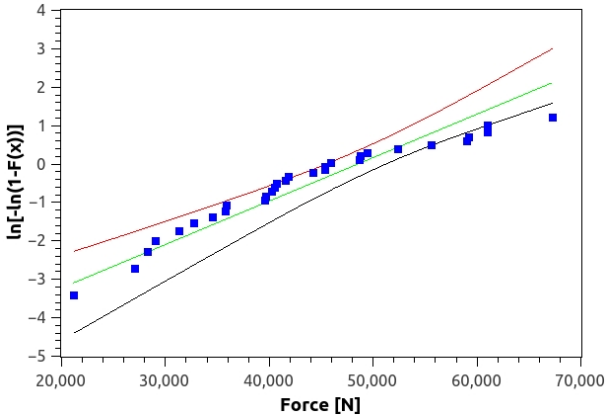

$H_s = 3$,$T_p = 5$, Element 603

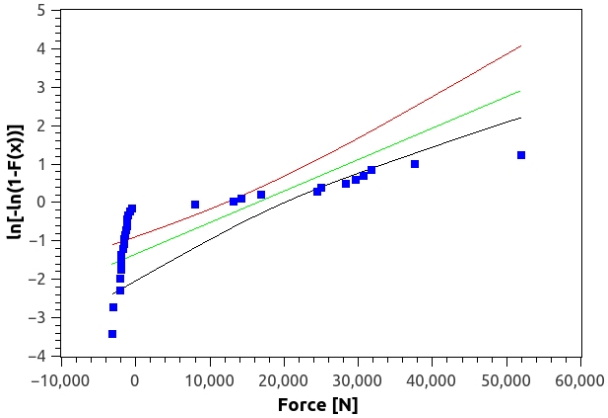

$H_s = 3$,$T_p = 16$, Element 603

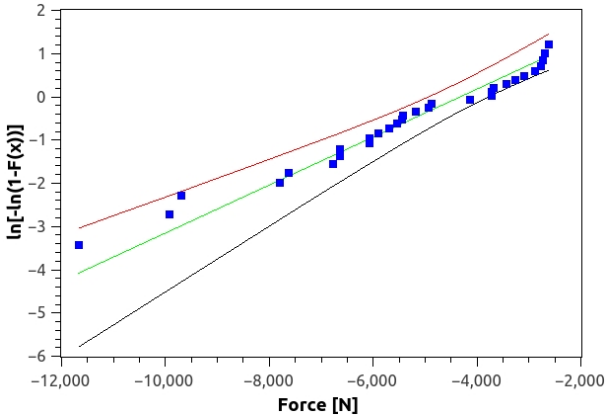

$H_s = 4$,$T_p = 7$, Element 603

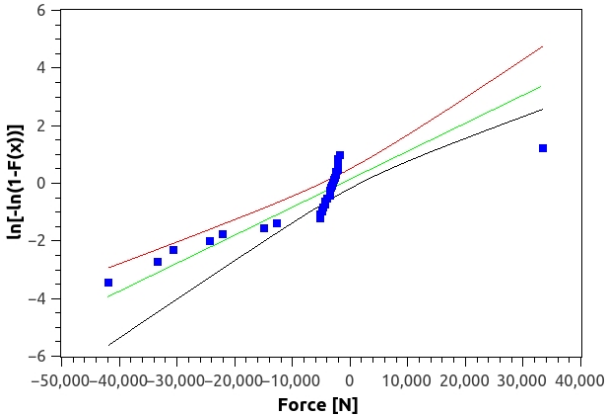

$H_s = 4$,$T_p = 15$, Element 603

B.3 S-curves for Sling Forces

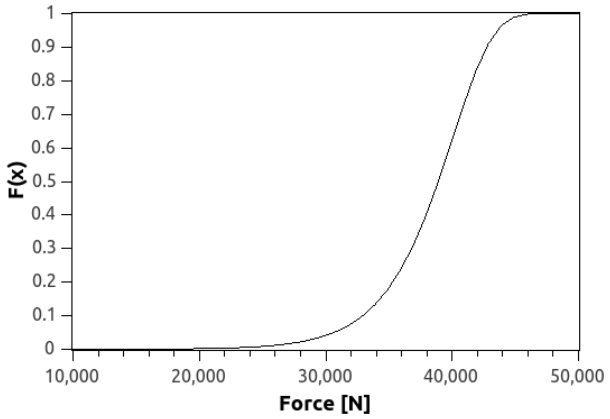

$H_s = 1$,$T_p = 12$, Element 600

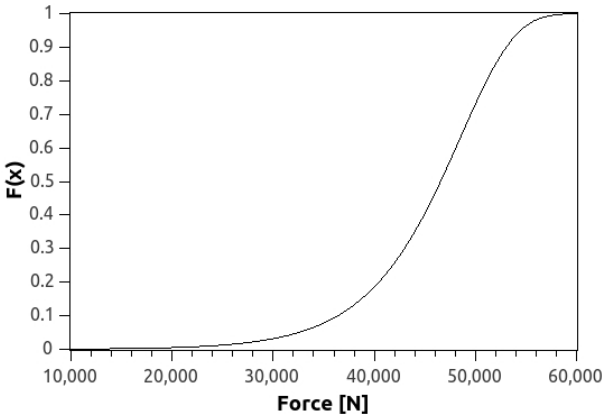

$H_s = 2$,$T_p = 4$, Element 600

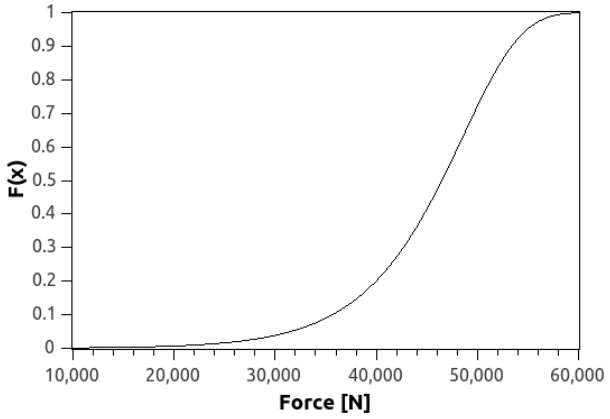

$H_s = 2$,$T_p = 4$, Element 603

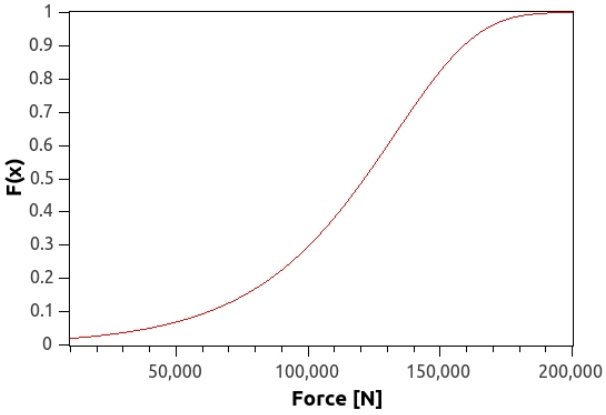

$H_s = 2$,$T_p = 16$, Wire

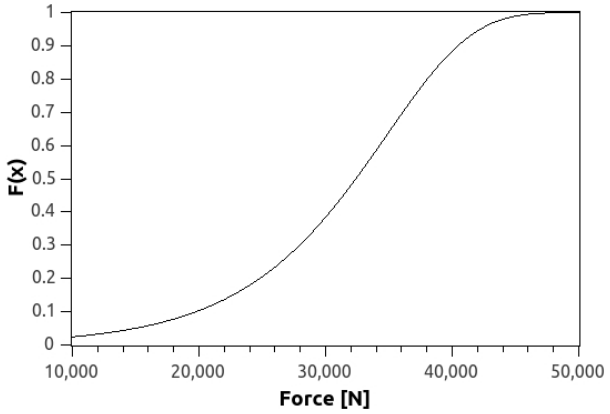

$H_s = 2$,$T_p = 16$, Element 600

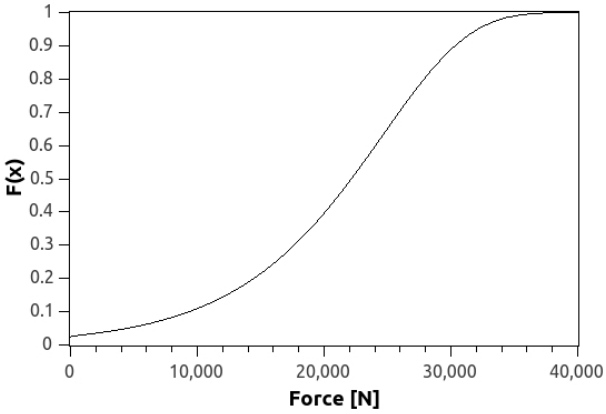

$H_s = 2$,$T_p = 16$, Element 601

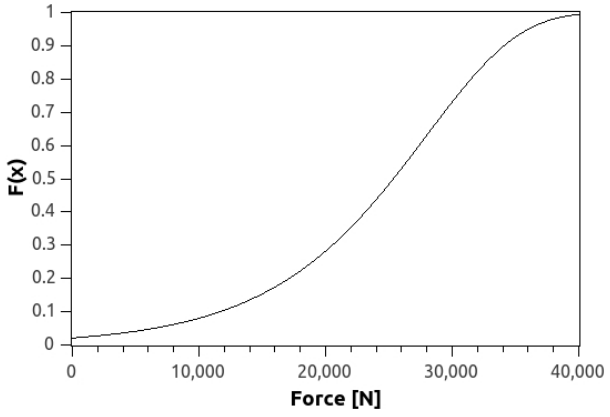

$H_s = 2$,$T_p = 16$, Element 602

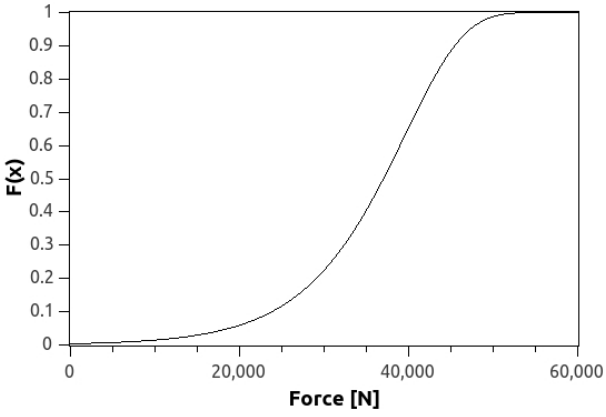

$H_s = 2$,$T_p = 16$, Element 603

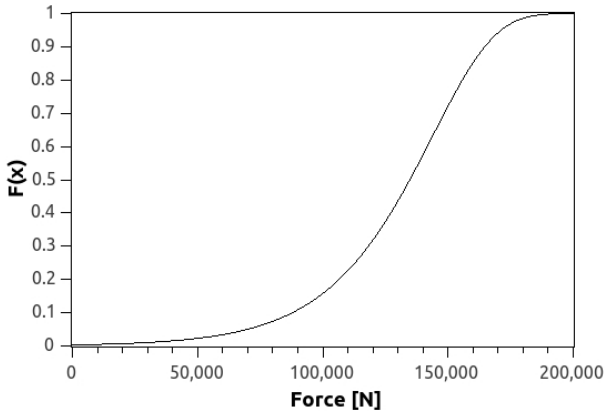

$H_s = 3$,$T_p = 5$, Wire

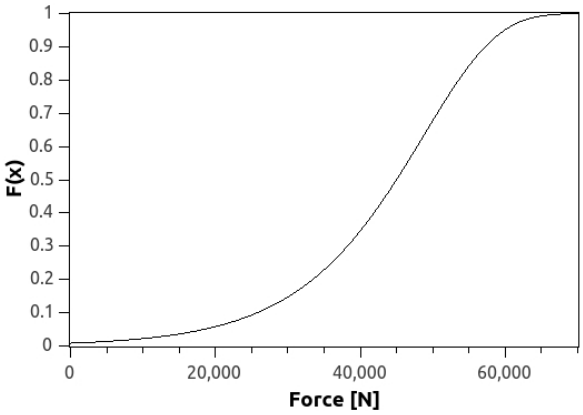

$H_s = 3$,$T_p = 5$, Element 600

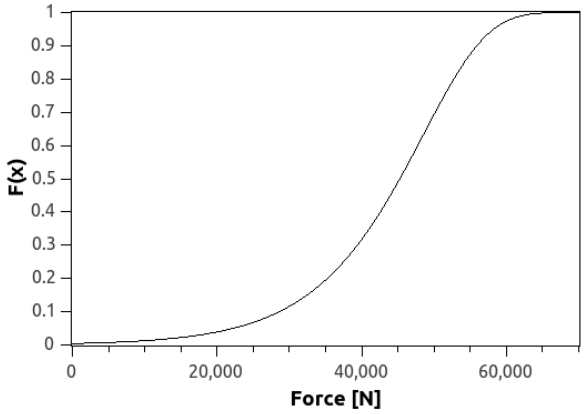

$H_s = 3$,$T_p = 5$, Element 603

Appendix C

MATLAB-scripts

./Appedix/acceleration_of_wire.m

```
%% Calculatin acceleration of wire elongation:

% The pupuse is to create a function of displacement of the start phase of
% the wire, so the acceleration goes for zero to zero in a continius
% motion.
clc; clear;
%% Defined paramters
c_2 = 100; % Peak parameter for acceleration
v = 1; % The derired lowering velocity
l = 100; % The desired lowering length
li = 49; % Initial length of wire

%% By formulase presented in .... displacement,acceleration can be given as:

S = @(c_2,t) 1/24 * t.^4 /(c_2);
vel = @(c_2,t) 1/6 * t.^3 /(c_2);
a = @(c_2,t,t_end) (t_end*t-t.^2)/(c_2);

t_end = nthroot(c_2*6*v, 3);

t=0:0.1:t_end;
t(length(t)+1)= t_end;
```

```
velo = vel(c_2,t);
Disp = S(c_2,t);
acc = a(c_2,t,t_end);

%% constant lowering velocity after ended acceleration to a defined lenght
Disp_end = Disp(length(Disp));

t_simulation = ((l-Disp_end)/v) + t_end;

t(length(t)+1) = t_simulation;


%Displacement factor
Disp_fac = Disp/li;
Disp_fac(length(Disp_fac)+1) = l/li;

%% Save the result to a file
time_disp = [t;Disp_fac];
acc_wire =[t(1:end-1);acc];

fileID = fopen('start_disp.plo','w');
fprintf(fileID,'%f %f\r\n',time_disp);
fclose(fileID);

fileID2 = fopen('acc_of_wire.plo','w');
fprintf(fileID2,'%f %f\r\n',acc_wire);
fclose(fileID2);
```

./Appedix/Slamming_general.m

```
close all; clear all;

%% Formulas

f_C_s1 = @(h,R) (5.15./(1+8.5*h./R)) + 0.275*h./R; % Exprimental slamming coff

% Coefficients:
  p1 = 1.3325;
  p2 = -12.763;
  p3 = 49.248;
  p4 = -97.585;
  p5 = 103.37;
  p6 = -51.53;
  p7 = 1.6097;
  p8 = 10.371;
  p9 = -6.5627;
  p10 = 3.14;

y_theroy = @(x) p1*x.^9 + p2*x.^8 + p3*x.^7 + p4*x.^6 + p5*x.^5 + p6*x.^4 +
    ...
    p7*x.^3 + p8*x.^2 + p9*x + p10;


% coefficients:
  ap1 = 0.35247;
  ap2 = -1.5803;
  ap3 = 2.7379;
  ap4 = 0.035908;

 y2 = @(x) ap1*x^3 + ap2*x^2 + ap3*x + ap4;


% Coefficients (with 95% confidence bounds):
       a0 =       1.994;
       a1 =      -1.503;
```

```
        b1 =      -0.2733;
        a2 =       -0.462;
        b2 =     -0.01653;
        a3 =      -0.0231;
        b3 =       0.1697;
        w =        1.231;

% General model Fourier3:
     f = @(x) a0 + a1*cos(x*w) + b1*sin(x*w) + ...
           a2*cos(2*x*w) + b2*sin(2*x*w) + a3*cos(3*x*w) + b3*sin(3*x*w);



%% Plot

%% Experimental slamming coefficent pr unit R and length
% h=0:0.01:2.5;
% R=1;
% figure
% plot(h/R,f_C_s1(h,R))
% hold on
% fplot(y_theroy,[0,2.5])
% hold on
% fplot(y2,[0,2.5])
% hold on
% fplot(f,[0,2.5])



%% Slamming in still water experimental Cs



% Assumtions:
V = 1; %m/s konstant velocity
R = 1; %m
L = 45; %m
h=0:0.01:2*R;
```

```
% Parameters
rho = 1025;
g = 9.81;

% Calculations

% changing area/Volume

y = sqrt(8.*h*R-4.*h.^2);

c = atan2((y/2),(R-h));

A = 0.5*R^2 *(2.*c-sin(2.*c));

Vol = A*L;
time = h/V;

F_buoy = Vol*rho*g;

F_slam = rho*f_C_s1(h,R)*R*V^2*L;

F_tot = F_slam + F_buoy;

Res =[h;F_slam];

figure
plot(h,F_slam)
figure
plot(h,F_buoy)
figure
plot(h,F_tot)

fileID = fopen('Slamming.plo','w');
fprintf(fileID,'%f %f\r\n',Res);
fclose(fileID);
```

./Appedix/postpromain.m

```
clc; clear all;

[W_water, lim_slack] = model();

[Result] = reader();

[aa bb] = size(char(Result.name));


if exist('Surf_elev') ==1
    maxsurf(Result);
end

[F_monitor_201,F_monitor_201_max,F_monitor_201_min,x_min] = force(Result);


%[analyse] = slack_limit(F_monitor_201,Result,W_water);

if aa>1
[coeff_table,gumby_aks] = Gumbel(x_min);

montecarlo(coeff_table,gumby_aks,x_min,lim_slack);
end

save('postpro.mat')
```

./Appedix/reader.m

```
function [Result]=reader()

direction = '../Results/';

dummy1 = dir(direction);

dummy2 = char (dummy1.name);

[a b] = size(dummy2);
Foldernames = dummy2(3:a,:);

[a b] = size(Foldernames);

disp('Folders to postprosses')
Foldernames


for i=1:a

    dummy5=regexprep(Foldernames(i,:),' ','');

    dummy3=dir([direction,dummy5,'/*.plo']);
    [aa bb] = size(dummy3);

    k=0;
    g=0;
    o=0;
    p=0;

    if (aa > 0)
    %if exist([direction,dummy5,'/',dummy3(1).name]) ==2 %%If there exsist a
        plot file

        for j=1:aa
```

```
dummy4 = load([direction,dummy5,'/',dummy3(j).name]);

Result(i).name = dummy5;

%saves the time to struct
Result(i).values.time = dummy4(:,1);

%rules for sorting results
matchStr1 = regexp(dummy3(j).name,'\wElement_Force','match');
matchStr2 = regexp(dummy3(j).name,'\wNodal_Displacement','match');
matchStr3 = regexp(dummy3(j).name,'\wNodal_Velocity','match');
matchStr4 = regexp(dummy3(j).name,'\wSurface_Elevation','match');

% saves the elemet foce to struct
if strcmp(matchStr1,'_Element_Force')
    k=k+1;
    c = regexp(dummy3(j).name,'\wElement_Force\w*','match');
    c=char(c);  c(:,1)='';

    Result(i).values.forces(k).element= c;
    Result(i).values.forces(k).value= dummy4(:,2);
end

% saves the nodal diso to struct
if strcmp(matchStr2,'_Nodal_Displacement')
    g=g+1;
    c = regexp(dummy3(j).name,'\wNodal_Displacement\w*','match');
    c=char(c);  c(:,1)='';

    Result(i).values.Displacement(g).element= c;
    Result(i).values.Displacement(g).value= dummy4(:,2);
end

 % saves the nodal vel to struct
if strcmp(matchStr3,'_Nodal_Velocity')
    o=o+1;
```

```
                c = regexp(dummy3(j).name,'\wNodal_Velocity\w*','match');
                c=char(c);  c(:,1)='';

                Result(i).values.Velocity(o).element= c;
                Result(i).values.Velocity(o).value= dummy4(:,2);
            end

             % saves the Wave elevation vel to struct
            if strcmp(matchStr4,'_Surface_Elevation')
                p=p+1;
                c = regexp(dummy3(j).name,'\wSurface_Elevation\w*','match');
                c=char(c);  c(:,1)='';

                %Result(i).values.Surface(p).element= c;
                Result(i).values.Surf_elev= dummy4(:,2);
            end

        end
    else
        disp(['Simulation unstable at',' ',Foldernames(i,:)])
    end

end



end
```

./Appedix/force.m

```
function [F_monitor_201, F_monitor_201_max,F_monitor_201_min,x_min]=force(
    Result)

Elem = 18;

[aa bb] = size(char(Result.name));
F_monitor_201=zeros(aa,length(Result(end).values.forces(Elem).value));


dt = Result(1).values.time(2)-Result(1).values.time(1);


%% lag en sort funksjon som finner Force in monitor
%%%%%%%%%%
%%

for i=1:aa

    for j=1:length(Result(i).values.forces(1).value)
        F_monitor_201(i,j) = Result(i).values.forces(Elem).value(j);
    end
end


for i=1:length(F_monitor_201(:,1))
    a=length(Result(i).values.forces(Elem).value);
    dt = Result(i).values.time(2)-Result(i).values.time(1);
    start = floor(20/dt);

    F_monitor_201_max(i) = max(F_monitor_201(i,start:a));
    F_monitor_201_min(i) = min(F_monitor_201(i,start:a));
    I_max(i)= find(Result(i).values.forces(Elem).value==F_monitor_201_max(i));
```

```
    I_min(i)= find(Result(i).values.forces(Elem).value==F_monitor_201_min(i));
end

b = char(Result.name);
fileID=fopen('result_psotpro.dat','w');
fprintf(fileID,'analyse\tForce_max\tTime\tForce_min\tTime\n');
for i=1:length(F_monitor_201_max)
    fprintf(fileID,'%s\t%f\t%f\t%f\t%f\n',b(i,:),F_monitor_201_max(i),Result(i
        ).values.time(I_max(i)),F_monitor_201_min(i),Result(i).values.time(
        I_min(i)));
end
fclose(fileID);

if aa>1


    F_max_min = {'Analyse', 'F_max', 'F_min'};

    for i=1:aa
        F_max_min{1+i,1} = char(Result(i).name);
        F_max_min{1+i,2} = F_monitor_201_max(i);
        F_max_min{1+i,3} = F_monitor_201_min(i);
    end

    k=0;
    g=1;
    for i=2:aa
        %% Sort after analyse
        f1 = char(F_max_min(i,1));
        f2 = char(F_max_min(i+1,1));
        if (strcmp(f1(1:end-3),f2(1:end-3)) == 1)
            k=1+k;
            x_min{1,g} = f1(1:end-7);
            x_min(k+1,g) = F_max_min(i,3);
            x_min(k+2,g)=F_max_min(i+1,3);
        else
```

```
            g=g+1;
            k=0;
        end
    end


    temp=cell2mat(x_min(2:end,:));

    %temp2 = sort(temp,1,'descend');
    temp2 = sort(temp,1);
    for i=1:length(temp(:,1))
        for j=1:length(temp(1,:))
            x_min{1+i,j} = temp2(i,j);
        end
    end
else
    x_min=1;
end
end
```

./Appedix/Gumbel.m

```
function [coeff_table,gumby_aks] = Gumbel(x_min)

%% Makes Gumbel data

%Cumulative distributution
[Nsmalest_responce Nanalyses] = size(x_min(2:end,:));
N=Nsmalest_responce;
i=1:Nsmalest_responce;
Fx=i./(Nsmalest_responce+1);

%Construct y-axsis
gumby_aks=log(-log(1-Fx));

%% Finds the coefficies for all the responses:(a and b)
 for j = 1:Nanalyses
      a=cell2mat(x_min(2:end,j));
      mean_exdata(j) = mean(a);    %Mean of extreme responce
      std_exdata(j) = std(a);      %Standard dev. extreme responce

%Appendix F, Statoil(Haver)
%but valid when m goes towards infinity.
      beta_G(j) =  std_exdata(j)/1.28255;
      alpha_G(j) = mean_exdata(j) + 0.57722*beta_G(j);

     coeff_table(1,1+(j-1)*2) = x_min(1,j);
     coeff_table{1,2+(j-1)*2} = 0;
     coeff_table(2,1+(j-1)*2) = {'alpha'};
     coeff_table(2,2+(j-1)*2) ={'beta'};

     coeff_table{3,1+(j-1)*2} = alpha_G(j);
     coeff_table{3,2+(j-1)*2} = beta_G(j);

 end

end
```

./Appedix/montecarlo.m

```
function [] = montecarlo(coeff_table,gumby_aks,x_min,lim_slack)
N_mont_sim=10000; % Have to be in 10
grid = 400;

for j =1:length(cell2mat(x_min(2,:)))
    x_data = cell2mat(x_min(2:end,:));
    low = floor(x_data(1,j));
    high = ceil(x_data(end,j));

    %% montecarlo

    %Makes axes for Gumbel plots
    alpha1 = cell2mat(coeff_table(3,1+(j-1)*2));
    beta1 = cell2mat(coeff_table(3,2+(j-1)*2));

    u = alpha1 + beta1 * log(-log(rand(1,length(gumby_aks),N_mont_sim)));

    x=low:1000:high;

    %Makes Gumbelfunktion
    Gumbel_reg= @(alpha, beta, x) (x-alpha)/beta;

    %% Montecarlo simulering
    for i=1:N_mont_sim

        mean_mc = mean(u(:,:,i));
        std_mc = std(u(:,:,i));

        beta(j,i) = std_mc/1.28255;
        alpha(j,i) = mean_mc + 0.57722*beta(j,i);

        %plot(x,sort(Gumbel_reg(alpha, beta, x)));
        % scatter(sort(u(:,:,i),'descend'),gumby_aks);
    end
```

```
% 90% conf.int lines
regline_c = @(alpha_m,beta_m,x) (x./beta_m) - (alpha_m./beta_m);
dgrid =(high - low)/(grid*1.3);
for g=1:grid*1.3
    x_conf(j,g) = low + dgrid*g;
    a(j,:) = sort(regline_c(alpha(j,:),beta(j,:),x_conf(j,g)));
    topconf(j,g) = a(j,0.95*N_mont_sim);
    bunconf(j,g) = a(j,0.05*N_mont_sim);
end

figure
title(char(x_min(1,j)));
hold on

plot (x_conf(j,:),topconf(j,:),'--k','LineWidth',1)
plot (x_conf(j,:),bunconf(j,:),'--k','LineWidth',1)
scatter(x_data(:,j),gumby_aks,'k')
plot(x,Gumbel_reg(alpha1, beta1,x),'-r','linewidth',3);
scatter(lim_slack,Gumbel_reg(alpha1, beta1,lim_slack),'b');
hold off

figure
x_scurve = min(x)-1e6 :1000: max(x)+1e6;
plot(x_scurve,1-exp(-exp(Gumbel_reg(alpha1, beta1,x_scurve))));

%% Save resutlt to plot files
Res = [x_data(:,j)';gumby_aks];
Confint = [x_conf(j,:);bunconf(j,:);topconf(j,:)];
Line = [x;Gumbel_reg(alpha1, beta1,x)];
Limit = [lim_slack, 0; ...
    lim_slack, Gumbel_reg(alpha1, beta1,lim_slack)];
S_curve = [x_scurve; (1-exp(-exp(Gumbel_reg(alpha1, beta1,x_scurve))))];

 fileID1 = fopen(['Res',char(x_min(1,j)),'.plo'],'w');
 fileID2 = fopen(['Confint',char(x_min(1,j)),'.plo'],'w');
 fileID3 = fopen(['Regline',char(x_min(1,j)),'.plo'],'w');
```

```
    fileID4 = fopen(['Limit',char(x_min(1,j)),'.plo'],'w');
    fileID5 = fopen(['Scatter',char(x_min(1,j)),'.plo'],'w');
    fileID6 = fopen(['Scurve',char(x_min(1,j)),'.plo'],'w');

  fprintf(fileID1,'Confint\n');
  fprintf(fileID1,'x\tylow\tyhigh\r\n');
  fprintf(fileID1,'%f %f %f\r\n',Confint);
  fprintf(fileID2,'x\tylow\tyhigh\r\n');
  fprintf(fileID2,'%f %f %f\r\n',Confint);

  fprintf(fileID1,'Regression line\n');
  fprintf(fileID1,'x\ty\r\n');
  fprintf(fileID1,'%f %f\r\n',Line);
  fprintf(fileID3,'x\ty\r\n');
  fprintf(fileID3,'%f %f\r\n',Line);

  fprintf(fileID1,'Limit\n');
  fprintf(fileID1,'x\ty\r\n');
  fprintf(fileID1,'%f %f\r\n',Limit);
  fprintf(fileID4,'x\ty\r\n');
  fprintf(fileID4,'%f %f\r\n',Limit);

  fprintf(fileID1,['Results:',char(x_min(1,j)),'\n']);
  fprintf(fileID1,'Scatter\n');
  fprintf(fileID1,'x\ty\r\n');
  fprintf(fileID1,'%f %f\r\n',Res);
  fprintf(fileID5,'x\ty\r\n');
  fprintf(fileID5,'%f %f\r\n',Res);

  fprintf(fileID1,'S-curv\n');
  fprintf(fileID1,'x\ty\r\n');
  fprintf(fileID1,'%e %e\r\n',S_curve);
  fprintf(fileID6,'x\ty\r\n');
  fprintf(fileID6,'%e %e\r\n',S_curve);

  fclose(fileID1);
```

```
    fclose(fileID2);
    fclose(fileID3);
    fclose(fileID4);
    fclose(fileID5);
    fclose(fileID6);
end




end
```